UI_4	*C2/c*, a = 13.967, b = 8.472, c = 7.510 Å, β = 90.54°. U 4*f*, 0,0.152,1/4 I(1) 8*f*, 0.123,0.118,–0.086 ; I(2) 8*f*, –0.134,0.382,0.100
HfI_4	*C2/c*, a = 11.787, b = 11.801, c = 12.905 Å, β = 116.3°. All atoms 8*f*. Hf 0.4244,0.3610,0.3753 ; I(1) 0.3270,0.3830,0.1309 I(2) 0.4470,0.1351,0.3866 ; I(3) 0.1898,0.3761,0.3632 I(4) 0.4369,0.6154,0.3808
PrI_2	$F\bar{4}3m$, a = 12.360 Å. All atoms 16 *e*, *x*,*x*,*x* etc. Pr, x = 0.3606 ; I(1), x = 0.1115 ; I(2(, x = 0.6257

Identify the anion packings (all are **cp**) and the way the cations occupy the interstices.

12. A tetragonal tetrahedral layer (§ 6.4.2) consists of two 4^4 nets of Y stacked AB, with a 4^4 net of X of twice the density in between [so there are $\{Y\}X_4$ tetrahedra]. The stoichiometry is X_2Y_2. If n such layers are joined together the stoichiometry is $X_{2n}Y_{n+1}$ (the case $n = \infty$ corresponds to **fluorite** structure X_2Y). In compounds with the KCu_4S_3 structure there are double tetrahedral layers (n = 2) of $\{Cu\}S_4$ tetrahedra interwoven with layers of K in $\{K\}S_8$ cubes:

KCu_4S_3	*P4/mmm*, a = 3.899, c = 9.262 Å, c/a = 2.38. K in 1 *b*: 0,0,1/2 Cu in 4 *i*: ±(0,1/2,*z* ; 1/2,0,*z*), z = 0.1603 S(1) in 1 *a*: 0,0,0 ; S(2) in 2 *h*: ±(1/2,1/2,*z*), z = 0.2944

Verify that the S packing consists of 4^4 nets stacked ABB... and that Cu atoms are in $\{Cu\}S_4$ tetrahedra . Compare the Cu...Cu distance in the layers with the Cu...Cu distance in elemental Cu (**ccp** with a = 3.615 Å). Speculate on the oxidation states of the atoms.

13. $AlCr_2C$ is one of the so-called H phases found for aluminum-transition metal carbides and nitrides. Many other isopuntal compounds are known including examples with two non-metallic components (which are still called H phases):

$AlCr_2C$	$P6_3/mmc$, a = 2.860, c = 12.82 Å, c/a = 4.48. Al in 2 *d*: ±(1/3,2/3,3/4) Cr in 4 *f*: ±(1/3,2/3,*z* ; 1/3,2/3,1/2–*z*), z = 0.086 ; C in 2 *a*: (0,0,0 ; 0,0,1/2)
Ti_2SC	$P6_3/mmc$, a = 3.210, c = 11.20 Å, c/a = 3.49. S in 2 *d*: ±(1/3,2/3,3/4) Ti in 4 *f*: ±(1/3,2/3,*z* ; 1/3,2/3,1/2–*z*), z = 0.099 ; C in 2 *a*: (0,0,0 ; 0,0,1/2)

Describe the two compounds above in terms of stacking of 3^6 nets (using $ABC,\alpha\beta\gamma$). What (if any) sets of atoms approximate closest packing in each case? What are the coordination polyhedra around S and C? [Compare Ti_2SC with TiP (§ 4.6.3).]

14. Here is a simple packing of unit diameter spheres:

I4/mmm, $a = 1 + \sqrt{2}$, $c = \sqrt{2}$. Centers in 8 *i*: $I \pm (x,0,0 ; 0,x,0)$, $x = 1/(2 + \sqrt{2})$

Identify the net in the layers normal to **c**, and the coordination number of the packing.

CHAPTER 7

NETS AND INFINITE POLYHEDRA

7.1 Introduction

In this chapter, in contrast to the last, we discuss some arrays of points with low coordination number, particularly 3- or 4-coordination. These are less usefully considered as sphere packings, and are more commonly described as *nets*. In some cases it is useful to consider the nets as the edges and vertices of packings of polyhedra. As in the previous chapter, the emphasis is mainly on the simpler high-symmetry patterns that occur in a variety of structural contexts. Now a systematic organization is more difficult as nets may be derived and described in more than one way. To improve continuity we have included in the main body of the text some material that might otherwise have been relegated to the Notes. In particular section numbers in this chapter that are marked with an asterisk may be of lesser interest to some readers and may be omitted in a first reading.

The diamond structure is a familiar example of a 4-coordinated (or 4-connected) net and many other 4-connected nets arise as structures of alumino-silicates (including the two most common crystalline materials in the earth's crust: quartz and feldspar). In the latter case the Si (or Al) atoms are the nodes (or vertices) of the net and the -O- bonds are to be considered the links (or edges). The frameworks of zeolites (mainly alumino-silicates and alumino-phosphates) are currently of great interest as their catalytic and other properties are largely determined by their structures. Other important 4-connected nets occur in covalent solids and as the hydrogen-bonded networks in polymorphs of ice and in hydrates.

Nets can also have mixed coordination; thus the net describing the atoms in Si_3N_4 (= $^{iv}Si_3{}^{iii}N_4$), in which Si is connected to four N, and N is connected to three Si, is referred to as (3,4)-connected. An important class of nets with mixed coordination is that corresponding to frameworks of corner-connected octahedra and tetrahedra. For example, in $Fe_2(SO_4)_3$, $\{Fe\}O_6$ octahedra share corners with $\{S\}O_4$ tetrahedra and *vice versa*. The Fe and S atoms are at vertices and the -O- links correspond to edges of a (4,6)-connected net.

We usually describe nets in crystallographic terms. We generally give unit cell parameters and coordinates of vertices that correspond to an idealized conformation in which the edges are of equal length, and in which the volume, subject to this constraint, is a maximum. This conformation is also one of maximum symmetry. Some nets occur in a variety of crystal structures and often then have lower symmetry.

There appears to be no *simple* method of giving a purely topological definition of nets, but a partial topological characterization of 3- and 4-connected nets is nevertheless useful, so we discuss this topic first. A *systematic* description of nets is difficult and efforts to enumerate possibilities have not succeeded in any rigorous manner (many hundreds of 4-connected nets have been described in the literature).

The topology of nets is a source of some fascinating, and mostly unsolved, problems. For comments on these aspects see Appendix 3.

We caution the reader that it is often *very* difficult to appreciate the structure of a three-dimensional net and virtually impossible to do such things as enumerate rings from a drawing. On the other hand models can be made simply and inexpensively (see Notes) and it will be found that these are invaluable (and sometimes essential) aids to understanding.

7.1.1 Circuits, rings and Schläfli symbols

Three-dimensional nets can be considered as infinite periodic graphs; we then tend to talk of *vertices* (atoms) and *edges* (bonds)—a common practice in graph theory. A *path* is a continuous sequence of edges, and a *circuit* is a closed path beginning and ending at the same vertex. The term *ring* is used in a special sense, described below, that is consonant with chemical usage. Any two edges with a common vertex define an *angle* at that vertex.

Recall that in Chapter 5 we often characterized finite polyhedra and two-dimensional nets by Schläfli symbols, which gave in cyclic order the size of the polygons common to a vertex. For 3- and 4-connected three-dimensional nets it is a common practice to extend the idea of a Schläfli symbol to include these cases also. Now, instead of polygons, either *shortest circuits* or *shortest rings* are used and we must first make clear the definition of these terms and be careful to distinguish between them.

For each angle at a vertex we can find a circuit which is a path that starts out at the vertex in question (the *home* vertex), goes out along one edge, and returns home along the second edge of the angle. The shortest such path (one that traverses the least number of edges) is the shortest circuit associated with that angle and is signified by the number of edges it contains. Some authors characterize three-dimensional nets by giving a "Schläfli symbol" that indicates the size of the shortest circuit at each angle; we give an example of this procedure below.

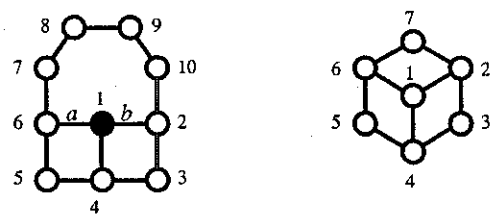

Fig. 7.1. Two fragments of nets discussed in the text.

The use of shortest circuits is not always consistent with our earlier treatment of polyhedra and two-dimensional nets as we now explain. In Fig. 7.1 (left) let the circle labeled "1" be the home vertex, and let *a* and *b* be two edges defining the angle *ab* at vertex "1." The rest of the numbered vertices represent a fragment of a net, which may be finite (i.e. the net of a polyhedron) or an infinite two- or three-dimensional net. There is a 6-circuit 1,2,3,4,5,6 containing this angle, but there is a "short cut" back to vertex 1 from vertex 4. To be consistent with earlier usage, we should not consider circuits that have such short cuts and count only those without them. Another circuit containing the angle *ab* is 1,6,7,8,9,10,2; this circuit does not contain short cuts as the path along the circuit between any two vertices on the circuit is a shortest path between them. Such circuits are variously called "fundamental circuits," "primitive rings," or just "rings;" here we will use the simplest term "ring" and reject the 6-circuit 1,2,3,4,5,6 as not being a ring but accept the 7-circuit 1,6,7,8,9,10,2 as a ring.

It is not hard to see that an infinite net will have only a finite number of rings for each vertex, whereas there is an infinite number of circuits. Interesting unsolved problems are how the number and sizes of rings affect properties such as density, and what constraints there are on ring size.

Referring to Fig. 7.1 (right) we can see that the circuit 1,2,3,4,5,6 is not counted as a ring, but 2,3,4,5,6,7 is. The latter ring is however made up of smaller ones (1,2,3,4 and 1,4,5,6 and 1,2,6,7) in the sense that traversing all the edges of the smaller rings will result in traversing all the edges of the larger one. Rings that cannot be decomposed in such a manner have been called "strong rings."

It is useful to recognize that the graphs of finite polyhedra usually contain rings that do not enter into the Schläfli symbol. Figure 7.2 (left) is a conventional representation of a cube: on the right is a Schlegel diagram. The circuit 1,4,8,7,6,2 (shown as heavier lines) is a 6-ring. The presence of 6-rings is not reflected in the Schläfli symbol (4^3) for the cube.

The reader might like to verify that there are also 6-rings (hexagons) in the cuboctahedron, 3.4.3.4 (see e.g. Fig. 6.8, p. 215).

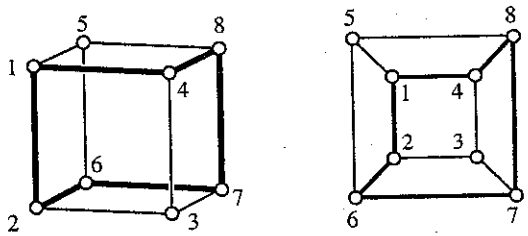

Fig. 7.2. Left: a conventional representation of a cube. Right: a corresponding Schlegel diagram. A 6-ring is shown as heavier lines.

Three angles meet at each node of a three-connected net. In contrast to plane nets, in three-dimensional nets more than one ring may be included in an angle (see also the next section), so we modify the Schläfli symbol to read $X_x \cdot Y_y \cdot Z_z$ where X, Y, Z are numbers that represent the ring size and x,y,z are numbers that indicate the numbers of rings meeting at that angle; subscript "1" is omitted. Thus $8 \cdot 8 \cdot 8_2$ indicates that at two of the angles there is an 8-ring and at the third angle there are two 8-rings. Note that many authors omit the subscripts, and the symbol for the vertex in this example is then written 8^3.

Just as polyhedra often contain larger rings than those used to specify the Schläfli

symbol, three-dimensional nets often contain larger rings in an analogous manner. (Remember that we use only the *shortest* rings at a vertex to construct the vertex symbol.)

To make clear the distinction between the use of circuits and rings, we give another example. Fig. 7.3 shows a fragment of a net. The 3-connected vertex shown as a filled circle has a 4-ring, a 6-ring and a 10-ring at the three angles, so using rings the symbol is 4.6.10 (the fragment shown might represent part of the net of the truncated icosidodecahedron). The 10-ring is at the angle *ab*. There is also an 8-circuit (1,2,3,4,5,6,7,8) at the same angle, but we do not count it as a ring because there is a short cut between vertices 1 and 4.

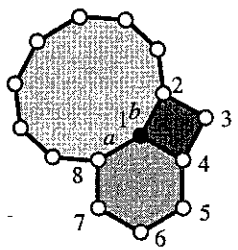

Fig. 7.3. Rings surrounding a 4.6.10 vertex (filled circle). The angle *ab* is contained in the 10-ring (lightly shaded) and also in the 8-circuit (not a ring) 1,2,3,4,5,6,7,8.

7.1.2 Schläfli symbols for 4-connected nets

Let us arbitrarily label the four edges meeting at a vertex of a 4-connected net *a*, *b*, *c* and *d*. A pair of edges, such as *ab* define an angle at that vertex. There are six angles at each vertex defined by pairs of edges: (*ab*, *cd*), (*ac*, *bd*), (*ad*, *bc*). Pairs of angles in parentheses have no common edge and are referred to as *opposite* angles. Pairs of angles with a common edges are referred to as *adjacent.*

Fig. 7.4. Illustrating two 6-rings containing the same angle (heavy lines) at a vertex (filled circle) in the diamond net. This figure is a fragment of Fig. 7.10 (left).

For a given angle there may well be several distinct shortest rings. For example, in the diamond structure (§ 7.3.1) two 6-rings are contained in each angle as sketched for one angle in Fig. 7.4.

In order to facilitate comparison with the (rather large) literature on 4-connected nets we sometimes use two kinds of "Schläfli" symbol. A "short" one that specifies just the shortest circuit contained in each angle (most commonly found in the literature) and a "long" one that recognizes only rings and is described next by example.

In the structure of a feldspar (§ 7.3.9) such as $CaAl_2Si_2O_8$, the net of the Al and Si atoms has two kinds of vertex.[1] If we use just the shortest *circuits* at each angle, the symbols for both vertices are $4^2.6^3.8$; however, using *rings* we can distinguish the two vertices. The smallest rings and circuits associated with each angle are given below for each vertex. Also listed are the numbers of such rings and circuits for each angle.

	vertex 1				vertex 2			
angle	ring	number	circuit	number	ring	number	circuit	number
ab	4	1	4	1	4	1	4	1
cd	6	1	6	1	6	2	6	2
ac	4	1	4	1	4	1	4	1
bd	6	1	6	1	8	1	8	3
ad	8	2	8	6	6	1	6	1
bc	10	10	6	1	6	2	6	2

We now write a *long Schläfli symbol* for each vertex as follows. We write, in order, the symbols of the rings with a subscript for the number of rings (omitting the subscript "1"). Note that we pair circuits by opposite angles and, subject to that constraint, write the smallest numbers first. The symbols for the two vertices are therefore:

vertex 1 $4{\cdot}6{\cdot}4{\cdot}6{\cdot}8_2{\cdot}10_{10}$
vertex 2 $4{\cdot}6_2{\cdot}4{\cdot}8{\cdot}6{\cdot}6_2$

Not all nets have distinctive vertex symbols even using long symbols: the pair **diamond** and **lonsdaleite** (see below) is a conspicuous example; for both nets the vertex symbol is $6_2{\cdot}6_2{\cdot}6_2{\cdot}6_2{\cdot}6_2{\cdot}6_2$.

Note that in our usage short symbols (using shortest circuits) employ *super*scripts which (including the implied "1"s) add up to three for 3-connected nets and to six (for the six angles) for 4-connected nets. Long symbols contain three entries for a 3-connected net and six entries for a 4-connected net and these are separated by a "·" and may (often do) employ *sub*scripts in some of the entries. Although the procedure may appear somewhat complicated, it is in fact very readily implemented using a computer, and is of considerable help in identifying nets of a given topology in structures.

7.1.3 Coordination sequences

We briefly mentioned *coordination sequences* for structures in § 6.8.2. Each different kind of vertex in a net has associated with it a coordination sequence (*CS*) which is the

[1] But not (as one might first expect) with Si on one kind of vertex and Al on the other. The edges of the nets correspond to the -O- bonds to (Si,Al) atoms. Ca is accommodated in cavities in the net and is ignored in the present context.

sequence $n_1, n_2, \ldots n_k, \ldots$ of numbers of kth topological neighbors. In the language appropriate for discussion of nets we simply define a kth neighbor of a vertex to be one for which the *shortest* path to that vertex consists of k edges.

Figure 7.5 illustrates the concepts of topological neighbors and *CS* for the two-dimensional net 4^4. The reference vertex (filled circle) has four neighbors (dark shading) connected to it by an edge, so $n_1 = 4$. The second neighbors (light shaded) of the reference vertex are first neighbors of the first neighbors (other than the reference vertex) and clearly $n_2 = 8$. Similarly the third neighbors (open circles) of the reference vertex are the first neighbors of the second neighbors of the reference vertex that are not first neighbors of the reference vertex (or, more simply, the third neighbors are those for which the shortest path to the reference vertex consists of three edges). It should be clear that $n_3 = 12$. In fact it should be clear (drawing a few more shells may help) that $n_k = 4k$ in this instance and that the *CS* is 4, 8, 12, 16,....

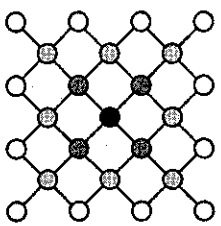

Fig. 7.5. Illustrating the topological neighbors of a vertex in the two-dimensional net 4^4 (see text).

Recall that the *CS* is concerned only with the topology of the net. In Fig. 7.5 the 4^4 net is illustrated in its most symmetrical form and it should be obvious that the eight second topological neighbors are not all the same geometrical distance from the reference vertex.

We give examples of *CS*'s for some nets in the sections below. One of their main uses is in computer recognition of nets, but it should be emphasized that occasionally two different nets have the same *CS* so that strictly speaking it can only be proved that two structures have different topologies.[1] The *CS* for the two vertices of the feldspar net are 4, 10, 20, 38, 58,... and 4, 10, 22, 38, 56,... respectively. We know of no example of two different nets in which the vertices have simultaneously the same *CS* and Schläfli symbol.

7.1.4 Further definitions

Other terms that have obtained some currency are now defined.

A *uninodal* net is one in which all vertices are congruent. In its maximum symmetry form all vertices will be related by symmetry operations (be equivalent).

A *uniform* net is one in which the shortest rings at each angle are equal in size. A familiar two-dimensional example is 6^3.

[1]The reader can readily verify that the *CS* for the two-dimensional net 3.4.6.4 is the same as that for 4^4.

A *quasi-regular* net is one in which all vertices and all edges are equivalent.[1]

A *regular* net has all vertices, all edges and all angles equivalent. A regular net is necessarily uniform. The net of the diamond structure is the only regular three-dimensional 4-connected net; the corresponding regular 3-connected net is described next.

*7.2. 3-connected nets

We have met some plane 3-connected nets before, notably the honeycomb (6^3). This is very frequently found as a layer in a crystal structure (e.g. graphite). A number of three-dimensional nets which can be realized with equal edges and angles of 120° between the edges, are known, and some are of sufficient interest to describe here.

The first three-dimensional net is an invariant cubic lattice complex:

Y^*	$I4_132$, $a = \sqrt{8}$
	$10_5{\cdot}10_5{\cdot}10_5$ in 8 *a*: I + (1/8,1/8,1/8 ; 3/8,7/8,5/8)κ
	or 8 *b*: I + (7/8,7/8,7/8 ; 5/8,1/8,3/8)κ

These two sets of positions produce structures that are enantiomers of each other and they are symbolized $^+Y^*$ and $^-Y^*$ respectively (for reasons which will be apparent later).

Although there are only four vertices in the repeat unit (the primitive cell), the structure is difficult to illustrate. Fig 7.6 shows two projections of $^+Y^*$. Note (on the left) that there are four-fold helices along [001] of one hand (anticlockwise along +z, i.e. 4_1) in the structure, and that (right) there are likewise three-fold helices along [111] that are all of the same hand (3_2). The helices are of opposite hand in $^-Y^*$. The Schläfli symbol is $10_5{\cdot}10_5{\cdot}10_5$ (five 10-rings meet at each angle). This net occurs as the Si arrangement in $SrSi_2$ and isostructural compounds. It is the only regular three-dimensional 3-connected net. For a stereo picture of this net see § 7.11.8.

The axes of the 4_1 helices are arranged as in the **β-Mn** cylinder packing and the axes of the 3_2 helices are arranged as in the **$SrSi_2$** cylinder packing (hence the name of the latter).

It is interesting that the same structure can be derived in several ways. Positions 8 *c* of $P4_132$ are (x,x,x ; 3/4–x,3/4–x,3/4–x ; $\bar{x}$,1/2+x,1/2–x ; 1/4–x,3/4+x,1/4+x)κ and 8 *c* of the enantiomorphic group $P4_332$ are (x,x,x, ; 1/4–x,1/4–x,1/4–x ; $\bar{x}$,1/2+x,1/2–x ; 3/4–x,1/4+x,3/4+x)κ. We have the special cases:

$P4_132$	8 *c*: x = 1/8 or 5/8 → 8 *a* of $I4_132$
$P4_332$	8 *c*: x = 3/8 or 7/8 → 8 *b* of $I4_132$

In the crystal structure of $SrSi_2$ (for data see Appendix 5), the Si atoms are at positions 8 *c* of $P4_332$ with $x = 0.423$ so they constitute a slightly distorted version of $^-Y^*$ (the Si-Si-Si angles are 118°). We may write the compound as $Sr^{2+}(Si^-)_2$ and then recognize that Si^- is

[1]One sometimes sees the term "regular" for what we term "quasi-regular" but this conflicts with established usage for plane nets and polyhedra. The polyhedra 3.4.3.4 and 3.5.3.5 are quasiregular.

isoelectronic with P. The formation of three non-coplanar P-P bonds in elemental P is ascribed to the presence of a non-bonding pair of valence electrons, and it is tempting to suppose that similar considerations apply to the Si-Si bonding in $SrSi_2$.

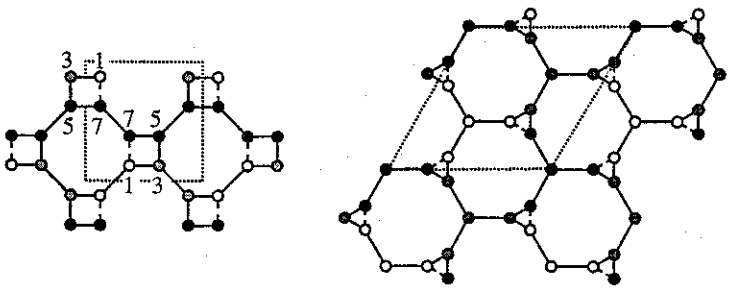

Fig. 7.6. Left: The lattice complex $^{+}Y^{*}$ projected on (001). The unit cell is shown by broken lines and numbers are heights in multiples of *c*/8. Right: The same structure projected on (111). Open, shaded and filled circles are at 0, 1/3 and 2/3 of a primitive translation vector {(**a**+**b**+**c**)/2 along [111]}.

The invariant positions of $P4_332$ are 4 *a*: (1/8,1/8,1/8 ; 3/8,7/8,5/8)κ and 4 *b*: (5/8,5/8,5/8 ; 1/8,7/8,3/8)κ and the invariant positions of $P4_132$ are 4 *a*: (3/8,3/8,3/8 ; 1/8,5/8,7/8)κ and 4 *b*: (7/8,7/8,7/8 ; 1/8,3/8,5/8)κ. The symbols for these lattice complexes are ^{+}Y and ^{-}Y respectively (see § 6.3.10). We can combine these as follows:

$P4_132$ $\quad 4\,a + 4\,b \rightarrow 8\,b$ of $I4_132$ $(2^{-}Y \rightarrow {}^{-}Y^{*})$
$P4_332$ $\quad 4\,a + 4\,b \rightarrow 8\,a$ of $I4_132$ $(2^{+}Y \rightarrow {}^{+}Y^{*})$

This shows incidentally that $I4_132$ has both 4_1 and 4_3 axes. If we had atoms *A* on positions 4 *a* and *X* on 4 *b* (of $P4_132$ or $P4_332$) we would get a simple (unknown) structure with *A* surrounded by an equilateral triangle of *X* (and *vice versa*). Note that it is its own "antistructure" (interchanging *A* and *X* produces the same structure).

A second cubic 3-connected net, called 6.8^2 *D*, can be constructed with angles of 120°:

6.8^2 *D* $\quad Pn\bar{3}m$, $a = \sqrt{18}$
6·8·8 in 24 *i*: $\pm(1/2,x,\bar{x}\ ;\ 0,1/2-x,\bar{x}\ ;\ 0,x,1/2+x\ ;\ 1/2,1/2-x,1/2+x)\kappa$, $x = 1/3$

A fragment of the structure is shown in Fig. 7.7. A notable feature is the groups (joined by edges) of 12 coplanar vertices parallel to {111}. The Schläfli symbol is 6·8·8. There are two kinds of edge: those on 6-rings, and those not on six-rings. The 6-rings and 8-rings of this structure can be considered as covering an infinite surface (named *D* in Appendix 4) and hence form an infinite polyhedron as discussed later for some 4-coordinated structures.

A related net, called 6.8^2 *P*, with the same Schläfli symbol (6·8·8) is also shown in Fig. 7.7. Parameters for unit edge length and regular hexagons are:

6.8^2 *P* $\quad Im\bar{3}m$, $a = 5.266$
6·8·8 in 48 *k*: $I + (\pm x,\pm x,\pm z)\kappa$, $x = 0.3275$ and $z = 0.0949$

The angles are 120° and 114.1° (2×). For slightly different parameters, the bond angles can be made all equal to 118.5°. Like the previous net this can be considered as an infinite polyhedron 6·8·8.[1]

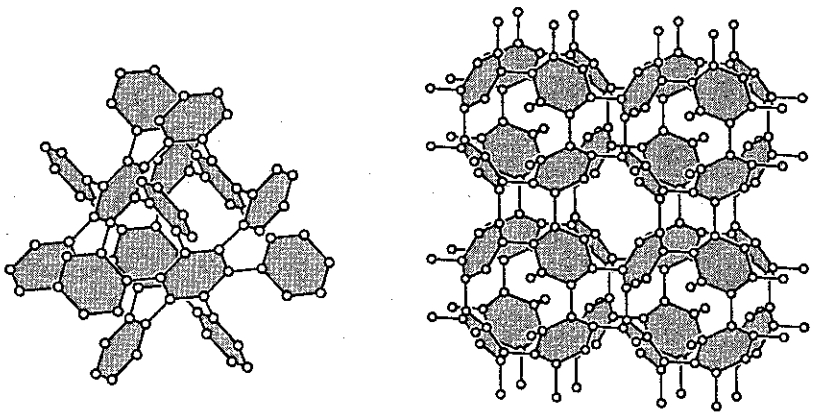

Fig. 7.7. Two cubic 3-connected nets, 6·8·8. Left: 6.8^2 *D*. Right: 6.8^2 *P*.

Another 3-connected net occurs in silicides such as $ThSi_2$ (for crystallographic data for the compound see Appendix 5). It can also be constructed with 120° bond angles:[2]

$ThSi_2$ net $\quad I4_1/amd$, $a = \sqrt{3}$, $c = 6$
vertices $(10_2{\cdot}10_4{\cdot}10_4)$ in 8 *e*: $I \pm (0,1/4,z\ ;\ 0,3/4,1/4+z)$, $z = -1/24$

This net is sketched in Fig. 7.8. The Schläfli symbol is $10_2{\cdot}10_4{\cdot}10_4$.

Three-connected nets can also occur in framework oxides with -O- links serving as edges as described for the structure of B_2O_3 below. In P_2O_5 {P}O_4 tetrahedra share *three* corners with neighbors (so the stoichiometry is $PO_{3/2}O = 1/2\ P_2O_5$). In one polymorph, isolated P_4O_{10} molecules are formed in which the P atoms are at the vertices of a tetrahedron (see Fig. 5.18, p. 150). In a second form the P-O-P links form a honeycomb

[1]These two 6.8^2 nets have been considered as possible structures for three-coordinated carbon; see M. O'Keeffe *et al.*, *Phys. Rev. Letts.* **68**, 2325 (1992); this reference explains the origin of the names. The $Pn\bar{3}m$ structure is a particularly favorable candidate; it is known to organic chemists as the "Riley structure" as it was apparently first suggested by H. L. Riley [see *e.g.* J. Gibson, *et al.*, *J. Chem. Soc.* 456 (1946)]. The (hypothetical) carbon is called "polybenzene."

[2]This is another net that has been considered as a possible carbon structure; interestingly carbon with this structure is predicted to be denser than graphite and metallic. [R. Hoffmann *et al.*, *J. Amer. Chem. Soc.* **103**, 4831 (1983)].

(6^3) layer. In the third, and apparently most stable, form the P-O-P links have the topology of the $ThSi_2$ net (see Exercise 11).

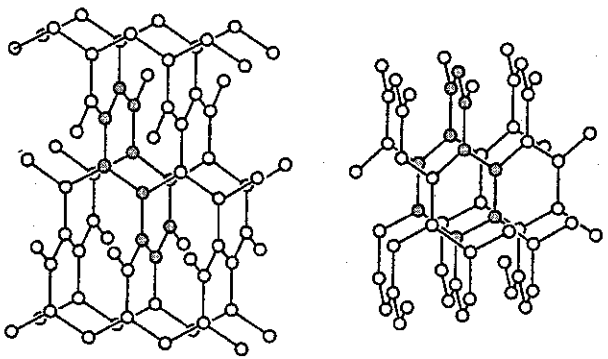

Fig. 7.8. Left: the 3-connected net of the Si atoms in $ThSi_2$. Right: the 3-connected net of the B atoms in B_2O_3. The c axis is vertical and the shaded vertices fall on a 10-ring in each case.

Another 3-connected net (Fig 7.8) that can be constructed with 120° bond angles again contains 10-rings. It is the net of the B atoms in B_2O_3 (for crystallographic data see Appendix 5) and is trigonal:

B_2O_3 net $P3_112$, $a = \sqrt{3}$, $c = 9/2$
vertices $(10{\cdot}10_2{\cdot}10_2)$ in 6 *c*: $(x,y,z\ ;\ \bar{y},x{-}y,1/3{+}z\ ;\ y{-}x,\bar{x},2/3{+}z\ ;\ x,x{-}y,\bar{z}\ ;$ $y{-}x,y,1/3{-}z\ ;\ \bar{y},\bar{x},2/3{-}z\ )$, $x = 1/3$, $y = 1/6$, $z = 1/9$

7.3. 4-Connected nets

The number of 4-connected nets found in crystal structures is very large. Well over 100 different topologies are known for framework silicates, particularly natural and synthetic zeolites. Some of these have a large number of topologically-distinct vertices and resist simple classification. In this chapter we confine ourselves mainly to relatively simple examples of nets with particular emphasis on those, such as that of the diamond structure, which arise in a number of different contexts. Some of the structures we describe do not appear to have been recognized yet in crystal structures. These have been assigned an arbitrary number for identification.[1]

Recall that unless explicitly stated otherwise, crystallographic parameters refer to unit edge (bond) length. For some nets (e.g. **diamond**) this is sufficient to completely

[1]These index numbers are known to the computer program EUTAX. [See also M. O'Keeffe & N. E. Brese, *Acta Crystallogr.* A**48**, 663 (1992).] With the recent flurry of activity in synthesis of new zeolites and related materials we find that we are continually replacing index numbers with names of known materials.

determine the structure; for other structures we give parameters for maximum volume subject to the constraint of equal edge length. Densities are expressed as r = number of vertices per unit volume (for nets of unit edge). In the context of framework aluminosilicates, there is considerable interest in the framework density (*FD*), usually expressed as the number of tetrahedral atoms (Al,Si) per 1000 Å^3. As the Si...Si distance is typically 3.06 Å in framework silicates, $FD \approx 1000r/3.06^3 = 34.9r$ Å^{-3}.

7.3.1 **Diamond, lonsdaleite** *and their polytypes*

The diamond net is of course that of the diamond form of carbon and is also found as the structure of the stable forms of Si, Ge and (at low temperatures) Sn. As it occurs in many structure types it will prove profitable to become familiar with it. In the structure every point is connected to four neighbors at the vertices of a regular tetrahedron as shown in Fig. 7.9. A formal description is as follows:

diamond $Fd\bar{3}m$, $a = 4/\sqrt{3}$, $r = 0.650$
vertices in 8 *a*: $F \pm (1/8,1/8,1/8)$

The positions of the vertices correspond to the lattice complex *D*.

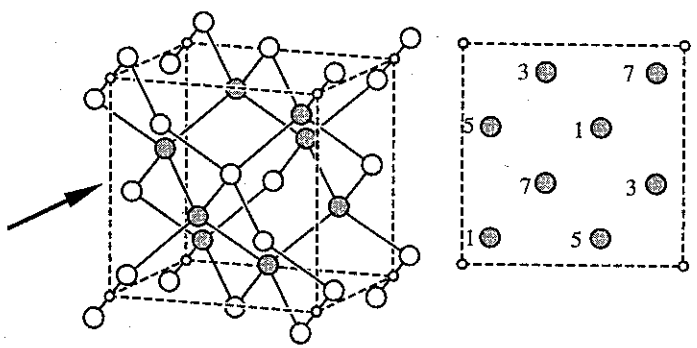

Fig 7.9. The diamond net. On the left in clinographic projection. The unit cell is outlined with dashed lines and points within the cell are shaded. On the right is shown a projection down the direction shown as an arrow (which corresponds to a unit cell edge) of the atoms shaded in the drawing on the left. Numbers are atom heights in multiples of 1/8. Small circles are centers of symmetry at the unit cell origin.

The long Schläfli symbol for this structure is $6_2{\cdot}6_2{\cdot}6_2{\cdot}6_2{\cdot}6_2{\cdot}6_2$. As we will see, some other nets have the same symbol.

It should be obvious from the formal description above, that the diamond array consists of two **ccp** arrays (origins at 1/8,1/8,1/8 and –1/8,–1/8,–1/8), each array occupying half of the tetrahedral sites of the other. If the two arrays are occupied by different kinds of atom, we have the **sphalerite** structure of ZnS. Recall that in § 6.1.5 we described **sphalerite**

as a "close packing" of S with Zn in tetrahedral sites (or *vice versa*). Now we see that the structure is equally well (perhaps better) described as a bond network.

A related 4-connected net occurs as the structure of lonsdaleite, a rare allotrope of carbon.[1] A formal description is:

lonsdaleite $P6_3/mmc$, $a = \sqrt{(8/3)}$, $c = 8/3$, $r = 0.650$
vertices in 4 *f*: $\pm(1/3,2/3,z\ ;\ 2/3,1/3,1/2+z)$, $z = 1/16$

The parameters are for the idealized structure with unit edge length and angles equal to the "tetrahedral" angle $\cos^{-1}(-1/3) = 109.47°$.

It should be obvious from the above description [notice that $c/a = \sqrt{(8/3)}$] that, as in **diamond**, the vertices fall on two **cp** arrays (but now **hcp**) separated by $c/8$. The vertices of one array are in one half the tetrahedral sites of the second one, and *vice versa*. If the two arrays consist of different kinds of atom we have the **wurtzite** form of ZnS.

Fig. 7.10 shows the diamond and lonsdaleite structures side by side for comparison. In the figure the direction up the page is [111] for the diamond structure and [001] for lonsdaleite. To facilitate the comparison, note that the diamond structure can be described using a hexagonal cell with vertices in $R \pm (0,0,1/8)$, $a = \sqrt{(8/3)}$, $c = 4$. It should also be noted that the nets could also be described as a stacking of puckered 6^3 nets (3-connected) with additional bonds between the layers. In terms of the symbols introduced in the previous chapter (§ 6.1.6) the stacking of (puckered) 6^3 nets (G) in lonsdaleite is G_1G_1... and in diamond it is $G_1G_2G_3$.... Later we will describe some other 4-connected nets derived from 6^3 in related ways.

In the diamond structure all the 6-circuits are skew hexagons in "chair" conformation. In lonsdaleite the hexagons not normal to [001] are in "boat" conformation (see Fig. 7.10).

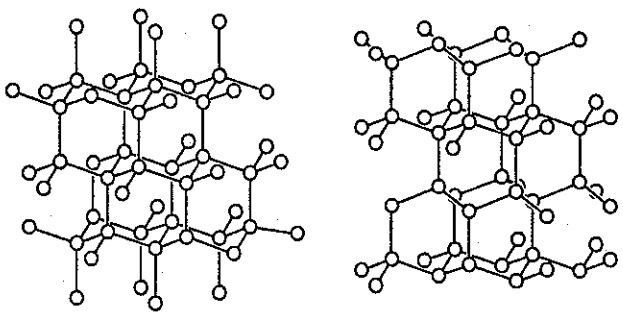

Fig 7.10. Left: the diamond structure in clinographic projection with [111] vertical on the page. Right: the lonsdaleite structure with [001] vertical on the page.

[1]Named for Kathleen Lonsdale who made many contributions to carbon chemistry, notably the first demonstration (by X-ray diffraction) of the planarity of the benzene ring. She was the first woman to be elected to fellowship in the Royal Society of London.

The Schläfli symbol of the lonsdaleite net is the same as that of diamond, *viz.* $6_2{\cdot}6_2{\cdot}6_2{\cdot}6_2{\cdot}6_2{\cdot}6_2$. Accordingly to distinguish between these nets topologically we need to consider numbers of kth neighbors. These are:

k	1	2	3	4	5	6	7	8	9	10
diamond	4	12	24	42	64	92	124	162	204	252
lonsdaleite	4	12	25	44	67	96	130	170	214	264
difference	0	0	1	2	3	4	6	8	10	12

It may be seen that lonsdaleite has more topological neighbors (i.e. is *topologically denser*[1]) than diamond for third and subsequent neighbors. In these cases simple expressions, in which brackets indicate rounding *down* to an integer, obtain for n_k, the number of kth neighbors:

diamond: $n_k = [5k^2/2] + 2$ (7.1)

lonsdaleite: $n_k = [21k^2/8] + 2$ (7.2)

Diamond and lonsdaleite structures may be derived from, respectively, cubic and hexagonal eutaxy by filling one-half of the tetrahedral sites (either all those pointing down, or all those pointing up). Related *polytypes* can be obtained in a similar way from more complicated closest packings. The simplest of these, derived from *hc* (4*H*) packing (i.e. two *hc* **cp** arrays with points of one array in tetrahedral interstices of the other), is:

carbon 4*H* $P6_3/mmc$, $a = \sqrt{(8/3)}$, $c = 16/3$, $r = 0.650$
c vertices in 4 *e*: $\pm(0,0,z\ ;\ 0,0,1/2+z)$, $z = 3/32$
h vertices in 4 *f*: $\pm(1/3,2/3,z\ ;\ 1/3,2/3,1/2-z)$, $z = 5/32$

A commonly encountered projection of these, and related structures, is shown in Fig. 7.11. For diamond, this is a projection on (110) of the cubic cell; for the hexagonal cell of the other two nets it is on $(11\bar{2}0)$. Single lines represent bonds in the plane of the projection; double lines represent bonds out of the plane but superimposed in projection. Readers interested in topics such as stacking faults in Si and similar defects will find it well worth the effort it takes to learn to interpret such diagrams. In particular notice that the double lines represent a zig-zag chain of vertices seen in projection; we encounter such a motif repeatedly in the next few sections.

"Diamond" (used as an abrasive) made by shock compression of graphite is usually a rather disordered mixture of polytypes. SiC also occurs as many polytypes; a cubic **sphalerite** form (known as β-SiC), a **wurtzite** form, and other hexagonal and rhombohedral forms. The term α-SiC is sometimes used for the non-cubic forms. Under the trade name "carborundum" it is used on a large scale as an abrasive. The polytypes have been studied very extensively as SiC is also potentially a valuable material for

[1]In the *topological* sense. In geometric terms the two nets in their most regular forms with equal edges have the same density (vertices per unit volume).

microelectronic applications. Unfortunately the electronic properties are very sensitive to structure and it is still far from certain what factors determine which polytype will form, and most preparations consist of intergrowths of different polytypes. The structure and isotopic composition of meteoritic SiC (moissanite) is also currently of considerable interest.

In the Notes (§ 7.11.4) we describe some of these polytypes in more detail and give coordinates for idealized versions of some of the simpler structures.

Forms of silica (SiO_2) with vertex-sharing $\{Si\}O_4$ tetrahedra and with the Si-(O)-Si nets having the **diamond** and **lonsdaleite** topology are known as cristobalite and tridymite respectively.

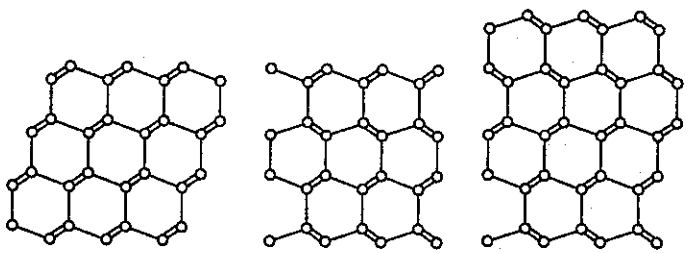

Fig. 7.11. Left: the diamond structure projected on (110). Middle: the lonsdaleite structure projected on $(11\bar{2}0)$. Right: the *hc* diamond polytype similarly projected. Double lines represent bonds up and down out of the plane of the paper.

*7.3.2 Two more uniform nets, 6^6

Fig. 7.12 shows a net that is a first cousin to the diamond-lonsdaleite family (compare Fig. 7.11). It is also uniform (6^6) but now the extended symbol is $6{\cdot}6{\cdot}6{\cdot}6_2{\cdot}6_2{\cdot}6_2$. There are also ten 10-rings meeting at each vertex in addition to the nine 6-rings. We have not found a good name for this net so it is arbitrarily named **net #9**. A crystallographic description is (note that it is denser than **diamond**):

net #9 *Fddd*, $a = 4.644$, $b = 3.061$, $c = 1.532$, $r = 0.735$
$6{\cdot}6{\cdot}6{\cdot}6_2{\cdot}6_2{\cdot}6_2$ in 16 *e*: $F \pm (x,1/8,1/8\ ;\ 1/4{-}x,\ 1/8,1/8)$, $x = 0.3057$

Another simple uniform net (which we call **net #5**) is also shown in Fig. 7.12. Like the previous net (and **lonsdaleite**) there are only four vertices in the primitive cell. The extended symbol is $6{\cdot}6{\cdot}6_2{\cdot}6_2{\cdot}6_3{\cdot}6_3$. There are also eight 8-rings and ten 10-rings meeting at each vertex in addition to the nine 6-rings. A crystallographic description is:

net #5 $P4_122$, $a = 2.030$, $c = 1.414$, $r = 0.686$
$6{\cdot}6{\cdot}6_2{\cdot}6_2{\cdot}6_3{\cdot}6_3$ in 4 *a*: $(0,x,0\ ;\ 0,\bar{x},1/2\ ;\ x,0,3/4\ ;\ \bar{x},0,1/4)$, $x = 0.3258$

Despite their simplicity, model builders will find constructing these last two nets a challenge, and counting rings by hand quite difficult.

It appears that all uniform 4-connected nets are 6^6 (some more examples are given below).[1] In contrast uniform 3-connected nets ranging from 7^3 to 12^3 are known (see Notes).

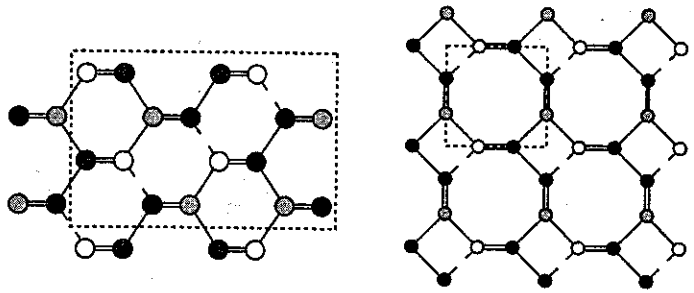

Fig 7.12. Left: **net #9** projected on (001) with **a** horizontal on the page. Open circles are at $z = 1/8$, lightly shaded circles at $z = 3/8$, darker shaded at $z = 5/8$ and filled circles at $z = 7/8$. Right: **net #5** projected on (001). Open circles are at $z = 0$, lightly shaded circles at $z = 1/4$, darker shaded at $z = 1/2$ and filled circles at $z = 3/4$. In both figures broken lines represent bonds to atoms with either $z < 0$ or $z > 1$.

7.3.3 Nets derived from 6^3: CrB_4

As mentioned above, it is possible to derive 4-connected nets in a formal way by linking stacked planar 3-connected nets. **Lonsdaleite** is a simple example of a 4-connected net derived by linking 6^3 nets (Fig. 7.13, left). Two more ways of deriving 4-connected nets from 6^3 are also shown in Fig. 7.13. In the figure, open and filled circles are to be interpreted as links up and down from a given layer and in opposite directions in adjacent layers so that each vertex is 4-connected. This description is sufficient to specify the topology (connectivity) of the net. Note that edges connecting pairs of open or filled circles correspond to 4-rings seen in projection. Except for **lonsdaleite**, all nets derived in this way contain 4-rings.

Each of the two new nets derived in the figure is uninodal and the long Schläfli symbol is also the same in both cases: $4{\cdot}6_2{\cdot}6{\cdot}6{\cdot}6{\cdot}6$ (short symbol 4.6^5).

The first new net, in the middle in Fig. 7.13, is the net of the B atoms in CrB_4 (which has the orthorhombic structure described for MnB_4 in § 4.6.5—see also Appendix 5) so we call it the **CrB_4** net. The other net is found as the arrangement of Ga atoms in $CaGa_2O_4$ (edges correspond to Ga-O-Ga bonds). A formal description of the first net is:

CrB_4 *I4/mmm*, $a = 3$, $c = \sqrt{2}$, $r = 0.629$
$4{\cdot}6_2{\cdot}6{\cdot}6{\cdot}6{\cdot}6$ in 8 *h*: $I \pm (\pm x,x,0)$, $x = 1/6$.

[1] An example of a net with only 7-rings is given below (§ 7.5.1), but one angle contains *no* rings.

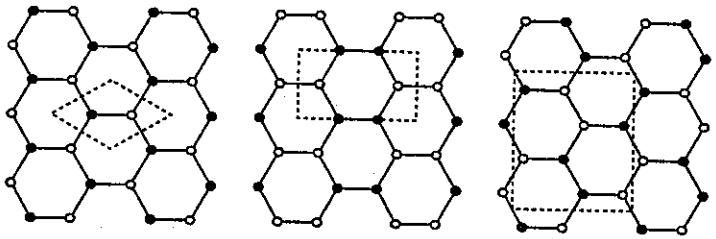

Fig. 7.13. Derivation of 4-connected nets from stacked 6^3 nets (see text). On the left, **lonsdaleite** is derived, in the middle **CrB_4**, and on the right **$CaGa_2O_4$**. In each case additional bonds go up (down) from open (filled) circles to identical nets above (below) the ones shown.

The net is illustrated in several ways in Fig. 7.14. On the left it is projected on (001), a projection that suggests that it could also be derived from the planar 4.8^2 net in an obvious way. This projection should also be compared with that of **net #109** on the left of Fig. 7.15. The projection in the middle of Fig 7.14 corresponds to that in the middle of Fig. 7.13 (but rotated by 90°).

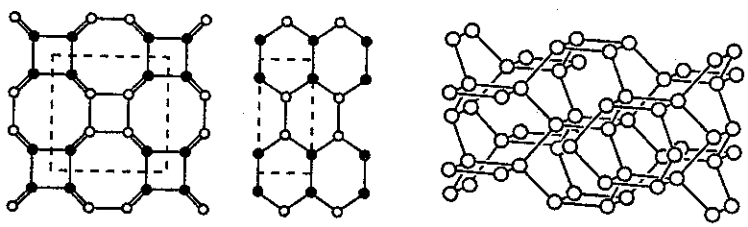

Fig. 7.14. The CrB_4 net. Left: a projection on (001); filled and open circles are at $z = 0$ and 1/2 respectively. Middle: the structure projected on (100); filled circles are at $x = \pm 1/6$ and open circles at $x = \pm 1/3$. Right: as a clinographic projection (c vertical).

We meet the **CrB_4** net in several disguises. The 8 *h* positions of *I4/mmm* can split into two groups of 4 corresponding to the positions 4 *f* and 4 *g* of $P4_2/mnm$:

4 *f*: $\pm(x,x,0\ ;\ 1/2+x,1/2-x,1/2)$ 4 *g*: $\pm(x,\bar{x},0\ ;\ 1/2+x,1/2+x,1/2)$

If these positions are separately occupied by Be and O atoms (with $x \approx 1/6$) we obtain the structure of β-BeO (for the real β-BeO structure see Appendix 5).

The same net appears as the Al,Si net in one form of $CaAl_2Si_2O_8$ (cf. the **paracelsian** net in § 7.3.6 which is the net of another form of $CaAl_2Si_2O_8$).

The reader is encouraged to draw the second net (that of $CaGa_2O_4$). This net also occurs as the Al,P net in the mineral variscite, $AlPO_4{\cdot}2H_2O$ (the corresponding net in metavariscite, which has the same composition, has the **CrB_4** topology). The crystallographic description is:

$CaGa_2O_4$ *Cmca*, $a = 2.823$, $b = 3.291$, $c = 2.794$, $r = 0.616$
$4{\cdot}6_2{\cdot}6{\cdot}6{\cdot}6{\cdot}6$ in 16 *g*: $C \pm (\pm x,y,z\ ;\ \pm x,1/2-y,1/2+z)$,
$x = 0.177$, $y = 0.133$, $z = 0.087$

**7.3.4 Two nets related to CrB_4 with zig-zag rods*

Fig. 7.14 shows (left) how **CrB_4** may be derived from the two-dimensional net 4.8^2 by replacing some of the edges (those not on squares) by zig-zag lines (which are shown as double lines in the projection) representing edges connecting layers above and below. A related net can be derived from 4.8^2 by an analogous procedure if the squares are slightly tilted out of the plane as shown in Fig. 7.15 (left). We label this **net #109**.

Another net that occurs as the (Al,P) framework in a form of $AlPO_4$ known as $AlPO_4$-31 is derived similarly from the two-dimensional net 4.6.12 [see Fig. 7.15 (right)].

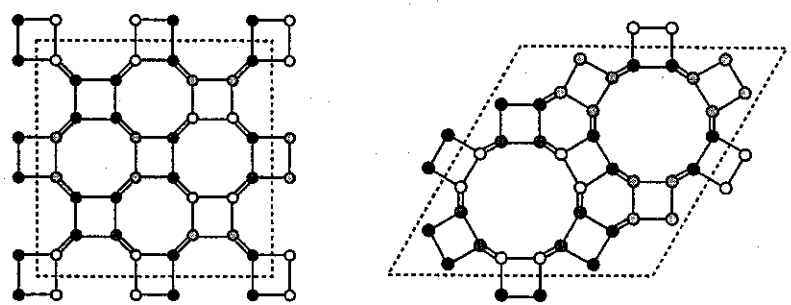

Fig. 7.15. Left: **net #109** projected on (001). Increasing depth of shading indicates elevations of z/8, 3z/8, 5z/8 and 7z/8. Right: **$AlPO_4$-31** projected on (001). Increasing depth of shading indicates elevations of z/12, 3z/12, 5z/12, 7z/12, 9z/12 and 11z/12.

Crystallographic data for these structures are:

net #109 $I4_1/amd$, $a = 5.856$, $c = 1.423$, $r = 0.656$
$4{\cdot}6_2{\cdot}6{\cdot}6{\cdot}6{\cdot}6$ in 32 *i*: $I \pm (x,y,z$; etc.), $x = 0.085$, $y = 0.080$, $z = 0.125$

$AlPO_4$-31 $R\bar{3}m$, $a = 6.800$, $c = 1.578$, $r = 0.570$
$4{\cdot}6_2{\cdot}6{\cdot}6_2{\cdot}6{\cdot}6_3$ in 36 *i*: $R \pm (x,y,z$; etc.), $x = 0.1992$, $y = 0.251$, $z = 0.25$

The nets of this and the previous section can be distinguished by numbers of topological neighbors n_k (the coordination sequence). Values for the first three are rather close to each other as might be expected for nets with the same Schläfli symbols.

k	*1*	*2*	*3*	*4*	*5*	*6*	*7*
CrB_4	4	11	24	41	62	90	122
$CaGa_2O_4$	4	11	24	41	63	91	123
net # 109	4	11	24	42	65	95	131
$AlPO_4$-31	4	11	22	37	59	85	114

7.3.5 $SrAl_2$, **cancrinite**, *and related nets with double zig-zags*

Two more ways of connecting 6^3 nets are shown in Fig. 7.16. These both give rise to uninodal nets that are of interest in crystal chemistry. The net on the left is found as the Al arrangement in $SrAl_2$, so we name it after that compound.[1] The same topology also occurs (considerably distorted from the geometry given above) as the network of bonds in α-Np.

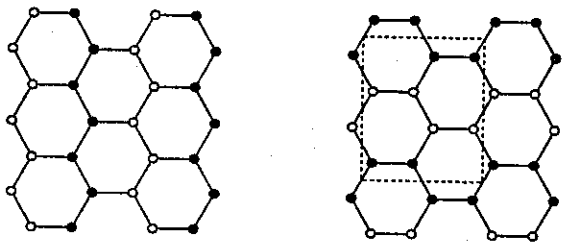

Fig. 7.16. Derivation of the $SrAl_2$ (left) and **paracelsian** (right) nets from 6^3 (compare Fig. 7.13).

A description of the $SrAl_2$ net is:

$SrAl_2$ *Imma*, $a = 3.268$, $b = 1.681$, $c = 2.631$, $r = 0.554$
4·6·4·6·6·8_2 in 8 *i*: $I \pm (\pm x,1/4,z)$, $x = 0.153$, $z = 0.103$

The structure is simply illustrated as a projection down the short axis (**b**); it is shown in this way as Fig. 7.17 (left).

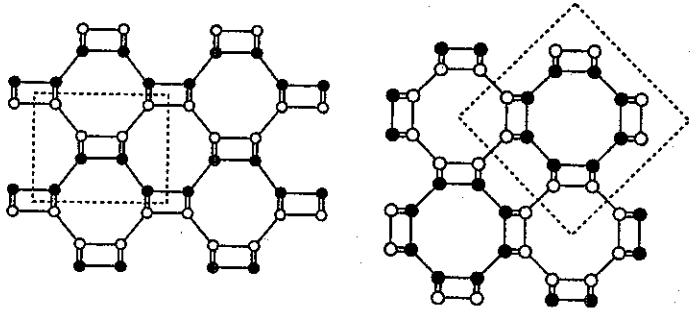

Fig 7.17. Left the $SrAl_2$ net projected on (010). **a** is horizontal on the page. Filled and empty circles are at $y = 1/4$ and 3/4 respectively. Right: **MAPO-39** projected on (001). Filled and empty circles are at $z = 0$ and 1/2 respectively. In both cases single lines are edges in the plane of the projection; double lines represent edges up and down out of the plane.

[1]The "type" compound is often taken as $CeCu_2$, structural data for which are to be found in Exercise 3.11. If you did that exercise, compare your drawing with Fig. 7.17.

Other occurrences of this net are as the (Al,Si) framework in $RbAlSiO_4$ and in the synthetic zeolite known as Li-A with stoichiometry $LiAlSiO_4{\cdot}H_2O$.

A closely related net occurs in the synthetic zeolite with (Mg,Al,P) as framework atoms known as MAPO-39. The formal description of this net is:

MAPO-39 *I4/mmm*, $a = 4.150$, $c = 1.708$, $r = 0.544$
4·6·4·6·6·8 in 16 *l*: $I \pm (\pm x,y,0\ ;\ \pm y,x,0)$, $x = 0.121$, $y = 0.291$

The relationship of this net to $SrAl_2$ should be apparent from Fig. 7.17. Both structures feature double zig-zags of vertices which make up a puckered ladder as shown schematically on the left in Fig. 7.18. The two nets differ only in the way the double zig-zags are interconnected. Note that in Fig. 7.17 the projection is along the axis of the double zig-zag (which projects as a rectangle).

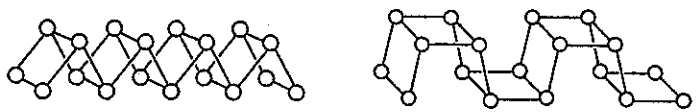

Fig. 7.18. Left: part of a double zig-zag. Right: part of a double crankshaft.

The net on the right in Fig. 7.16 occurs as the (Al,Si) framework in paracelsian and is discussed in § 7.3.6.

Another simple net containing double zig-zags occurs in the structure of cancrinite, which has ideal formula $CaNa_6Al_6Si_6O_{24}CO_3{\cdot}2H_2O$. This net is shown in projection in Fig. 7.19. Crystallographic data are:

cancrinite $P6_3/mmc$, $a = 4.000$, $c = 1.633$, $r = 0.530$
4·6·4·6·6·6 in 12 *j*: $\pm(x,y,1/4\ ;\ y,x,3/4\ ;\ \bar{y},x{-}y,1/4\ ;\ x{-}y,\bar{y},\ 3/4\ ;$
$y{-}x,\bar{x},1/4\ ;\ \bar{x},y{-}x,3/4)$, $x = 1/12$, $y = 5/12$

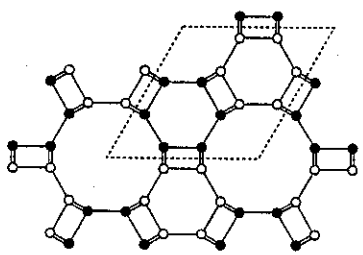

Fig. 7.19. The **cancrinite** net projected on (001). Open circles are at $z = 1/4$ and filled circles at $z = 3/4$. Double lines represent "zig-zags" viewed in projection.

Note that the unit cell consists of hexagons centered at 1/3,2/3,1/4 and 2/3,1/3,3/4 so the centers of the hexagons are stacked in a sequence *AB*... as in hexagonal close packing. We

will meet a number of related nets based on stackings of hexagons in § 7.8.5.

**7.3.6. Some nets derived from 4.8^2 with double crankshafts*

The derivation in Fig. 7.13 of some 4-connected nets from 6^3 by addition of a fourth link (either "up" to a net above or "down" to a net below), suggests that nets could be similarly derived from stacked 4.8^2 nets. Four uninodal examples, one of which we have already met, are given here. Fig. 7.20, which is to be interpreted in the same way as Figs. 7.13 and 7.16, provides a definition of their topologies. Another way of deriving nets from 4.8^2 is suggested by Fig. 7.17; we meet yet another way in our discussion of the feldspar net.[1]

A feature of the structures in this and the next section is the occurrence of rods of atoms arranged in what is known as a "double crankshaft" configuration as shown in the right-hand part of Fig. 7.18 (above).

On a double crankshaft rod, all vertices are three-connected and related 4-connected nets (discussed here) differ in the mode of cross-linking the rods, which all have their axes parallel. In projection along the axis of the double crankshaft it appears as a rectangle with two links "up" on one long edge and two links "down" on the opposite edge. (In Fig. 7.20 we have used an idealized representation in which the rectangles appear as squares—contrast Figs. 7.17 and 7.19.)

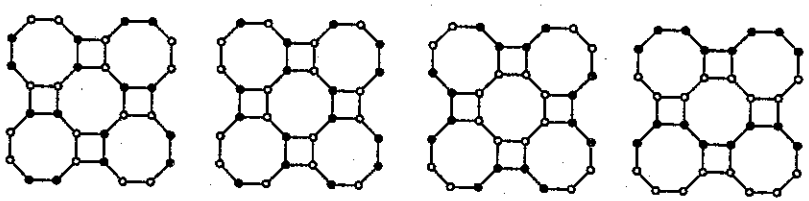

Fig 7.20. An idealized representation of 4-connected nets derived from stacked 4.8^2. From the left: **net #75**, the **paracelsian** net [compare Fig. 7.16 (right)], the **merlinoite** net, and the **gismondine** net. Fourth edges go up from open circles and down from filled circles.

The net derived second from the left in Fig. 7.20 is in fact the same as that shown on the right of Fig. 7.16; (see below). It occurs as the (Al,Si) framework in paracelsian, $BaAl_2Si_2O_8$.[2] Other compounds with the same framework are danburite, $CaB_2Si_2O_8$ and hurlbutite, $CaBe_2P_2O_8$.

A crystallographic description of the **paracelsian** net is:

paracelsian *Cmcm*, $a = 3.252$, $b = 3.118$, $c = 2.850$, $r = 0.554$
$4{\cdot}6{\cdot}4{\cdot}6{\cdot}6{\cdot}8_3$ in 16 *h*: $C \pm (\pm x,y,z\ ;\ \pm x,y,1/2{-}z)$, $x = 0.154$, $y = 0.355$, $z = 0.075$

[1]For a systematic account of the derivation of 4-connected nets from 4.8^2 see J. V. Smith, *Amer. Mineral.* **63**, 960 (1978).

[2]The celsian modification of $BaAl_2Si_2O_8$ has the feldspar structure (§ 7.3.9).

The net derived on the left in Fig. 7.20 has the same Schläfli symbol as **paracelsian**. We have not identified it in a known material so it is arbitrarily labeled **net #75**. The description is:

net #75 *I4/mcm*, $a = 4.509$, $c = 2.844$, $r = 0.553$
$4{\cdot}6{\cdot}4{\cdot}6{\cdot}6{\cdot}8_3$ in 32 *m*: $I \pm (x,y,\pm z\ ;\ \bar{y},x,\pm z\ ;\ x,\bar{y},1/2{\pm}z\ ;\ y,x,1/2{\pm}z)$,
$x = 0.101$, $y = 0.243$, $z = 0.176$

As it is very useful to be able to interpret projections of nets, in Fig. 7.21 we repeat the two projections of **paracelsian** using the coordinates given above.[1] In the first (left) the projection [on (001)] is along the axes of the double crankshafts and the second (second left) the projection [on (100)] is normal to the double crankshafts.

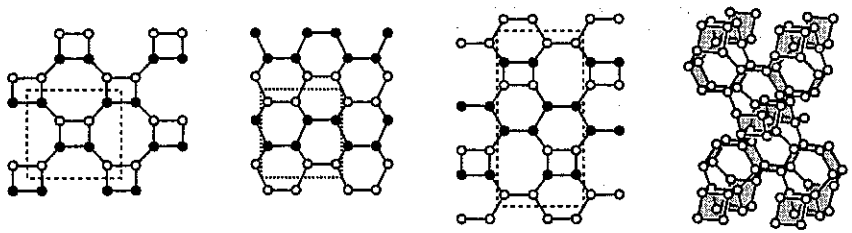

Fig. 7.21. Left: **paracelsian** projected on (001) with **b** up the page. Open circles are vertices at $z = 0.07$ and 0.43; filled circles are vertices at $z = 0.57$ and 0.93. Double crankshafts project as rectangles. Second left: the same net projected on (100) with **b** up the page. Open circles are vertices at $x = 0.15$ and 0.85; filled circles are vertices at $z = 0.35$ and 0.65. Double crankshafts project as single crankshafts of all filled or all open circles. Second right: **net #78** projected on (100) with **c** up the page. Open circles are vertices at $x = 0.17$ and 0.83; filled circles are vertices at $z = 0.33$ and 0.67. Right: the same net in clinographic projection with double crankshafts shaded.

These two projections suggest the possibility of a family of nets with double crankshafts running in two perpendicular directions. The simplest such net (and possibly the only one with one kind of vertex) is shown in the two right-hand drawings of Fig. 7.21. Data for this net (#78) are:

net #78 $I4_1/amd$, $a = 3.020$, $c = 6.210$, $r = 0.565$
$4{\cdot}6{\cdot}4{\cdot}8_2{\cdot}6{\cdot}6$ in 32 *i*: $I \pm (x,\dot{y},z$; etc.), $x = 0.165$, $y = 0.085$, $z = 0.069$

The other two nets of Fig. 7.20 are found in the structures of merlinoite and in gismondine; they both have Schläfli symbols $4{\cdot}4{\cdot}4{\cdot}8_2{\cdot}8{\cdot}8$ (note the short symbol is now $4^3.6^2.8$ in both cases) and are illustrated in Fig. 7.57 (p. 342). These nets are less dense than the other two, and alumino-silicates based on these frameworks accommodate a substantial amount of water (as typical for zeolites). Ideal formulas are merlinoite, $K_5Ca_2Al_9Si_{23}O_{64}{\cdot}24H_2O$, and gismondine, $CaAl_2Si_2O_8{\cdot}4H_2O$.

[1]Once one learns to "read" such diagrams, it will be found very easy to construct "spaghetti" models.

merlinoite *I4/mmm*, $a = 4.482$, $c = 3.312$, $r = 0.481$
4·4·4·8_2·8·8 in 32 *o*: $I \pm (x,\pm y,\pm z\ ;\ y,\pm x,\pm z)$, $x = 0.112$, $y = 0.269$, $z = 0.151$.

gismondine $I4_1/amd$, $a = 10/3$, $c = \sqrt{80}/3 = 2.981$, $r = 0.483$
4·4·4·8_2·8·8 in 16 *g*: $I \pm (\pm x,1/4\pm x,7/8)$, $x = 3/20$

Coordination sequences for nets of this and the last section, n_k, are:

k	*1*	*2*	*3*	*4*	*5*	*6*	*7*
$SrAl_2$, MAPO-39	4	10	21	36	54	78	106
paracelsian	4	10	21	37	57	81	109
#75	4	10	21	37	57	81	110
#78	4	10	21	37	58	83	111
cancrinite	4	10	20	34	54	78	104
merlinoite	4	9	18	32	49	69	93
gismondine	4	9	18	32	48	67	92

The nets are generally distinguished by numbers of neighbors, n_k, although **$SrAl_2$** and **MAPO-39** have the same sequence (but these nets are distinguished by their Schläfli symbols). Notice that **$SrAl_2$**, **paracelsian**, **net #75** and **net #78** have very similar geometrical densities (r) and also have very similar numbers of topological neighbors (n_k). The same is true for **merlinoite** and **gismondine**. Generally it is found (see § 7.5) that the geometrical density, r, and the topological density as measured by sum of n_k (over, say ten coordination shells), are rather well correlated.

7.3.7 Another net with double crankshafts:* **gmelinite

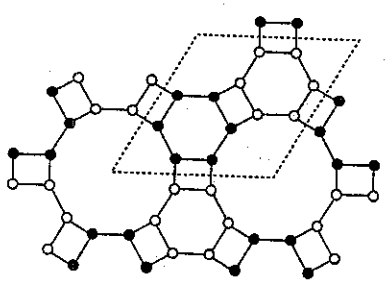

Fig. 7.22. The **gmelinite** net projected on (001). Open circles are vertices at $z = 0.09$ and 0.41 and filled circles are vertices at $z = 0.59$ and 0.91. Lines joining filled circles and lines joining open circles represent edges normal to **c** (i.e. parallel to the plane of the paper). The other lines represent edges going up and down so the rectangles represent double crankshafts in projection.

Another simple net with double crankshafts is found as the (Al,Si) framework of the natural zeolite gmelinite, which has approximate formula $Na_{2-x}Ca_xAl_2Si_4O_{12}{\cdot}6H_2O$. As shown in Fig. 7.22, the structure is now derived from the two-dimensional net 4.6.12.

Note that the structure contains hexagonal prisms centered at 1/3,2/3,1/4 and 2/3,1/3,1/4. The hexagon stacking could therefore be symbolized *AABB*... Contrast **cancrinite** (Fig. 7.19, p. 307) in which hexagons are stacked *AB*... Crystallographic data are:

gmelinite $P6_3/mmc$, $a = 4.418$, $c = 3.149$, $r = 0.451$
4·4·4·8·6·8 in 24 *l*: $\pm(x,y,z\ ;$ etc.), $x = 1/3$, $y = 0.440$, $z = 0.091$

7.3.8 Alternating "up-down" nets

There is a large class of nets derived from a stacking of 3-connected two-dimensional nets with fourth links from each vertex in the layer alternating up to a layer above or down to a layer below. For such alternation to be possible, the rings in the two-dimensional net must all be even, and for a given two-dimensional net there is only one distinct three-dimensional "up-down" net. Accordingly there are only three nets in this class with one kind of vertex; they are derived from 6^3, 4.8^2 and 4.6.12 respectively. The net derived from 6^3 is in fact **lonsdaleite** (§ 7.3.1). The net derived from 4.8^2 is found as the Zn and Sb net of $TlZn_2Sb_2$ so we name it after that compound (recall that bold face names refer to structures—in this case a net). The net derived from 4.6.12 is found in the aluminophosphate zeolite known as **$AlPO_4$-5**. Data for the last two (illustrated in Fig. 7.23) are:

$TlZn_2Sb_2$ *I4/mcm*, $a = 3.235$, $c = 2.639$, $r = 0.580$
4·6_2·6·6_3·6·6_3 in 16 *l*: $I \pm (x,x+1/2,z$; etc.), $x = 0.147$, $z = 0.190$

$AlPO_4$-5 *P6/mcc*, $a = 4.515$, $c = 2.599$, $r = 0.523$
4·6_2·6·6_3·6_2·6_3 in 24 *m*: $\pm(x,y,z$; etc.), $x = 0.455$, $y = 0.122$, $z = 0.192$

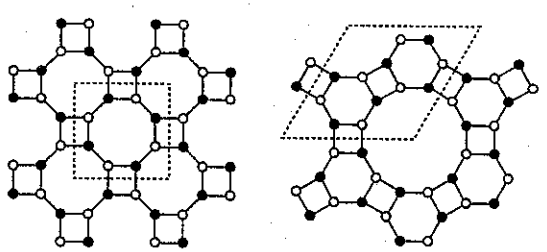

Fig 7.23. Left: projection of **$TlZn_2Sb_2$** on (001). Right: projection of **$AlPO_4$-5** on (001). In both cases open circles are vertices at $z = 0.39$ and 0.61, and filled circles are vertices at ± 0.19. Edges go down from filled circles to a layer below, and up from empty circles to one above.

A conspicuous feature of these nets is the rods of atoms that project as a square with connections up-down-up-down (UDUD).[1] This may be contrasted with the double crankshaft which projects as a rectangle with connections UUDD. A fragment of an UDUD rod is shown in Fig. 7.24.

[1]For the case of of two or more rods fused together (when the "squares" become rectangles) see § 7.11.8

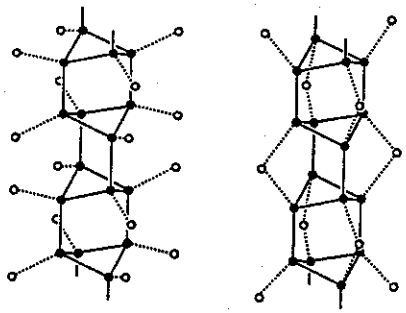

Fig. 7.24. Left: a fragment of $TlZn_2Sb_2$ (Fig. 7.23) illustrating an UDUD rod (full lines and filled circles). Right: the same rod with connecting vertices as in **scapolite**.

Several other "up-down" nets found in zeolites are described in § 7.8.4. A simple net with UDUD rods occurs in minerals of the scapolite family.[1] We include it here as it illustrates several useful points. Crystallographic data are:

scapolite *I4/mmm*, $a = 4.338$, $c = 2.294$, $r = 0.556$
$4{\cdot}5_2{\cdot}8_2{\cdot}8_2{\cdot}8_2{\cdot}8_2$ in 8 *i*: $I \pm (x,0,0\ ;\ 0,x,0)$, $x = 0.163$
$4{\cdot}8_2{\cdot}5{\cdot}5{\cdot}5{\cdot}5$ in 16 *n*: $I \pm (0,y,\pm z\ ;\ y,0,\pm z)$, $y = 0.339$, $z = 0.280$

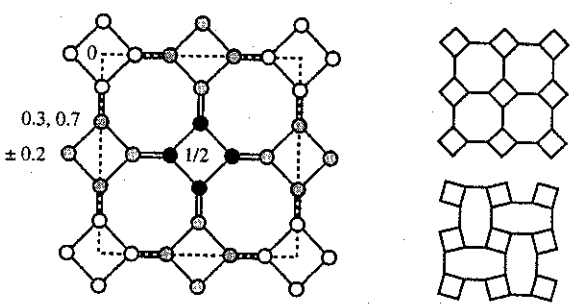

Fig. 7.25. Left: the **scapolite** net projected on (001). Numbers are elevations in units of c. Right: the 4.8^2 net in its most-symmetrical, minimum-density form (top) and partly collapsed (bottom).

The net consists of UDUD rods linked by single squares of vertices. In Fig 7.24 (right) one vertex of each such square is shown as an open circle. Fig. 7.25 shows the structure in projection on (001) and it is worth the effort it takes to read the projection. Note in particular that squares at $z = 0$ and $z = 1/2$ represent planar square groups, but that the other squares represent UDUD rods. As usual we show pairs of edges inclined up and down as

[1]Scapolite has approximate formula $Na_4Al_3Si_9O_{24}Cl$. Remember that the net is the structure of only the tetrahedrally-coordinated atoms (in this case Al and Si).

double lines.

The crystallographic data given above for **scapolite** are for the highest symmetry form and the most open structure. In fact it is common for nets of this sort to "collapse" to a denser structure, with the extent of collapse determined by the nature (and size) of the material in the cavities of the net (in scapolite this is Na and Cl, other members of the family contain CO_3 and SO_4 groups). Fig. 7.25 also shows schematically a common mode of collapse of a rod structure (such as **scapolite**) based on 4.8^2 nets.

An isolated UDUD rod of $\{T\}O_4$ tetrahedra has stoichiometry T_2O_5. In narsarsukite such rods are joined by columns of vertex-sharing $\{Ti\}O_6$ octahedra to produce a structure with composition $Na_2TiO(Si_2O_5)_2$. (For more on narsarsukite, see Exercise 7.12.14.)

7.3.9 **Feldspar** *and* **coesite**

The feldspars are a large and complex group of minerals with general formula $A(Al,Si)_4O_8$. The (Al,Si) atoms are on a 4-connected net linked by O atoms. In the structure of coesite (a high-pressure polymorph of SiO_2) the Si atoms are on a different, but closely related net. Derivation of the feldspar net from 4.8^2 is shown in Fig. 7.26. To interpret this figure, it should be noted that distorted 4.8^2 nets are packed in a two layer repeat; the net in solid lines alternating with that shown by broken lines. Filled and open circles represent respectively edges going (almost) vertically up and down from the solid-line net to the broken-line net above or below.

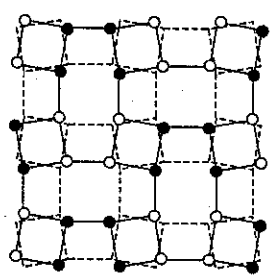

Fig. 7.26. Derivation of the feldspar net from 4.8^2. See text.

A crystallographic description of this net (as usual with unit edges and in its highest-symmetry, maximum-volume form) is:

feldspar *C2/m*, $a = 3.189$, $b = 3.951$, $c = 2.346$, $\beta = 115.4°$, $r = 0.599$
vertices in 8 *j*: $C \pm (x,\pm y,z)$
$4{\cdot}6_2{\cdot}4{\cdot}8{\cdot}6{\cdot}6_2$: $x = 0.287$, $y = 0.373$, $z = 0.376$
$4{\cdot}6{\cdot}4{\cdot}6{\cdot}8_2{\cdot}10_{10}$: $x = 0.000$, $y = 0.231$, $z = 0.213$

Note that the net of the real mineral is somewhat collapsed from the maximum volume form. Parameters more representative of real minerals (again for unit edge) are $a = 2.780$, b

= 4.202, c = 2.314, β = 116.0°, r = 0.659, vertices in 0.215, 0.381, 0.337 and 0.011, 0.176, 0.222. Ordering of silicon and aluminum in real materials also lowers the symmetry and leads in some instances to larger unit cells; the topology of the net stays the same, of course.

Why, with simple, symmetrical nets such as those of the previous sections available, did nature choose this more-complex, lower-symmetry net as the basis of the structure of the most common of all minerals on the face of the earth?

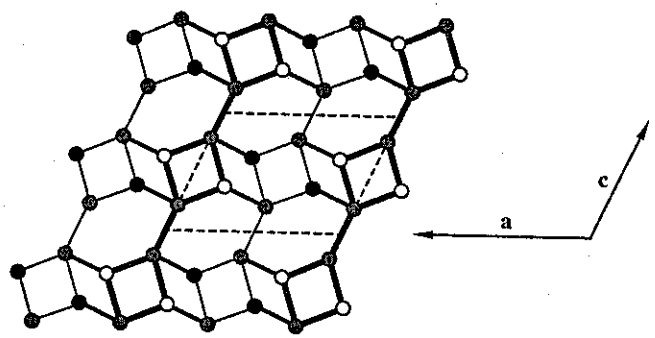

Fig 7.27. Projection of the feldspar net on (010). The points shown are a slab with $1/2 < y < 1$. A second slab lies beneath and related to the first by a mirror plane at y = 1/2. Shaded circles represent one type of vertex, open and filled circles the other. Vertices connected by heaviest lines are approximately in a plane and above the plane of those connected by the lightest lines. Additional edges go vertically up from vertices shown by open circles and down from vertices shown as filled circles.

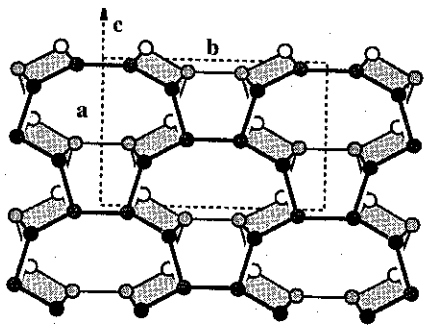

Fig. 7.28. Feldspar projected on (001) showing the twisted double crankshafts (shaded). An **ab** face of the unit cell is shown and the arrow marked **c** is the projection of that axis on the plane. Open, lightly shaded, darker shaded and filled circles are vertices at elevations approximately 0.45, 0.80, 1.32 and 1.67 above the plane. As **c** is not normal to the page successive layers are displaced up the page by the projection of **c**. The coordinates used in the drawing are for the denser of the two sets given above.

As an aid to constructing a model a projection of the **feldspar** net is shown in Fig. 7.27. The twisted double crankshafts now run horizontally across the page (parallel to **a**). In making a "spaghetti" model the best strategy is to first construct the double crankshafts, secondly link them to make the layer shown in the figure (the double crankshafts will now twist) and finally connect layers to their mirror images using the remaining unused links as shown in Fig. 7.28 in which the twisted crankshafts are seen in a projection on (001).

A related net, that is also made up of twisted double crankshafts, is that of the Si atoms in the coesite form of SiO_2 (a high-pressure polymorph; for data see Appendix 5). The net is made up of layers similar (topologically identical) to those shown for feldspar in Fig. 7.27. The linkage between layers makes the topology difficult to describe and results in rings of edges being looped as in a chain. Fig 7.29 (which should be contrasted with Fig. 7.28) shows how the layers of crankshafts are linked. Model builders should first construct double-crankshaft layers as for **feldspar**, then link them using Fig. 7.29 as a guide. Note that the middles of these linking edges are at centers of symmetry.

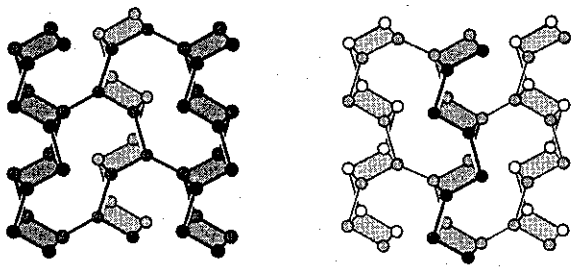

Fig. 7.29. The linkage of double-crankshaft layers in coesite shown in projection on (001). Only one double crankshaft of each layer is shown. On the left, the middle double crankshaft is connected to two higher in elevation, on the right the same (middle) double crankshaft is connected to two others of lower elevation. Vertices with the same shading have approximately the same elevation.

The coesite net contains odd (9-) rings. This means that if there are two kinds of atoms (A and B) at the vertices they cannot be arranged so that A has only B neighbors and *vice versa*. Data for a form of the coesite net are given below. Note the high density (r). Coesite is the densest known form of silica with Si in 4-coordination by oxygen.

coesite $C2/c$, a = 2.327, b = 4.152, c = 2.281, β = 120.8°, r = 0.845
vertices in 8 f: $C \pm (x,y,z\ ;\ x,\bar{y},1/2+z)$
$4{\cdot}8{\cdot}4{\cdot}9_7{\cdot}6{\cdot}8$: x = 0.157, y = 0.094, z = 0.088
$4{\cdot}6{\cdot}4{\cdot}6{\cdot}8{\cdot}9_2$: x = 0.019, y = 0.325, z = 0.041

7.3.10 Sodalite

A simple quasi-regular four-connected net that arises in many contexts is the net we call the **sodalite** net. A formal description is, for unit edge length:

sodalite $Im\bar{3}m$, $a = \sqrt{8}$, $r = 0.530$
4·4·6·6·6·6 in 12 *d*: $I \pm (1/4,0,1/2)\kappa$

We met this pattern earlier (§ 6.2) as that of the tetrahedral sites of **bcc** packing. It may also be recalled that this arrangement is that of the vertices of a space-filling by truncated octahedra (illustrated in Fig. 7.30). The centers of the truncated octahedra are on the nodes of a *bcc* lattice.

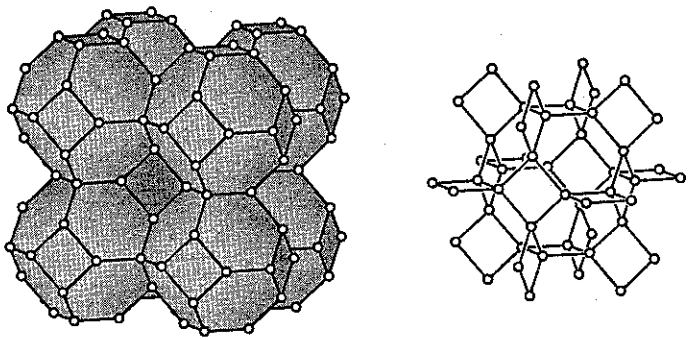

Fig. 7.30. Left: space-filling by truncated octahedra (4.6^2). Right: the edges and vertices shown as the four-connected **sodalite** net.

The net corresponds to the arrangement of the (Si,Al) atoms in the mineral sodalite[1]: $Na_4Si_3Al_3O_{12}Cl$, although in the real structure the O arrangement lowers the symmetry to $I\bar{4}3m$ (see Fig. 6.72, p. 275) and Si,Al ordering further lowers the symmetry to $P\bar{4}3n$. The positions of the vertices of the net are also those of the lattice complex W^*. The same pattern is shown as a 4-connected net in Fig. 7.30. The Schläfli symbol of the vertices is 4·4·6·6·6·6. Note that for a net derived from a packing of polyhedra each angle contains just one ring (the Schläfli symbol has no subscripts).

The number of topological neighbors is given by the very simple formula:

$$n_k = 2k^2 + 2 \qquad (7.3)$$

7.3.11 **NbO** *and* **quartz**

The positions of the Nb and O atoms in the simple cubic structure of NbO (for crystallographic data see Appendix 5) taken together are at the nodes of another quasi-regular net (Fig. 7.31). For unit edge length, the crystallographic description is:

[1]Minerals of this group are often called ultramarines. Ordering and the occurrence of incommensurate phases in sodalites such as $Ca_4Al_6O_{12}WO_4$ (CAW) and $Sr_4Al_6O_{12}MoO_4$ (SAM) are currently lively topics of investigation. Yet another sodalite composition is $Ca_4Al_6O_{13}$ (with one O atom in the cage).

NbO $Im\bar{3}m$, $a = 2$, $r = 0.75$
$6_2·6_2·6_2·6_2·8_2·8_2$ in 6 *b*: $I + (0,1/2,1/2)\kappa$

The vertices of the net correspond to the invariant lattice complex J^*.[1] They also represent the distribution of "octahedral sites" in the *bcc* structure and so the vertices are at the centers of the squares in the **sodalite** net. The Schläfli symbol of the vertices is $6_2·6_2·6_2·6_2·8_2·8_2$. Note that the edge angles are four of 90° and two of 180° and that the vertices fall on three mutually-perpendicular strings that intersect in pairs.

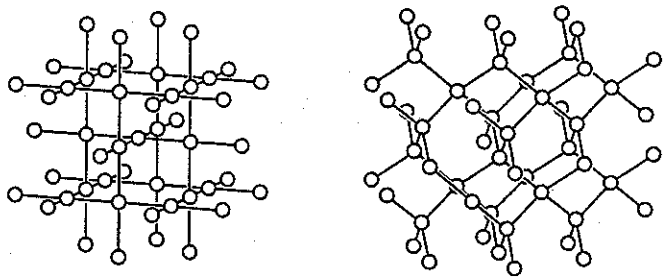

Fig. 7.31. Left: the **NbO** net. Right: the **quartz** net (c is vertical).

Another quasi-regular net, that we will see is related to the **NbO** net, is the **quartz** net. It describes the positions of the Si atoms in the quartz form of SiO_2 (the most stable form at room temperature and pressure). In the maximum volume configuration the structure is:

quartz $P6_222$, $a = \sqrt{(8/3)}$, $c = \sqrt{3}$, $r = 0.75$
$6·6·6_2·6_2·8_7·8_7$ in 3 *c*: 1/2,0,0 ; 0,1/2,2/3 ; 1/2,1/2,1/3

The net is enantiomorphic; its mirror image has symmetry $P6_422$ with coordinates 1/2,0,0 ; 0,1/2,1/3 ; 1/2,1/2,2/3. The structure (also illustrated in Fig. 7.31) again corresponds to an invariant lattice complex; the two enantiomers are labeled ^+Q and ^-Q respectively. The edges are all equivalent, so the net is quasiregular. The angles are two of 90°, two of $\cos^{-1}(-1/3) = 109.47°$ and two of $\cos^{-1}(-2/3) = 131.81°$.

The **NbO** and **quartz** nets have the same short Schläfli symbol: $6^4.8^2$ and the same density ($r = 0.75$). The relationship between them is shown in Fig. 7.32 in which a projection of the **NbO** net on (111) is compared with a projection of the **quartz** net on (001). It is to be noted that the repeat distance normal to the plane of projection is the same in the two cases, and that both nets contain the same number of vertices per unit volume (i.e. they have the same geometrical density). The main difference is that **NbO** contains three-fold spirals of two hands whereas **quartz** contains spirals of only one hand.

[1]Note that in NbO the Nb and O atoms (each 4-coordinated in a square by the other) are each on a *J* lattice complex; two such complexes separated by 1/2,1/2,1/2 combine to give J^*.

A third net is related to these two. It is of some interest because, like them, it has only three vertices in the primitive cell. The projection in Fig. 7.33 should make the family relationship clear (compare Fig. 7.32). Wells (see the Notes at the end of this chapter) calls it "net 2" so we label it **W2**. It is found as the arrangement of Ni atoms in heazlewoodite, Ni_3S_2 (for crystallographic data see Appendix 5), and is a rare example of a net containing *only* odd rings. A formal description is:

W2 $R32$, $a = 5/\sqrt{3}$, $c = \sqrt{5}$, $r = 0.558$
$3{\cdot}7{\cdot}7{\cdot}7{\cdot}7_2{\cdot}7_2$ in 9 d: $R + (x,0,0\ ;\ 0,x,0\ ;\ \bar{x},\bar{x},0)$, $x = 1/5$

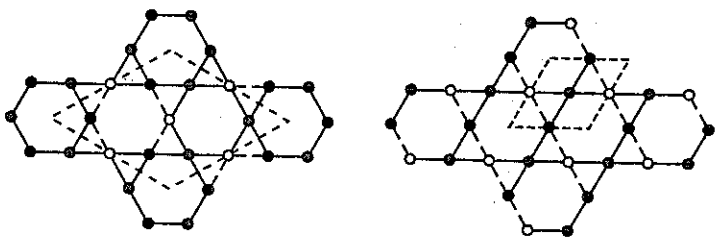

Fig. 7.32. Left: the **NbO** net projected on (111). Right: the **quartz** net projected on (001). Open, shaded and filled circles are at 0, 1/3 and 2/3 of the repeat distance normal to the plane of projection.

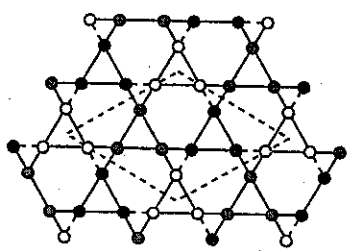

Fig. 7.33. The net **W2** drawn for comparison with Fig. 7.32

The nets differ in topological density: The values of n_k are given by:

$$\textbf{NbO} \qquad n_k = 3k^2 + 2 - (k \bmod 2) \tag{7.4}$$

$$\textbf{quartz} \qquad \begin{aligned} n_k &= 19k^2/6 + 2 && (k = 6i) \\ n_k &= [(19k^2 + 10)/6] && (2 < k \neq 6i) \end{aligned} \tag{7.5}$$

$$\textbf{W2} \qquad \begin{aligned} n_k &= 5k^2/2 && (k = 2i) \\ n_k &= 5k^2/2 + 7/2 && (k = 2i+1) \end{aligned} \tag{7.6}$$

Here i is a positive integer, and brackets indicate rounding down to an integer. $n_1 = 4$ for **W2** (as, of course, for all 4-connected nets). Topologically, **quartz** is the densest of

these nets (has most topological neighbors) and **W2** (which contains 3-rings) is topologically less dense than the other two. (See § 7.5 for a discussion of density.)

**7.3.12 More quasi-regular and/or uniform nets: γ-Si*

Three other nets of interest are described briefly here. They are all cubic and although there is only a small number of vertices in the repeat unit, they provide an interesting challenge to the model builder.

The first is found as the structure of a high-pressure polymorph of elemental silicon (for data see Appendix 5), so we call it the **γ-Si** net. Data for the idealized net are:

γ-Si $Ia\bar{3}$, $a = 2/(\sqrt{6} - \sqrt{3})$, $r = 0.739$
$6{\cdot}6_2{\cdot}6{\cdot}6_2{\cdot}6{\cdot}6_2$ in 16 c: $I \pm (x,x,x\ ;\ x,1/2{-}x,1/2{+}x)\kappa$, $x = (\sqrt{2} - 1)/4 = 0.1035$

The vertices in **γ-Si** have long Schläfli symbol $6{\cdot}6_2{\cdot}6{\cdot}6_2{\cdot}6{\cdot}6_2$ so that this is another uniform net. Note that there are two different angles: three of 97.94° and three of 118.13°.

There are several interesting features of the structure. If the value of x is increased to 1/8 = 0.125 the vertices are on the lattice complex Y^{**} which is the positions 16 b of $Ia\bar{3}d$ and corresponds to an intergrowth of the $^{+}Y^{*}$ and $^{-}Y^{*}$ lattice complex. We saw (§ 7.2) that these latter represent the two enantiomers of the Si net in $SrSi_2$. Thus **γ-Si** can be considered as derived from two inter-grown **$SrSi_2$** (3-connected) nets. The **γ-Si** and Y^{**} structures are compared in Fig. 7.34.

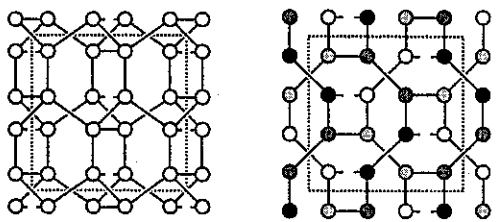

Fig. 7.34. Left: the γ-Si net projected on (001); vertices in the top layer are at approximately $z = 1.1c$ and $0.9c$ and those in the bottom layer at $0.4c$ and $0.6c$. Broken bonds go to layers above or below those shown in the figure. Right: The Y^{**} lattice complex shown as two intergrown three-connected nets ($^{\pm}Y^{*}$) projected on (001). Open circles at $c/8$, light shaded at $3c/8$, darker shaded at $5c/8$ and filled at $7c/8$.

The positions 16 c of $Ia\bar{3}$ can also be considered to be a combination of two sets of 8 a of $I2_13$: $I + (x,x,x\ ;\ x,1/2{-}x,1/2{+}x)\kappa$, with $x = u_1$ and $x = u_2$. If $u_1 + u_2 = 1/2$ the symmetry is actually still $Ia\bar{3}$. In γ-Si $u_1 = 0.104$ and $u_2 = 0.386$. If these are changed to $u_1 = 0.0$ and $u_2 = 0.25$ the structure is transformed to the body-centered cubic array (described with a cell of twice the edge length). This suggests that the material found after application of pressure may have transformed from a body-centered cubic lattice at high pressure as the pressure was released. It has been suggested that the diamond form of

carbon will transform to **γ-Si** at very high pressure (about 800 GPa).[1]

As **γ-Si** approximates the Y^{**} structure (two intergrown Y^{*} nets) it contains intergrown 3_1 and 3_2 helices of Si atoms each arranged as in $\mathbf{SrSi_2}$. For this reason the cylinder packing consisting of two interlaced $\mathbf{SrSi_2}$ packings was named the **γ-Si** packing in § 6.7.3.

Two other invariant lattice complexes are 4-connected nets. They are of less importance in crystal chemistry and are frustratingly difficult to illustrate (as our figures below attest), but we include them here for completeness. Model makers will find that they are challenging to construct but very beautiful.

S^{*} $Ia\bar{3}d$, $a = \sqrt{(32/3)}$, $r = 0.689$
$6{\cdot}6{\cdot}6_2{\cdot}6_2{\cdot}6_2{\cdot}6_2$ in 24 *d*: $I \pm (3/8,0,1/4\ ;\ 1/8,0,3/4)\kappa$

This is another uniform net. It is also quasi-regular. A feature of the structure is that there are large non-intersecting tunnels parallel to <111> arranged as in the **garnet** cylinder packing (§ 6.7.3). The projection on (111) shown in Fig. 7.35 reveals one such set of tunnels.

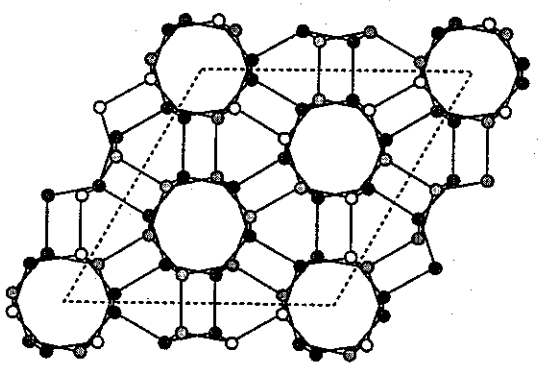

Fig. 7.35. The lattice complex S^{*} projected on (111). Points in order of increasing depth of shading are at heights (in units of la+b+cl/2) of 1/12, 3/12, 5/12, 7/12, 9/12 and 11/12.

The second invariant lattice complex is an enantiomorphous pair:

$\mathbf{HL4_3}$ $I4_132$, $a = \sqrt{(32/3)}$, $r = 0.344$
^{+}V $3{\cdot}3{\cdot}10_2{\cdot}10_2{\cdot}10_3{\cdot}10_3$ in 12 *c*: $I + (1/8,0,1/4\ ;\ 3/8,0,3/4)\kappa$
^{-}V $3{\cdot}3{\cdot}10_2{\cdot}10_2{\cdot}10_3{\cdot}10_3$ in 12 *d*: $I + (5/8,0,1/4\ ;\ 7/8,0,3/4)\kappa$

This is also a quasi-regular net. The net is very open; now two 3-rings meet at each vertex (Fig. 7.36 emphasizes this aspect of the structure) and the other rings in the structure

[1]R. Biswas *et al.*, *Phys. Rev.* **B35**, 9559 (1988).

are ten 10-rings meeting at each vertex. The structure is the third of four 4-coordinated rare sphere packings discussed by Heesch and Laves (see § 7.5.2) so we label it $\mathbf{HL4_3}$.

In much the same way as $^{+}Y^{*}$ and $^{-}Y^{*}$ can interpenetrate (Fig. 7.34) so can ^{+}V and ^{-}V to produce the lattice complex V^{*} which corresponds to the positions 24 *c* of $Ia\bar{3}d$:

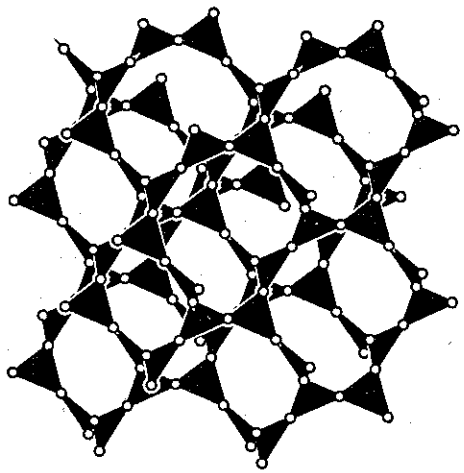

Fig. 7.36. A clinographic projection of the lattice complex ^{+}V ($\mathbf{HL4_3}$).

7.3.13 Silica (SiO_2) and water nets: **keatite** *and* **moganite**

The planet we inhabit is made largely of silicates, and its surface consists largely of water (solid and liquid) and framework silicates. Silica (SiO_2) itself is of importance in a variety of contexts, and at least twelve polymorphs have been described. Low pressure forms of silica consist of framework structures of $\{Si\}O_4$ tetrahedra sharing vertices and the 4-connected nets corresponding to some of these structures have been met already: here we discuss several others. Silica is also found as a very-high-pressure **rutile** form (with six-coordinated Si) known as stishovite. BeF_2 and GeO_2 and ternary derivatives such as $AlPO_4$ also adopt at least some of the silica structures. Note that most of the silica polymorphs have lower symmetry than the idealized net on which the structure is based.

Solid water (ice) in its low pressure forms is also based on 4-connected nets of O atoms joined by -H... bonds and the nets are the same as in some of the silica polymorphs. In higher pressure forms the structures are based on two inter-penetrating 4-connected nets.

(i) Quartz, the stable form of silica at ordinary temperature and pressure, was described in § 3.6 and the 4-connected net discussed in § 7.3.11.

(ii) At high temperature, quartz transforms to cristobalite which is based on the

diamond net (§ 7.3.1). This is the net of ice I_c which is stable at very low temperatures. Ice VII (formed at pressures above about 2 GPa = 20 kbar) consists of two inter-penetrating cristobalite nets.

(iii) Tridymite is a (possibly metastable) form of silica based on the **lonsdaleite** net. This is the net of the familiar ice (I_h) stable at atmospheric pressure below 0 °C.

(iv) Coesite is the first crystalline phase of silica obtained when quartz is subject to pressure (about 2 GPa). The net of this structure was discussed in § 7.3.9.

(v) Melanophlogite is rare naturally-occurring form of silica that is based on the net of the Type I gas hydrate net (§ 7.6).

(vi) Keatite is another rare metastable form of silica. The net (Fig. 7.37) contains two kinds of node and occurs also as the structure of γ-Ge (a form recovered from high pressure) and as the net of ice III (which is produced from ice I_h at a pressure of about 200 MPa). Data for keatite SiO_2 and γ-Ge are given in Appendix 5. The keatite cell is tetragonal ($P4_32_12$, $a = 7.46$, $c = 8.61$ Å); in the maximum volume form of the net, $r = 0.668$. The Schläfli symbols are Si(1): $5{\cdot}5{\cdot}5_2{\cdot}7_2{\cdot}8_2{\cdot}8_2$ and Si(2): $5{\cdot}7{\cdot}5{\cdot}7{\cdot}5{\cdot}7_2$.

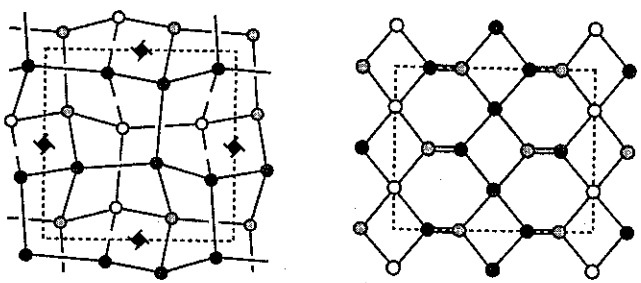

Fig. 7.37. Left: the Si atoms of keatite projected on (001). Increasing depth of shading indicated vertices at approximately $z = 0$, 1/4, 1/2, and 3/4. The positions of the 4_3 axes in the unit cell (broken lines) is indicated. Right: the **moganite** net projected on (010). **a** is horizontal across the page. Progressively darker shaded circles represent vertices at $y = 0$, 1/4, 1/2 and 3/4.

(vii) Moganite is another polymorph of SiO_2 which is reported[1] to be monoclinic (*I2/a*). Recent results suggest that moganite occurs more commonly than once supposed in fibrous forms of "quartz" known as chalcedony, agate, chert, flint, etc.[2] The idealized 4-connected net of the Si atoms is illustrated in Fig. 7.37. For unit edge crystallographic data are:

[1]G. Miehe & H. Graetsch, *Eur. J. Mineral.* **4**, 693 (1992).
[2]P. J. Heaney & J. E. Post, *Science* **255**, 441 (1992).

moganite *Ibam*, $a = 3.53$, $b = 1.61$, $c = 2.89$, $r = 0.731$
$4{\cdot}4{\cdot}6_2{\cdot}6_2{\cdot}8_2{\cdot}8_2$ in 4 *a*: $I \pm (0,0,1/4)$
$4{\cdot}8_6{\cdot}6{\cdot}6{\cdot}6{\cdot}6$ in 8 *j*: $I \pm (x,y,0\ ;\ 1/2+x,1/2-y,0)$, $x = 0.167$, $y = 0.250$

For more on **moganite** and its relationship to **quartz** see § 7.11.7. Crystallographic data for the real material are given in Appendix 5.

(viii) When molten silica is cooled, it forms a glass (amorphous silica) which is a random network of vertex-sharing $\{Si\}O_4$ tetrahedra. This is often referred to as *quartz glass* but the term "quartz" should be restricted to the crystalline polymorph. An amorphous silica is also obtained when quartz is compressed at low temperatures; amorphous ice can similarly be obtained from crystalline ice.

(ix) The structure of ice VI (stable between about 0.6 and 2 GPa at room temperature) is based on two inter-penetrating **edingtonite** nets (see § 7.8.7)

7.4 Nets and infinite polyhedra

We now expand our consideration of nets constructed from polyhedra sharing faces. They may be derived as a space filling (tiling) by finite polyhedra or considered as an infinite surface tiled with polygonal faces (infinite polyhedra). The most important of these nets are those of zeolites. The simplest such structure, the **sodalite** net, was described in § 7.3.10.

7.4.1 **Linde A**: *an infinite polyhedron* $4^2.6^2$

The first such new net is that of the zeolite known as Linde *A*:

Linde *A* $Pm\bar{3}m$, $a = 1 + \sqrt{8} = 3.828$, $r = 0.428$
$4{\cdot}6{\cdot}4{\cdot}6{\cdot}4{\cdot}8$ in 24 *k*: $(0,\pm y,\pm z\ ;\ 0,\pm z,\pm y)\kappa$, $y = 1/(4 + \sqrt{2}) = 0.1847$, $z = 2y$

In Fig. 7.38 (left) the structure is illustrated as an assembly of cubes and truncated octahedra (4.6^2) sharing square faces. Considered as a 4-connected *net* it has the Schläfli symbol $4{\cdot}6{\cdot}4{\cdot}6{\cdot}4{\cdot}8$ given above. However we can also consider this structure as an *infinite polyhedron*; at each vertex two squares and two hexagons meet, and the interior of this polyhedron is the space occupied by the cubes and truncated octahedra. Considered as a *polyhedron* the Schläfli symbol is $4^2.6^2$. Note the distinction between the net description and the polyhedron description—in the former we count rings at six angles at the vertices, in the latter we count (in cyclic order) only polygons on the surface of the polyhedron.

The empty space in the above structure consists of truncated cuboctahedra (4.6.8) sharing octagonal faces as shown in Fig. 7.38 (right). This is likewise an infinite polyhedron $4^2.6^2$ and the "interior" of the polyhedron is the space occupied by the truncated cuboctahedra.

It may be seen that we have two infinite polyhedra, each of which fills the empty space of the other. Such pairs of infinite polyhedra are termed *complementary*. Taken together they represent an example of space filling (tiling) by regular and/or Archimedean polyhedra. In each case the same polygons are on the surfaces of both polyhedra.

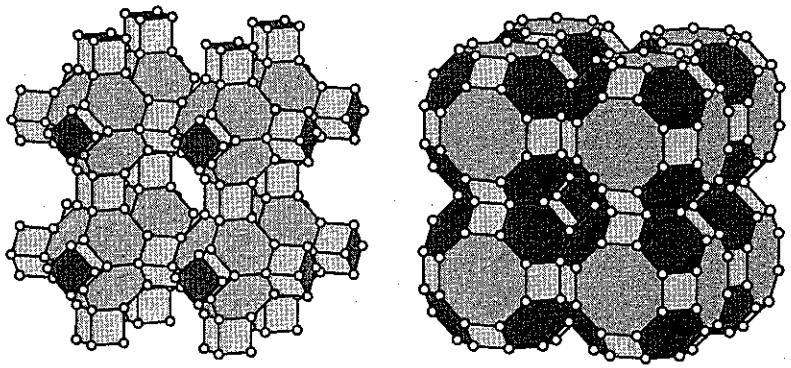

Fig. 7.38. The Linde *A* structure. Left: as an assembly of cubes and truncated octahedra. Right: as an assembly of truncated cuboctahedra.

For such an apparently complicated structure the number of topological neighbors is given by a very simple formula (brackets indicate rounding down to an integer):

$$n_k = [(8k^2 + 13)/5] \qquad (7.7a)$$

7.4.2 Zeolite **rho**: *infinite polyhedra* $4^3.6$ *and* 4.8.4.8

The structure of the zeolite known as **rho** gives rise to another 4-connected net that can also be described as a space-filling by Archimedean polyhedra as shown in Fig. 7.39. Data for unit edge are:

rho $Im\bar{3}m$, $a = 2 + \sqrt{8} = 4.828$, $r = 0.426$
4·4·4·6·8·8 in 48 *i*: $I + (1/4,\pm x,1/2\pm x\ ;\ 1/4,1/2\pm x,\pm x)\kappa$, $x = (\sqrt{2} - 1)/4 = 0.1035$

This structure may be considered as constructed of truncated cuboctahedra (4.6.8) and octagonal prisms ($4^2.8$) sharing octagonal faces.[1] From this point of view it is an infinite polyhedron $4^3.6$. The empty space is an identical infinite polyhedron, so it is its own complement. The combination of the infinite polyhedron and its complement corresponds a space-filling by truncated cuboctahedra and octagonal prisms.

[1]Compare Fig. 7.38 in which truncated cuboctahedra share octagonal faces without the intervening octagonal prisms.

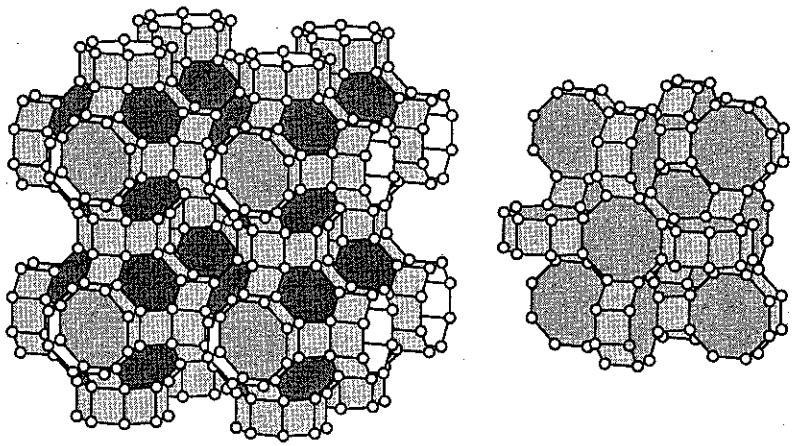

Fig. 7.39. The structure of zeolite **rho**. Left: as a packing of truncated cuboctahedra (4.6.8) and octagonal prisms ($4^2.8$) forming the polyhedron $4^3.6$. Right: as the polyhedron 4.8.4.8 formed from fused octagonal prisms.

Alternatively the same set of vertices may be described as derived from an assembly of octagonal prisms sharing square faces as also shown in Fig. 7.39. In this description, the structure is an infinite polyhedron 4.8.4.8. The complement of this infinite polyhedron is the one (not shown) derived from truncated cuboctahedra sharing their hexagonal faces.

Rho and **Linde A** have very similar densities, *r*. Remarkably, equation 7.7a (p. 324) holds for the coordination sequences of both structures.

7.4.3 Zeolite **ZK-5** *and an infinite polyhedron* $4^3.8$

We have already met two structures involving the truncated cuboctahedron (4.6.8). One description of the Linde *A* structure involved linking them by sharing octagonal faces (note that they also are linked by cubes). Similarly the zeolite rho structure was obtained by linking truncated cuboctahedra by octagonal prisms attached to the octagonal faces. A third possibility involves linkage by hexagonal prisms attached to the hexagonal faces. This produces a structure (Fig. 7.40) that is the framework of the zeolite known as ZK-5 and is an infinite polyhedron $4^3.8$. Considered as a 4-connected net the Schläfli symbol is 4·4·4·8·6·8. The crystallographic description is:

ZK-5 $Im\bar{3}m$, $a = 2/\sqrt{3} + \sqrt{8} + 2 = 5.983$, $r = 0.448$
4·4·4·8·6·8 in 96 *l*: $I \pm (x,\pm y,\pm z\ ;\ y,\pm x,\pm z)\kappa$,
$x = 1/2a = 0.0836$, $y = 1/4 - x/\sqrt{3} = 0.2018$, $z = 2y - x = 0.3199$

The *CS* is given by (cf. Eq. 7.7a):

$$n_k = [(12k^2 + 16)/7] \qquad (7.7b)$$

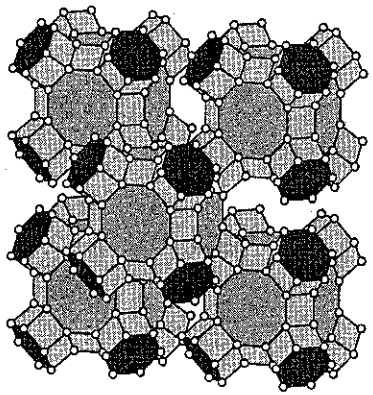

Fig. 7.40. Part of the zeolite **ZK-5** structure.

7.4.4 **Faujasite**: *a second infinite polyhedron* $4^3.6$

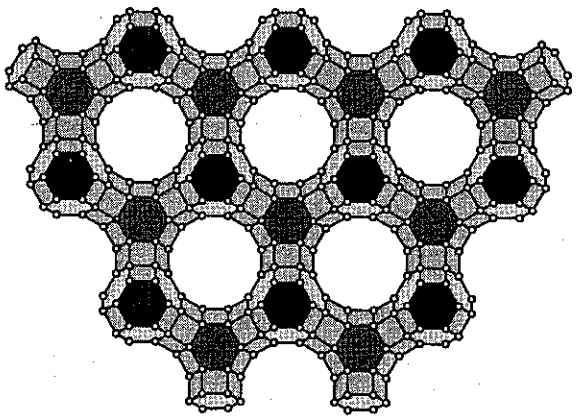

Fig. 7.41. A fragment of the faujasite structure projected on (111). The black hexagons are hexagonal prisms seen in projection and sharing a hexagonal face with a truncated octahedron underneath. The shaded regular hexagons are top faces of truncated octahedra connected to hexagonal prisms on the bottom face.

Another net that may be derived from a packing of polyhedra is that of the natural zeolite faujasite. This is obtained by fusing hexagonal prisms on four non-adjacent faces of a truncated octahedron (4.6^2). Adding four more truncated octahedra to the other hexagonal faces of the prisms results in a tetrahedral arrangement of the four truncated octahedra about

the first one. Continuing so that a **diamond** array of truncated octahedra is obtained produces the **faujasite** net, which is an infinite polyhedron $4^3.6$. A polytype is obtained if the truncated cuboctahedra are connected as in **lonsdaleite** (rather than as in **diamond**); it should be clear that an infinite number of other polytypes is possible. Fig. 7.41 shows part of one layer of the structure. Considered as 4-connected nets all vertices in these structures have symbol 4·4·4·6·6·12.

Crystallographic data for the cubic (**c-**) and hexagonal (**h-**) **faujasite** nets are:

c-faujasite $Fd\bar{3}m$, $a = 20/(\sqrt{18} - \sqrt{3}) = 7.966$, $r = 0.380$
4·4·4·6·6·12 in 192 *i*: $F \pm (x,y,z\ ;\ y,x,z\ ;\ x,1/4-y,1/4-z\ ;\ x,1/4-z,1/4-y\ ;$
$y,1/4-z,1/4-x\ ;\ y,1/4-x,1/4-z\ ;\ z,1/4-x,1/4-y\ ;\ z,1/4-y,1/4-x)\kappa$,
$x = (\sqrt{6} - 1)/40 = 0.0362$, $y = 1/8$, $z = 3/8 - 2x = 0.3025$

h-faujasite $P6_3/mmc$, $a = 5.633$, $c = 9.199$, $r = 0.380$
all vertices 4·4·4·6·6·12 in 24 *l*: $\pm(x,y,z$; etc.)
vertex 1: $x,y,z = 0.371, 0.097, 0.0181$; vertex 2: $x,y,z = 0.156, 0.489, 0.0706$
vertex 3: $x,y,z = 0.430, 0.037, 0.1069$; vertex 4: $x,y,z = 0.489, 0.156, 0.1957$

**7.4.5 An open structure, W^*8 and a related zeolite*

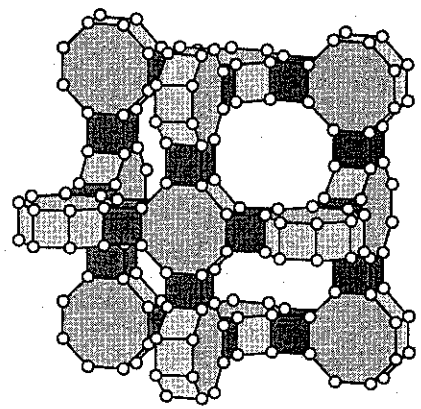

Fig. 7.42. Part of a rare net 4·4·4·8·4·12 (W^*8) shown as an infinite polyhedron $4^3.8$.

If cubes are inserted between the square faces common to the octagonal prisms in Fig. 7.39 (right), a very open 4-connected net 4·4·4·8·4·12 results (Fig. 7.42). An alternative description is as an infinite polyhedron $4^3.8$ (cf. the ZK-5 polyhedron, p. 325). For reasons to become apparent (§ 7.5.2) we label this net W^*8.

Crystallographic data for the W^*8 structure are (see also p. 373):

W^*8 $Im\bar{3}m$, $a = 4+\sqrt{8} = 6.828$, $r = 0.302$
4·4·4·8·4·12 in 96 *l*: $I \pm (x,\pm y,\pm z\ ;\ y,\pm x,\pm z)\kappa$, $2ax = 1$, $2ay = 3 + \sqrt{2}$, $2az = 3 + \sqrt{8}$

The density corresponds to a silicate with framework density FD = 10.5 tetrahedral atoms per 1000 Å^3. We do not know of a zeolite based on this framework; the most open known structures based on 4-connected nets have $FD \approx 12.5$. The 12-rings in W^*8 are not planar; they have angles of 135° (compare 150° for plane dodecagons). The structure also contains 24-rings.

A closely related structure occurs in the synthetic zeolite known as CoAPO-50 which has a framework with composition $Co_3Al_5P_8O_{32}$. The structure (Fig. 7.43) contains cubes connected by squares forming hexagonal layers containing 12-rings. The layers are joined by edges connecting opposite vertices of the cubes. Crystallographic data for the ideal form of this structure (which has a density close to that of **faujasite**) are:

CoAPO-50 $P\bar{3}1m$, a = 4.1815, c = 2.7321 r = 0.387
4·8·4·8·4·8 in 4 h: $\pm(1/3,2/3,\pm z)$, z = 0.1830
4·4·4·8·4·12 in 12 l: $\pm(x,y,z\ ;\ \bar{y},x{-}y,z\ ;\ y{-}x,\bar{x},z\ ;\ y,x,z\ ;\ x{-}y,\bar{y},z\ ;\ \bar{x},y{-}x,z)$,
x = 0.1381, y = 2/3, z = 0.3943

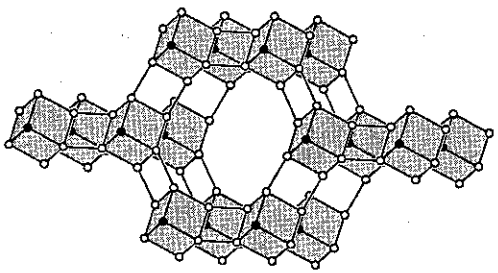

Fig. 7.43. The **CoAPO-50** net viewed almost down **c**.

A related net is that of **MAPSO-46** which is left as an exercise (7.12.12).

*7.5 Rare and dense 4-connected nets

In the Chapter 6 we discussed sphere packings with particular attention to the densest packings of equivalent spheres. It is natural to ask also what is the rarest (least dense) packing of equivalent spheres. If we require the sphere packing to be *stable*, i.e. each sphere to be in contact with at least four others with points of contact not all on the same hemisphere, we must consider 4-coordinated sphere packings, or what is equivalent, 4-connected nets with equal edges.

We remind the reader that the density, expressed as vertices per unit volume, we call the *geometric* density. In the context of nets, we consider one to be *topologically* dense if it has a large number of kth neighbors (obviously, all 4-connected nets have four first neighbors). As a measure of density in this respect, we arbitrarily use the cumulative sum of the numbers of topological neighbors, n_k, for the first ten coordination shells (i.e. k = 1 to 10) as a measure of the *topological* density. Appendix 3 elaborates on this topic.

The catalytic activity of zeolites is intimately bound up with the sizes of the rings in the structure, and considerable discussion has focused on topics such as the connection between ring size and density (in both senses). The same topic is also of interest in connection with glasses; for these a direct measure of ring sizes is generally unavailable, but can possibly be inferred from the density.

*7.5.1 Two dense nets

We consider here a second net (the first is **diamond**) with only two vertices in the repeat unit and a fourth net (the other three were described in § 7.3.11) with only three vertices in the repeat unit.

To derive the first new net we systematically remove one third of the edges of the 6-connected net of the primitive cubic lattice. The way that it is done is illustrated on the left in Fig. 7. 44. The arrangement of the vertices is cubic, but if the edges are considered, the symmetry is tetragonal: $P4_2/mmc$ a = 1, c = 2 with vertices in 2 a: 0,0,0 ; 0,0,1/2. The net can be distorted so that each vertex has only four (instead of six) geometrical nearest neighbors as suggested in the center of the figure. The symmetry is now $I4_1/acd$ and vertices are in 16 e: $I \pm (x,0,1/4\ ;\ x,1/2,3/4\ ;\ 1/4,1/4{-}x,0\ ;\ 1/4,3/4{-}x,0)$. For unit edge length and the next nearest distance as large as possible ($\sqrt{5}/2$), a = 2, $c = \sqrt{14}$ and x = 1/8 (r = 1.069). Note that distortion slightly increases the geometrical density.

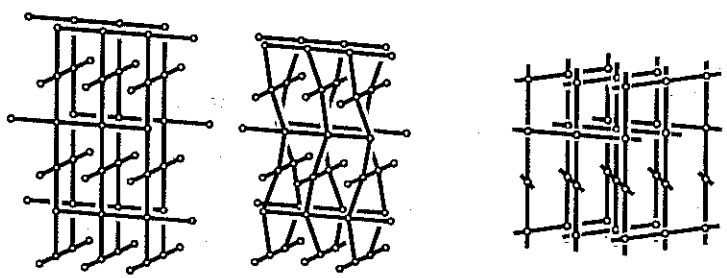

Fig 7.44. Left: the **$CdSO_4$** net derived from a primitive cubic array. Center: the same net distorted so that each vertex has only four geometric nearest neighbors. Right: a dense net with three vertices in the repeat unit.

This net is found as that of Cd,S (joined by -O-) in $CdSO_4$ ($HgSO_4$ is isostructural) hence the name, **$CdSO_4$** net. The short symbol for the vertices is $6^5.8$. It is interesting that one of the angles is not contained on any ring, as all circuits containing that angle have shortcuts (cf. § 7.1.1). We use ∞ to symbolize such an angle and the long Schläfli symbol becomes $6{\cdot}6{\cdot}6{\cdot}6{\cdot}6_2{\cdot}\infty$. It is very dense in the topological sense; the numbers of neighbors are:

$$n_1 = 4,\ n_2 = 12,\ n_k = 4k^2 - 6\ (k > 2) \qquad (7.8)$$

Our second dense net (Fig. 7.44, right) is derived analogously by deleting one half of the edges corresponding to nearest neighbor distances in a primitive hexagonal lattice. Taking into account the edges the symmetry is $P6_222$. Unlike the previous one, this net does not appear to be realizable with shortest distances corresponding only to equal edges. It does, however, have some interesting properties that merit mention. Like the previous net, one angle is not contained in a ring and the long symbol is $7_2{\cdot}\infty{\cdot}7_3{\cdot}7_3{\cdot}7_3{\cdot}7_3$ (short symbol $7^5.9$). It is the only 4-connected net that has been described that does not have at least one 6- or smaller ring. It also has the largest number of topological neighbors of any known 4-connected net, so we call it **dense** net; the numbers of neighbors are given by:

k	1	2	3	4	5	6	>6
n_k	4	12	36	72	122	188	$6k^2-30$

(7.9)

**7.5.2 Rare sphere packings*

This topic was considered many years ago by Heesch and Laves who found what was long considered to be the rarest (least dense) stable sphere packing. This structure is derived by replacing the vertices of the diamond net by groups of four spheres in contact (so that their centers form a regular tetrahedron). The tetrahedral groups are arranged so that they make contact along the diamond structure edges. We name this structure **HL4$_4$** or *D*4 (because the vertices of the *D* lattice complex are replaced by groups of four); see below for a crystallographic description.

A fragment of the structure is shown in Fig. 7.45. In the figure shaded tetrahedra replace vertices of the diamond net.

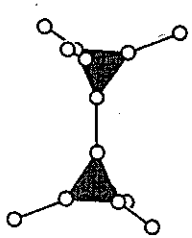

Fig. 7.45. Illustrating how **HL4$_4$** is obtained by decorating the vertices of **diamond**.

We call this process of replacing a vertex of a 4-connected net with a tetrahedral group of vertices *decorating*. It turns out that at least four other nets can be decorated in this way to give new uninodal nets. They are derived from the lattice complexes ^+Q (quartz), S^*, W^* (sodalite) and ^+V. We label them $^+Q4$, S^*4, W^*4 and $^+V4$. Here are their crystallographic data in abbreviated form:

HL4$_4$ (*D*4) $Fd\bar{3}m$, $a = \sqrt{8} + 4/\sqrt{3} = 5.1378$, $r = 0.236$ ($\rho = 0.1235$)
$3{\cdot}12_2{\cdot}3{\cdot}12_2{\cdot}3{\cdot}12_2$ in 32 *e*: $F \pm (x,x,x\,;\, x,1/4{-}x,1/4{-}x)\kappa$, $x = 1/(8+\sqrt{96}) = 0.0562$

$^+Q4$ $P6_222$, $a = 3.550$, $c = 3.885$, $r = 0.283$
$3{\cdot}12{\cdot}3{\cdot}12_2{\cdot}3{\cdot}12_7$ in 12 *k*, $x = 0.458$, $y = 0.115$, $z = 0.091$

S^*4 $Ia\bar{3}d$, $a = 7.168$, $r = 0.261$
$3{\cdot}12{\cdot}3{\cdot}12_2{\cdot}3{\cdot}12_2$ in 96 *h*, $x = 0.065$, $y = 0.224$, $z = 0.424$

W^*4 $Im\bar{3}m$, $a = 2 + 3\sqrt{2} = 6.2426$, $r = 0.197$ ($\rho = 0.1033$)
$3{\cdot}8{\cdot}3{\cdot}12{\cdot}3{\cdot}12$ in 48 *j*: $I \pm (0,y,\pm z\,;\, 0,z,\pm y)\kappa$,
$y = (1/2 + \sqrt{2})/a = 0.3066$, $z = (1/2 + 3/\sqrt{2})/a = 0.4199$

$^+V4$ $I4_132$, $a = 4 + \sqrt{8} = 6.8284$, $r = 0.151$ ($\rho = 0.0789$)
$3{\cdot}6{\cdot}3{\cdot}20_2{\cdot}3{\cdot}20_3$ in 48 *i*, $x = y = \sqrt{2}/8 = 0.1768$, $z = 0$

The last of these is the rarest, but does not correspond to a stable sphere packing as the four contacts of spheres are all on the same hemisphere. The others, and *D*4, are stable sphere packings. W^*4 is illustrated in Fig. 7.46 which shows how it is derived by decorating the **sodalite** net. It is possibly the rarest stable sphere packing. The density (fraction of space filled by spheres in contact is $8\pi/(2+3\sqrt{2})^3 = 0.1033$ (compare with the density of $\pi/\sqrt{18} = 0.7404$ for closest packing).

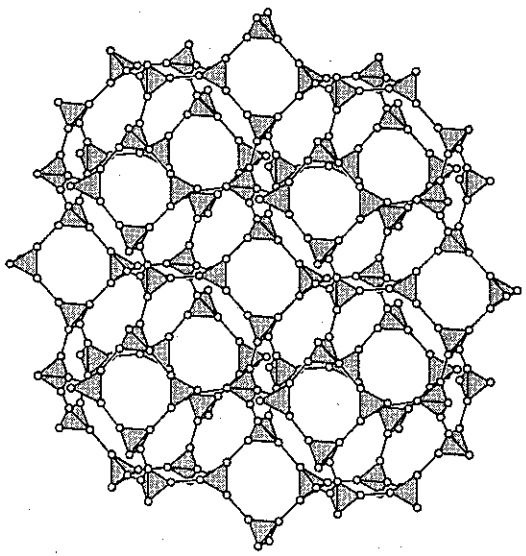

Fig. 7.46. The rare (low density) sphere-packing net W^*4 obtained by decorating the sodalite net with tetrahedral groups (shaded).

It is worth noting the apparently paradoxical fact that the most open nets are characterized by having a large number of small rings. The rare nets listed above all have

three 3-rings or four 4-rings in their symbols (they also have large rings as a consequence). On the other hand dense nets generally have a small number of 3- or 4-rings, often shortest rings of 6 (7 in the case of the **dense** net).

It is interesting that density (or rarity) in the geometrical sense is correlated with density in the topological sense. In Table 7.1 we list (for maximum volume form) the number of vertices per unit volume, r, for some mostly dense or rare nets. Also listed is c_{10}, the cumulative number of topological neighbors out to tenth neighbors. The net 4·4·4·8·4·12 (W^*8) was described in § 7.4.5. It can be derived by replacing the vertices of the sodalite (W^*) net by cubes of vertices (the centers of the cubes are on a **sodalite** net). It is possibly the rarest uninodal net that does not contain 3-rings.

Note that if the restriction to uninodal nets is lifted, nets (but not *stable* sphere packings) can be constructed of arbitrarily low density by repeating the process of decoration.[1]

Table 7.1. Some dense and rare nets compared

net	*Schläfli symbol*	r	c_{10}
dense	$7_2{\cdot}\infty{\cdot}7_3{\cdot}7_3{\cdot}7_3{\cdot}7_3$	1.155	2078
$CdSO_4$	$6{\cdot}6{\cdot}6{\cdot}6{\cdot}6_2{\cdot}\infty$	1.000	1488
coesite	$4{\cdot}6{\cdot}4{\cdot}6{\cdot}8{\cdot}9_2$	0.845	1324
	$4{\cdot}8{\cdot}4{\cdot}9_7{\cdot}6{\cdot}8$	0.845	1321
quartz	$6{\cdot}6{\cdot}6_2{\cdot}6_2{\cdot}8_7{\cdot}8_7$	0.750	1230
NbO	$6_2{\cdot}6_2{\cdot}6_2{\cdot}6_2{\cdot}8_2{\cdot}8_2$	0.750	1186
diamond	$6_2{\cdot}6_2{\cdot}6_2{\cdot}6_2{\cdot}6_2{\cdot}6_2$	0.650	980
sodalite	$4{\cdot}4{\cdot}6{\cdot}6{\cdot}6{\cdot}6$	0.530	790
W^*8	$4{\cdot}4{\cdot}4{\cdot}8{\cdot}4{\cdot}12$	0.302	453
$D4 = \mathbf{HL4_4}$	$3{\cdot}12_2{\cdot}3{\cdot}12_2{\cdot}3{\cdot}12_2$	0.236	496
W^*4	$3{\cdot}8{\cdot}3{\cdot}12{\cdot}3{\cdot}12$	0.197	409
$^+V4$	$3{\cdot}6{\cdot}3{\cdot}20_2{\cdot}3{\cdot}20_2$	0.151	350

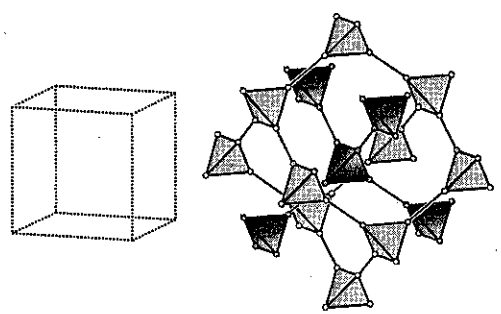

Fig. 7.47. The two inter-penetrating $D4$ nets (light and darker shaded) in $D4^*$.

The $D4$ (**$HL4_4$**) net (among others) can be intergrown with itself in a way such that the shortest distance between vertices of the two nets is greater than the edge length (in much the same way as $^+Y^*$ and $^-Y^*$ intergrow to produce Y^{**}, see § 7.3.12). The two intergrown $D4$ nets are called $D4^*$. The unit cell edge is now only half that the original *fcc* cell and a lattice vector translates from a vertex on one $D4$ net to an identical vertex on the other net (see Fig. 7.47).[1] The structure of $LiCo(CO)_4$ is based on this principle with $\{Li\}O_4$ and $\{Co\}C_4$ tetrahedra joined by C-O bonds. $Zn(CN)_2 = Zn(1)Zn(2)(CN)_4$ is isostructural. In the structure of ZnI_2 there are tetrahedral ZnI_4 groups joined by common corners to form a supertetrahedron (Fig. 5.18, p. 150) and the Zn arrangement is topologically the same. The Pb arrangement in NaPb is similar. (Data for these compounds are given in Appendix 5.)

$D4^*$ $\quad Pn\bar{3}m$, $a = \sqrt{2} + 2/\sqrt{3} = 2.5689$
vertice in 8 e: $\pm(x,x,x\ ;\ 1/2{+}x,1/2{+}x,\bar{x})\kappa$, $x = 1/(4 + \sqrt{24}) = 0.1124$

7.6 Clathrate hydrates, foam, and grains

Imagine a foam of equal-sized bubbles. The surface of the bubbles will form space-filling polyhedra with edges and faces curved so as to minimize their surface area. Three faces meet at an edge with dihedral angle 120° and four edges meet at a vertex with angles of 109.47°, so the vertices and edges will form a 4-connected net. The structures can also be considered as packings of polyhedra with 4-, 5- and 6-gon faces. As discussed by Kelvin over a hundred years ago, the simplest such net will be **sodalite** which, as we have seen (p. 315), is based on a space-filling by truncated octahedra.

Similar arrangements are found in a number of different contexts such as the crystallites of a fine-grained metal or ceramic and aggregates of biological cells. The crystal structures of clathrate hydrates are also based on these principles, for example the hydrogen-bonded framework of O atoms in $HPF_6{\cdot}6H_2O$ is **sodalite**. Framework silicates with structures based on these nets are known as *clathrasils*.

It is common in this context to use symbols for polyhedra that specify the number and types of faces. Specifically a symbol $[M^m.N^n....]$ refers to a polyhedron with m faces that are M-gons, n faces that are N gons, etc. Thus the space-filling truncated octahedron is a 14-hedron with six square faces and eight hexagonal and has symbol $[4^6.6^8]$. For polyhedra with three edges at every vertex the number of vertices is $(mM + nN + ...)/3$.

Interesting related space-filling polyhedra were discovered by Williams.[2] Converting two square faces and two hexagonal faces of $[4^6.6^8]$ into four pentagons will produce a polyhedron $[4^4.5^4.6^6]$ with symmetry $mm2$ that has four quadrangular, four pentagonal and six hexagonal faces as shown in Fig. 7.48. This polyhedron (with slightly curved edges) will fill space to produce the first Williams structure. Although there is just one kind of polyhedron, there are now four kinds of vertex.

Crystallographic data for the structure are:

[1]M. O'Keeffe & S. T. Hyde, *Zeits. Kristallogr.* (1996).

[1]Note that two intergrown D (**diamond**) nets are just **bcc** and again the unit cell for the intergrowth has half the edge of the original.

[2]R. E. Williams, *Science* **161**, 276 (1968).

Williams 1 $P4_2/ncm$, $a = 2.302$, $c = 7.909$, $r = 0.573$
4·4·6·6·6·6 in 4 *a*: ±(3/4,1/4,0 ; 3/4,1/4,1/2)
5·5·5·5·6·6 in 4*b*: ±(3/4,1/4,3/4 ; 1/4,3/4,3/4)
vertices in 8 *i*: ±(*x*,*x*,*z* ; 1/2–*x*,*x*,1/2+*z* ; *x*,1/2–*x*,1/2+*z* ; 1/2–*x*,1/2–*x*,*z*)
4·4·6·6·6·6, $x = 0.096$, $z = 0.0618$; 4·5·5·6·5·6, $x = 0.096$, $z = 0.1882$

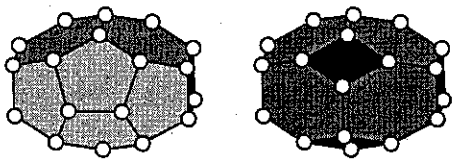

Fig. 7.48. The *mm*2 14-hedron in a space-filling configuration. The two aspects shown are related by rotation by 180° about a horizontal axis.

There is a second polyhedron with the same symbol $[4^4.5^4.6^6]$, now with symmetry 222, that also fills space. It is found in the structure of $BaCu_2P_4$ in which the Cu and P atoms form a 4-connected net (the coordinations are $\{Cu\}P_4$ and $\{P\}Cu_2P_2$). Crystallographic data for the net with unit edge are given below.

$BaCu_2P_4$ *Fddd*, $a = 2.334$, $b = 8.207$, $c = 4.488$, $r = 0.558$
4·4·5·6·6·6 in 16 *f*: *F* ± (1/8,*y*,1/8 ; 1/8,1/4–*y*,5/8), $y = 0.5065$
4·5·5·6·6·6 in 32*h*: *F* ± (*x*,*y*,*z* ; 3/4–*x*,3/4–*y*,*z* ; 3/4–*x*,*y*,3/4–*z* ; *x*,3/4–*y*,3/4–*z*),
$x = 0.195$, $y = 0.1826$, $z = 0.8145$

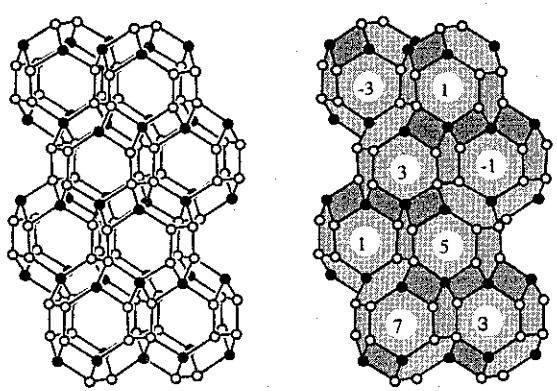

Fig. 7.49. The net of Cu (filled circles) and P in $BaCu_2P_4$ projected on (100). On the left as a 4-connected net and on the right as a packing of polyhedra. In the latter, the numbers are the *x* coordinates of the centroids of the polyhedra (Ba positions) in multiples of 1/8.

The structure (Fig. 7.49) contains equal numbers of both enantiomorphs of the polyhedron. Another feature of the structure is that it contains rods of $\{Cu\}P_4$ tetrahedra sharing opposite edges that run alternately along [101] and [10$\bar{1}$] and connected by P-P bonds. Ba atoms are at the centroids of the polyhedra (for crystallographic data see Appendix 5).

Continuing the process of converting squares + hexagons to pentagons will produce the second Williams space filling polyhedron $[4^2.5^8.6^4]$ with two square, eight pentagonal and four hexagonal faces. The structure of the polyhedron packing is now rather simple (Fig. 7.50):

Williams 2 $P4_2/mnm$, $a = 2.325$, $c = 3.880$, $r = 0.572$
5·5·5·5·6·6 in 4 *d*: ±(0,1/2,1/4 ; 1/2,0,1/4)
4·5·5·6·5·6 in 8 *j*: ±(*x*,*x*,±*z* ; 1/2+*x*,1/2–*x*,1/2±*z*), $x = 0.152$, $z = 0.129$

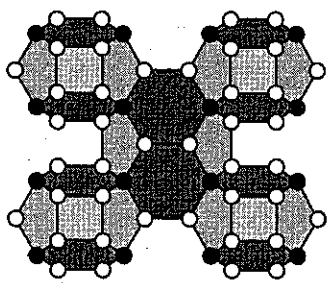

Fig 7.50. The $P4_2/mnm$ space filling by polyhedra shown projected on (110). Filled circles are the 5·5·5·5·6·6 vertices (in 4 *d*).

Finishing the process of eliminating squares produces a polyhedron $[5^{12}.6^2]$ with twelve pentagonal faces and two hexagonal faces.[1] This polyhedron does not fill space but the structure of the hydrogen-bonded framework of the cubic chlorine hydrate (of approximate composition $2Cl_2.15H_2O$) is made of a packing of pentagonal dodecahedra $[5^{12}]$ and these 14-hedra $[5^{12}.6^2]$ in the ratio 1:3 (Fig. 7.51). This is sometimes known as the type I hydrate structure. The same framework occurs in the naturally-occurring (impure) form of silica known as melanophlogite. The same structure is also found in alkali silicides and germanides typified by Na_4Si_{23} in which Si atoms are at the vertices and Na atoms center the larger polyhedra. A stereo view of the net is in Fig. 7.89 (§ 7.11.8).

The structure of the hydrates of a number of molecules such as $CHCl_3$ contains dodecahedra again and also 16-hedra $[5^{12}.6^4]$ packed in the ratio 2:1. This is known as the type II hydrate structure. The 16-hedron is shown in Fig. 7.52; it has symmetry $\bar{4}3m$.[2]

Data for the nets with unit edge length (this condition is sufficient to fix all the coordinates) are:

[1]This polyhedron is the dual of the bicapped hexagonal antiprism (Fig. 5.12, p. 143).
[2]This polyhedron is the dual of the Friauf polyhedron (Fig. 5.12, p. 143).

Type I $Pm\bar{3}n$, $a = 4.3021$, $r = 0.578$
5·5·5·5·6·6 in 6 *c*: $\pm(0,1/2,1/4)\kappa$
5·5·5·5·5·5 in 16 *i*: $\pm(x,x,\pm x\ ;\ 1/2+x,1/2+x,1/2\pm x)\kappa$, $x = 0.1829$
5·5·5·5·5·6 in 24 *k*: $\pm(0,y,\pm z\ ;\ 1/2,1/2+z,1/2\pm y\ )\kappa$, $y = 0.3099$, $z = 0.1162$

Type II $Fd\bar{3}m$, $a = 6.2054$, $r = 0.552$
5·5·5·5·5·5 in 8 *a*: $F \pm (1/8,1/8,1/8)$
5·5·5·5·5·5 in 32 *e*: $F \pm (x,x,x\ ;\ x,1/4-x,1/4-x)\kappa$, $x = 0.2180$
5·5·5·5·5·6 in 96 *g*: $F \pm (x,x,z\ ;\ x,1/4-x,1/4-z\ ;\ 1/4-x,x,1/4-z\ ;\ 1/4-x,1/4-x,z)\kappa$, $x = 0.1820$, $z = 0.3709$

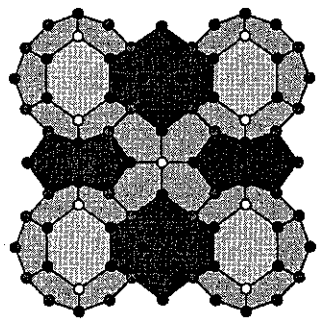

Fig. 7.51. A fragment of the Type I hydrate (clathrasil) structure viewed down [001]. Dodecahedra are shown with heavily shaded faces. Tetrakaidecahedra share hexagonal faces to form rods along <100>. The rods are packed (by sharing pentagonal faces) as in the β-W cylinder packing. Dodecahedra fill interstices in this rod packing.

The last structure (Type II) comes close to having all vertices 5^6. The unit cell contains sixteen 12-hedra, eight 16-hedra, 144 5-gons and sixteen 6-gons. It does not appear possible to make 4-connected nets with *all* 5-rings, although model builders (see Notes at the end of this chapter) will find that remarkably large clusters of packed pentagonal dodecahedra can be made before strain becomes too severe to continue. To construct a "spaghetti" model of the type II net it is best to make one 16-hedron and then to construct dodecahedra on each of its pentagonal faces (there is only one way to do this); it should be obvious how to proceed thereafter. A stereo view of the net is in Fig. 7.90 (§ 7.11.8).

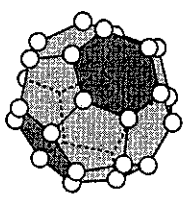

Fig 7.52. The hexakaidecahedron appearing in the Type II hydrate net.

The Type II net also occurs as Si or Ge frameworks in compounds M_xSi or M_xGe formed by decomposition (loss of M = alkali metal) of MSi or MGe at high temperatures under vacuum. The synthetic zeolite dodecasil 3C is also based on this net.

The polyhedra in this section have three polygons (not necessarily regular or even planar) meeting at each vertex. For such a polyhedron (see the exercises in Chapter 5) the number of faces, F and vertices, V are related by $2F = V + 4$, and the number of edges, $E = 3V/2$. If there are F_4 faces with four edges and F_5 faces with five edges then $2F_4 + F_5 = 12$. There is no constraint on the number of faces with six edges.

We revisit the clathrate hydrate structures in Appendix 4 where two further structures are mentioned. Attention is also directed to the structures of the zeolite clathrasils (§ 7.8.6).

7.7 A summary of the simpler 4-connected nets

Here (Table 7.2) is a list of the simpler uninodal 4-connected nets either with less than 4 vertices in the topological repeat unit or quasi-regular. Z is the number of vertices in the topological repeat unit (primitive unit cell). "l.c." refers to the symbol for an invariant lattice complex. It would be of interest to know if this list is complete. The list for $Z = 4$ would be quite long.[1] The **dense** net is uniform in that it contains only 7-rings.

Table 7.2. Names and properties of some simple 4-connected nets

net	*Z*	*symbol*	l.c.	*regular*	*uniform*
diamond	2	$6_2{\cdot}6_2{\cdot}6_2{\cdot}6_2{\cdot}6_2{\cdot}6_2$	D	yes	yes
$CdSO_4$	2	$6{\cdot}6{\cdot}6{\cdot}6{\cdot}6_2{\cdot}\infty$		no	yes
quartz	3	$6{\cdot}6{\cdot}6_2{\cdot}6_2{\cdot}8_7{\cdot}8_7$	^+Q	quasi	no
NbO	3	$6_2{\cdot}6_2{\cdot}6_2{\cdot}6_2{\cdot}8_2{\cdot}8_2$	J^*	quasi	no
W2	3	$3{\cdot}7{\cdot}7{\cdot}7{\cdot}7_2{\cdot}7_2$		no	no
dense	3	$7_2{\cdot}\infty{\cdot}7_3{\cdot}7_3{\cdot}7_3{\cdot}7_3$		no	yes
sodalite	6	$4{\cdot}4{\cdot}6{\cdot}6{\cdot}6{\cdot}6$	W^*	quasi	no
$HL4_3$	6	$3{\cdot}3{\cdot}10_2{\cdot}10_2{\cdot}10_2{\cdot}10_2$	^+V	quasi	no
$S^* = Ia\bar{3}d$ 24*d*	12	$6{\cdot}6{\cdot}6_2{\cdot}6_2{\cdot}6_2{\cdot}6_2$	S^*	quasi	yes

7.8 Zeolite nets

The current considerable interest in zeolites stems from their value as catalysts and "molecular sieves" and each year sees a number of new structures discovered. Their

[1]Nets not realizable with shortest distances between vertices corresponding to edges probably should be excluded. There are five *uninodal* nets with $Z = 4$ in this chapter, we know of only one other. See M. O'Keeffe, *Phys. Chem. Minerals* **22**, 504 (1995).

properties are, to a large extent, determined by their structures, so we devote some space to this topic (but by no means exhaust it).[1]

An invaluable guide to zeolite nets is the *Atlas of Zeolite Structure Types*[2] which includes eighty 4-connected nets of natural and synthetic zeolites. The *Atlas* contains stereo diagrams of each net, coordination sequences for each vertex, references and synonyms. Some structures appear dauntingly complex, but many can be described rather simply as they contain a short axis suitable for projection. Once one learns to "read" the projection, it will be found that the three-dimensional structure may readily be reconstructed (model making is highly recommended). As in many instances we provide coordinates for idealized nets (not given in the *Atlas*), they can be readily studied by computer.[3]

The term *zeolite* is not rigorously defined: it is used loosely to refer to any oxide with an open structure (say $r < 0.6$) based on a framework of corner connected $\{T\}O_4$ tetrahedra.[4] Some authors use the term *clathrasil* to refer to those structures without large channels (shortest ring at each angle a 6-ring or smaller). From this point of view **sodalite** is a clathrasil. *Pentasils* are open silica-rich alumino-silicate structures in which the smallest rings are 5-rings. Some of these are referred to as *silicalites*.

A number of simpler zeolite nets have already been described (an index to zeolite nets in this chapter is given in § 7.8.8, p. 353). Here we describe some more, using easily-recognized structural units (such as "zig-zag" or "crankshaft" rods) as an organizing principle. The reader uninterested in zeolites is invited to scan through this section quickly, pausing perhaps to admire some of the more-beautiful structures that occur.

*7.8.1 Zig-zag structures

In § 7.3.3-7.3.5 we described some nets, including those of zeolites Li-A, MAPO-39, $AlPO_4$-31 and cancrinite, which contain parallel zig-zag rods of vertices. The repeat distance for a unit edge zig-zag is typically about 1.65 time the edge length (about $1.65 \times 3.05 \approx 5$ Å for zeolites) and many zig-zag structures have one short axis of about this size, and have all vertices lying on mirror planes, so that they are readily shown in projection. In such a projection the framework appears as a two-dimensional 3-connected net. **Cancrinite** for example (Fig. 7.19, p. 307), projects as the 4.6.12 net.

[1]A good introduction to the properties and uses of zeolites is the article by J. M. Newsam in *Solid State Chemistry: compounds* (A. K. Cheetham & P. Day, eds.) Oxford (1992). A good source of data concerning zeolites is *Handbook of Molecular Sieves* by R. Szostak [Van Nostrand, New York (1992)].

[2]W. M. Meier & D. H. Olsen, *Atlas of Zeolite Structure Types*, Third Ed. Butterworth-Heinemann (1992). This also appeared as issue 5 of the journal *Zeolites*, **12** (1992). *Natural Zeolites* by G. Gotardi & R. Galli [Springer, Berlin (1985)] has good drawings that will be appreciated by model builders.

[3]The symmetry of real materials is generally lower that the maximum symmetry of the net. For structures for which we do not give coordinates, see the references given in the *Atlas of Zeolite Structure Types*. Note also that our coordinates may, in some instances, be rather different from those in real structures; they do however serve to define the topology of the net.

[4]When heated, zeolite minerals give off water as steam, and the name comes from the Greek for *boiling stone*. Purists insist that the term "zeolite" should be restricted to alumino-silicate minerals, but the wider sense used in this section (and in the *Atlas*) now has general currency.

A particularly simple net with both double and single zig-zags occurs in the zeolite known as NaJ with ideal composition $Na_2Al_2Si_2O_8{\cdot}H_2O$. The net is illustrated both as a projection down the zig-zags and in clinographic projection in Fig. 7.53. Crystallographic data are:

NaJ *Pmma*, $a = 1.576$, $b = 2.525$, $c = 2.525$, $r = 0.597$
$6{\cdot}6{\cdot}6{\cdot}6{\cdot}6_2{\cdot}6_2$ in 2 *g*: $\pm(1/4,1/2,z)$, $z = 0.378$
$4{\cdot}6_2{\cdot}4{\cdot}6_2{\cdot}6{\cdot}8_2$ in 4 *k*: $\pm(1/4,\pm y,z)$, $y = 0.198$, $z = 0.122$

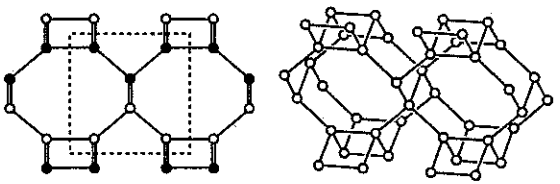

Fig. 7.53. The **NaJ** net. Left: projected on (100) with open and filled circles at $x = 1/4$ and 3/4 respectively. Right: in clinographic projection. Compare with Fig. 7.62 (**$AlPO_4$-25**) p. 346.

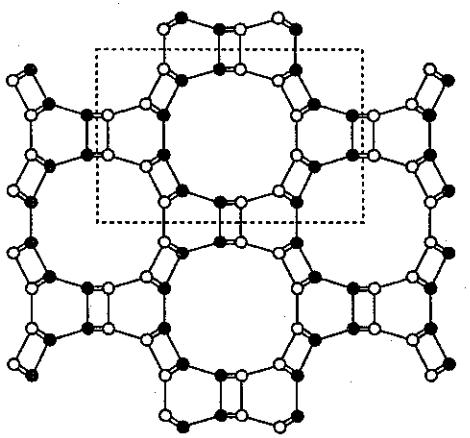

Fig. 7.54. The **MAPO-36** net projected on (001) with **b** horizontal on the page. Open and filled circles are at $z = 0$ and 1/2 respectively. Note that zig-zags are shown as double lines and that double zig-zags project as rectangles.

The net of the zeolite MAPO-36 (with a $MgAl_{11}P_{12}O_{48}$ framework) projects as 4.6.12 with the squares changed to rectangles representing a double zig-zag in projection (and the hexagons and dodecagons also distorted) as shown in Fig. 7.54 (contrast with **cancrinite**, Fig. 7.19, p. 307). Data for this net are:

MAPO-36 *Cmcm*, $a = 4.357$, $b = 6.687$, $c = 1.697$, $r = 0.485$
$4{\cdot}6{\cdot}4{\cdot}6{\cdot}6{\cdot}6_2$ in 8 *g*: $C \pm (\pm x,y,1/4)$, $x = 0.385$, $y = 0.040$
$4{\cdot}6_2{\cdot}4{\cdot}6_2{\cdot}6{\cdot}12_2$ in 8 *g*, $x = 0.319$, $y = 0.183$
$4{\cdot}6_2{\cdot}4{\cdot}6_2{\cdot}6{\cdot}12_2$ in 8 *g*, $x = 0.115$, $y = 0.251$

A number of zeolite nets with zig-zags project as two-dimensional nets containing pentagons. Two simple examples base on pentagon-octagon nets are those of bikitaite ($LiAlSi_2O_6.H_2O$) and $CsAlSi_5O_{12}$ (Fig. 7.55). Data are:

bikitaite *Cmcm*, $a = 2.365$, $b = 5.104$, $c = 1.656$, $r = 0.600$
$5_2{\cdot}6_2{\cdot}6{\cdot}6{\cdot}6{\cdot}6$ in 4 *c*: $C \pm (0,y,1/4)$, $y = 0.055$
$5{\cdot}5{\cdot}5{\cdot}5{\cdot}6{\cdot}8_2$ in 8 *g*: $C \pm (\pm x,y,1/4)$, $x = 0.289$, $y = 0.198$

$CsAlSi_5O_{12}$ *Cmcm*, $a = 1.602$, $b = 4.713$, $c = 5.151$, $r = 0.617$
$5{\cdot}6{\cdot}5{\cdot}6{\cdot}5_2{\cdot}6$ in 8 *f*: $C \pm (0,y,z\ ;\ 0,y,1/2-z)$, $y = 0.045$, $z = 0.088$
$5{\cdot}5{\cdot}5{\cdot}5{\cdot}6{\cdot}8_2$ in 8 *f*, $y = 0.255$, $z = 0.058$
$5{\cdot}6{\cdot}5{\cdot}6{\cdot}6_2{\cdot}8_2$ in 8 *f*, $y = 0.440$, $z = 0.153$

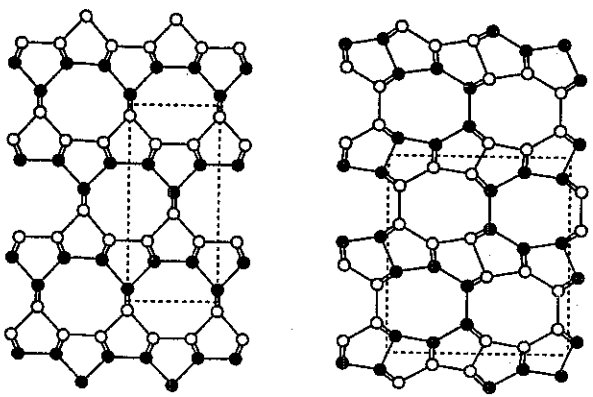

Fig. 7.55. Left **bikitaite** projected on (001) with **b** vertical on the page. Open and filled circles are at z = 1/4 and 3/4 respectively. Right: **$CsAlSi_5O_{12}$** projected on (100) with **c** vertical on the page. Open and filled circles are at $x = 0$ and 1/2 respectively.

The synthetic zeolites ZSM-12, ZSM-23 and theta-1 (essentially hydrous silica with small amounts of Na and Al) are also derived from two-dimensional nets, but now including either decagons or dodecagons (see Fig. 7.56). The nets of the first two contain seven different types of vertex, but **theta-1** has a simple description:

theta-1 *Cmcm*, $a = 4.575$, $b = 5.638$, $c = 1.625$, $r = 0.573$
$5{\cdot}5{\cdot}5{\cdot}5{\cdot}6_2{\cdot}10_2$ in 4 *c*: $C \pm (0,y,1/4)$, $y = 0.262$
$5{\cdot}5{\cdot}5{\cdot}5{\cdot}{\cdot}6_2{\cdot}\infty$ in 4 *c*, $y = 0.635$ (note the absence of a ring at one angle)
$5{\cdot}5{\cdot}5{\cdot}5{\cdot}6{\cdot}10_2$ in 8 *g*: $C \pm (\pm x,y,1/4)$, $x = 0.209$, $y = 0.210$
$5_2{\cdot}6_2{\cdot}6{\cdot}6_2{\cdot}6{\cdot}6_2$ in 8 *g*, $x = 0.307$, $y = 0.052$

ZSM-12 *C2/m*, $a = 8.03$, $b = 1.62$, $c = 3.92$, $\beta = 107.7$, $r = 0.58$

ZSM-23 *Pmmn*, $a = 1.62$, $b = 6.94$, $c = 3.59$, $r = 0.59$

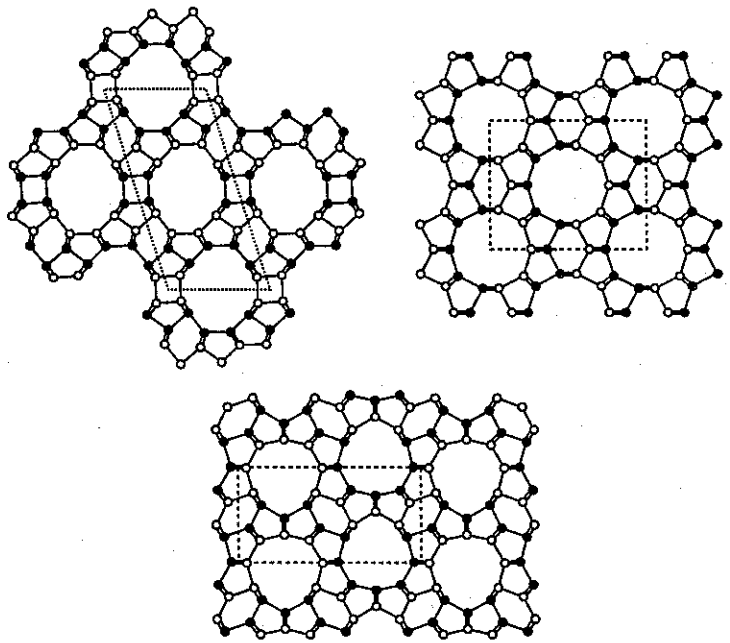

Fig. 7.56. Three zeolite nets with zig-zags (shown as double lines) projected down the short axis. Top left: **ZSM-12**. Top right: **theta-1**. Bottom: **ZSM-23**. Filled and open circles differ in elevation by 1/2 the vertical repeat distance.

**7.8.2 Crankshaft structures*

In § 7.3.6 (p. 308) we discussed some nets derived from the two-dimensional net 4.8^2 that contained vertices arranged on double crankshafts. In that section coordinates and a schematic illustration of **merlinoite** and **gismondine** were given. It might be noted that the repeat distance of a crankshaft is about 3.3 times an edge length: this translates into a repeat distance of about 3.3 × 3 Å = 10 Å for silicates and related materials (aluminophosphates etc.). In projections down the crankshaft axes, vertices are at elevations about ±0.15 (in units of the projection axis length) from mirror planes (which are either at 0 and 1/2 or at 1/4 and 3/4). Here we describe two more double crankshaft structures. The first is found in the aluminosilicate **phillipsite** and the second in a form of aluminum phosphate known as **$AlPO_4$-C**.

Crystallographic data for **phillipsite** and **AlPO$_4$-C** are:

phillipsite *Cmcm*, a = 3.446, b = 4.222, c = 4.359, r = 0.505
both vertices 4·4·4·8$_2$·8·8 in 16 *h*: $C \pm (\pm x,y,z\ ;\ \pm x,y,1/2-z)$
vertex 1: x = 0.145, y = 0.109, z = 0.044
vertex 2: x = 0.355, y = 0.243, z = 0.135

AlPO$_4$-C *Cmca*, a = 2.988, b = 5.897, c = 3.334, r = 0.545
4·4·4·8$_2$·8·8$_2$ in 16 *g*: $C \pm (\pm x,y,z\ ;\ \pm x,1/2+y,1/2-z)$,
x = 0.167, y = 0.051, z = 0.120
4·6·4·6·6·8$_2$ in 16 *g*, x = 0.167, y = 0.221, z = 0.120

These nets, together with **merlinoite** and **gismondine** are illustrated in Fig. 7.57. Note that in the figure the projection is down the axis of the double crankshaft (which projects as a rectangle). Note also that **merlinoite** contains octagonal prisms (shaded) centered at 0,0,0 and 1/2,1/2,1/2. Some relationships between the structures (all based on 4.8^2) should be apparent from the figure.

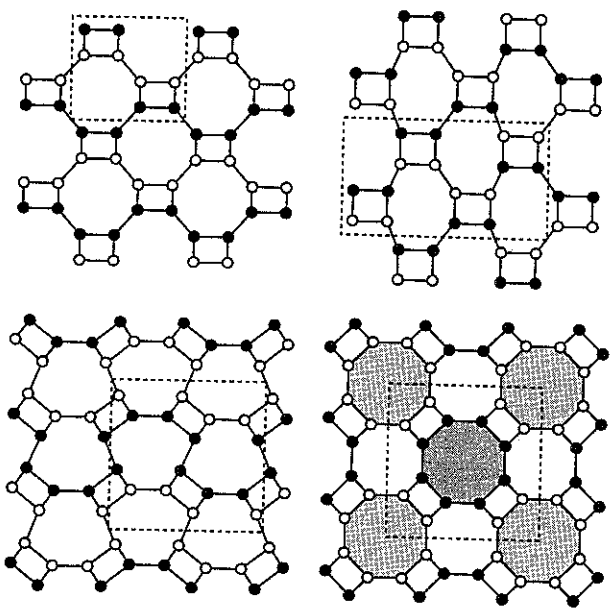

Fig. 7.57. Top left: **gismondine** projected on (100) with **c** vertical on the page. Top right: **AlPO$_4$-C** projected on (100) with **c** vertical on the page. Bottom left: **phillipsite** (100) with **b** vertical on the page. Bottom right: **merlinoite** projected on (001). In each case open circles are vertices at about ±0.15 and filled circles are vertices at about 0.5±0.15. Double crankshafts project as rectangles.

Another zeolite framework with double crankshafts is **gmelinite** (§ 7.3.7, p. 310); this is based on the two-dimensional net 4.6.12.

A simple zeolite framework containing both *single* and *double* crankshafts is found in **AlPO$_4$-12** (AlPO$_4$-33 has the same framework). Data for this structure (illustrated in Fig. 7.58) are:

AlPO$_4$-12 *Pmma*, a = 3.276, b = 2.498, c = 2.865, r = 0.512
4·8$_2$·4·8$_2$·6·8$_2$ in 4 *g*: $\pm(x,1/2,z\ ;\ 1/2-x,1/2,z)$, x = 0.097, z = 0.356
4·4·4·6·8·8 in 8 *l*: $\pm(x,\pm y,z\ ;\ 1/2-x,\pm y,z)$, x = 0.097, y = 0.200, z = 0.134

The short axis of **AlPO$_4$-12** is **b**. It might be noted that along this direction (horizontal in Fig. 7.58) vertices form rods (either all filled or all empty circles in the figure) that are referred to as "saw-tooth." We use a projection down saw-tooth rods in § 7.8.3 (next).

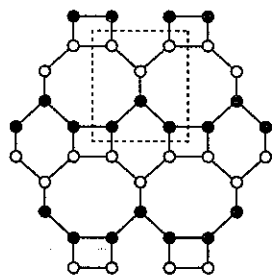

Fig. 7.58. AlPO$_4$-12 projected on (100) with **b** horizontal on the page. Double crankshafts project as rectangles. Vertices not on a double crankshaft are on a single crankshaft. Open circles are vertices at x = 0.1 and 0.4; filled circles are vertices at x = 0.6 and 0.9. Compare with Fig. 7.53 (**NaJ**), p. 339.

**7.8.3 Saw-tooth structures*

A rod intermediate between a zig-zag and a crankshaft is known as a saw tooth. A double saw-tooth rod is illustrated in Fig. 7.59. Now there are two kinds of vertex—the "teeth" (T) and the "base" (B)—in the ratio 1:2 on the rod. The repeat distance of a saw-tooth rod is about 2.4-2.6 times the edge length (about 2.5 × 3.0 Å = 7.5 Å in zeolites). The T vertices are on mirror planes at elevation either 0 and 1/2 or at 1/4 and 3/4 in projection down the rod, and the B vertices are about ±0.2 from the mirror planes. Again some zeolite structures are conveniently shown as projections, but the figures must be interpreted with care (see, for example, the legend for Fig. 7.60).

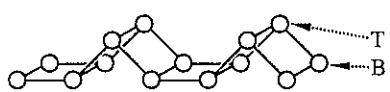

Fig. 7.59. A double "saw-tooth" rod. "B" and "T" indicate a base and a tooth vertex.

Two simple nets featuring double saw-tooth rods are found in the nets of the zeolites Linde-L and mazzite (both silica-rich aluminosilicates) shown in Fig. 7.60.

Linde L *P6/mmm*, $a = 6.007$, $c = 2.354$, $r = 0.489$
$4{\cdot}8_3{\cdot}4{\cdot}8_3{\cdot}6{\cdot}12$ in 12 *p*: $\pm(x,y,0$; etc.), $x = 0.096$, $y = 0.359$
$4{\cdot}4{\cdot}4{\cdot}6{\cdot}6{\cdot}8$ in 24 *r*: $\pm(x,y,z$; etc.), $x = 0.167$, $y = 0.500$, $z = 0.288$

mazzite $P6_3/mmc$, $a = 5.816$, $c = 2.505$, $r = 0.490$
$4{\cdot}8_2{\cdot}4{\cdot}8_2{\cdot}5{\cdot}6$ in 12 *j*: $\pm(x,y,1/4$; etc.), $x = 0.495$, $y = 0.161$
$4{\cdot}5{\cdot}4{\cdot}5{\cdot}8{\cdot}12$ in 24 *l*: $\pm(x,y,z$; etc.), $x = 0.096$, $y = 0.364$, $z = 0.050$

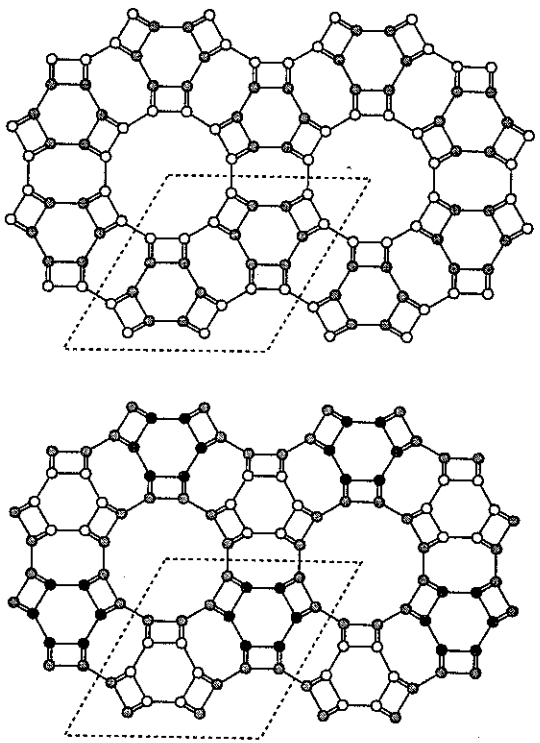

Fig. 7.60. Top: **Linde L** projected on (001). Open circles are T vertices at $z = 0$, shaded circles are B vertices at $z = \pm 0.29$. The latter form hexagonal prisms centered at 1/3,2/3,1/2 and 2/3,1/3,1/2. Bottom: **mazzite** projected on (001). Open and filled circles are T vertices at $z = 1/4$ and $z = 3/4$ respectively. Shaded circles on saw-tooth rods with teeth at $z = 1/4$ are B vertices at $z = -0.05$ and 0.55; shaded circles on saw-tooth rods with teeth at $z = 3/4$ are B vertices at $z = 0.45$ and 1.05. Note that here the rectangles are projections of the "double saw-tooth" rods of Fig. 7.59.

Some other saw-tooth nets found in silica-rich alumino-silicate nets are found in mordenite, dachiardite, ferrierite and ZSM-57. Symmetries and unit cell parameters (for unit edge) of these nets are:

mordenite *Cmcm*, $a = 5.60$, $b = 6.80$, $c = 2.42$, $r = 0.52$
dachiardite *C2/m*, $a = 5.84$, $b = 2.48$, $c = 3.30$, $\beta = 112.0°$, $r = 0.54$
ferrierite *Immm*, $a = 6.25$, $b = 4.34$, $c = 2.41$, $r = 0.55$
ZSM-57 *Imm2*, $a = 2.44$, $b = 4.63$, $c = 6.13$, $r = 0.52$

The nets are shown in projection in Fig. 7.61. To interpret the diagrams note that (a) filled and open circles are T vertices on mirror planes separated by 1/2 the projection distance; (b) shaded circles are B vertices at elevations of approximately 0.3 above and below the T vertices to which they are connected, (c) saw-tooth rods are shown as double lines.

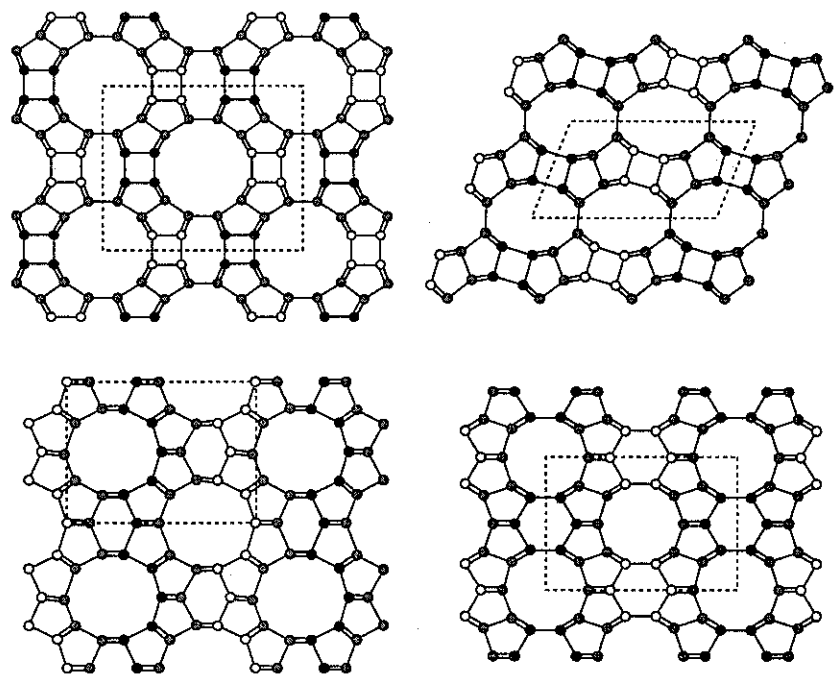

Fig. 7.61. Top left: **mordenite** projected on (001) with **a** horizontal on the page. Bottom left: **ZSM-57** projected on (100) with **c** horizontal on the page. Top right: **dachiardite** projected on (010) with **c** horizontal on the page. Bottom right: **ferrierite** projected on (001) with **a** horizontal on the page. See also the text.

**7.8.4 More up-down structures*

In § 7.3.8 we described two nets (one was of the zeolite **AlPO$_4$-5**) based on "up-down" connections of two-dimensional nets. Some rather complicated $AlPO_4$ structures that have recently been discovered are based on this principle, so again there is a short axis, and they are readily depicted as projections down that axis (Fig. 7.62). The repeat distance along the projection axis is about 2.7 the edge length (i.e. about 8.4 Å in aluminophosphates). Note that these nets contain only even rings and that in the real materials Al and P alternate (lowering the symmetry).

Data for the two simpler of these nets with unit edge are:

VPI-5 *P*6$_3$/*mcm*, $a = 6.086$, $c = 2.674$, $r = 0.406$
4·6$_3$·4·6$_3$·6·6$_4$ in 12 *k*: ±(*x*,0,*z* ; etc.), $x = 0.4227$, $z = 0.063$
4·6$_2$·6·6$_3$·6$_2$·6$_3$ in 24 *l*: ±(*x*,*y*,*z* ; etc.), $x = 0.1786$, $y = 0.5120$, $z = 0.563$

AlPO$_4$-25 *Cmma*, $a = 2.603$, $b = 4.800$, $c = 3.149$, $r = 0.610$
6·6$_2$·6·6$_2$·6$_2$·6$_2$ in 8 *n*: *C* ± (±*x*,1/4,*z*), $x = 0.308$, $z = 0.849$
4·6$_2$·6·6$_3$·6$_2$·6$_3$ in 16 *o*: *C* ± (±*x*,*y*,*z* ; ±*x*,1/2−*y*,*z*),
$x = 0.192$, $y = 0.099$, $z = 0.651$

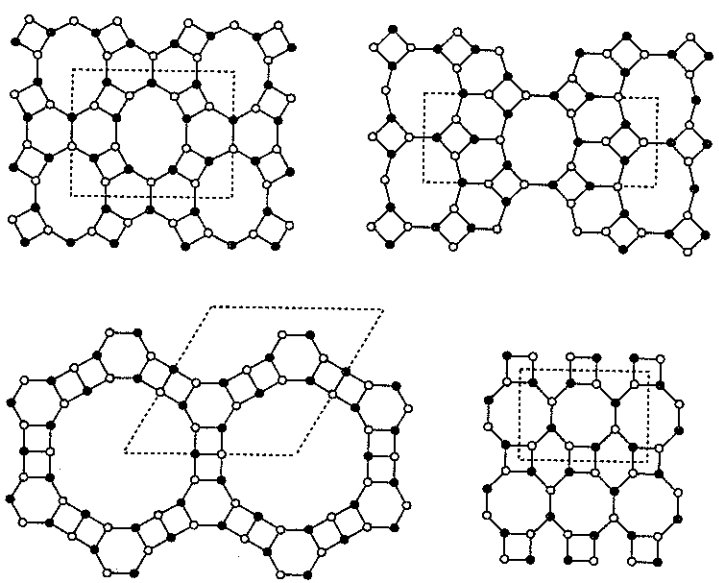

Fig. 7.62. Top left: **AlPO$_4$-11** projected on (100) with **b** horizontal on the page. Top right: **AlPO$_4$-41** projected on (001) with **b** horizontal on the page. Bottom left: **VPI-5** projected on (001). Bottom right: **AlPO$_4$-25** projected on (100) with **b** horizontal on the page. Additional edges go "up" from open circles and "down" from filled circles.

The **AlPO$_4$-41** net has symmetry *Cmcm* and four different kinds of vertex; The **AlPO$_4$-11** net has symmetry *Imma* and three different kinds of vertex.

Another member of this family that has recently been discovered is known as **AlPO$_4$-8**. This beautiful structure, shown (again slightly idealized) in Fig. 7.63, has five different kinds of vertex and contains 14-rings. The symmetry of the net is also *Cmcm*.

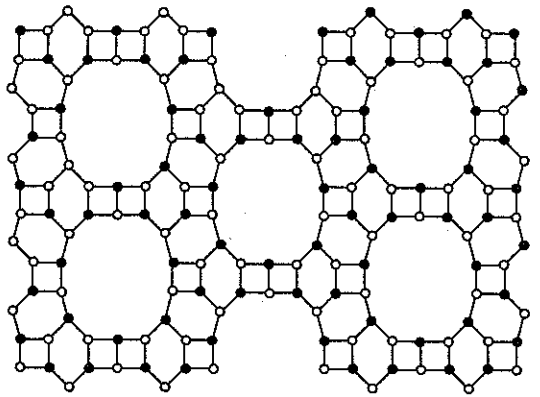

Fig. 7.63. AlPO$_4$-8 projected on (001) with **a** horizontal on the page.

**7.8.5 The "ABC-6" family*

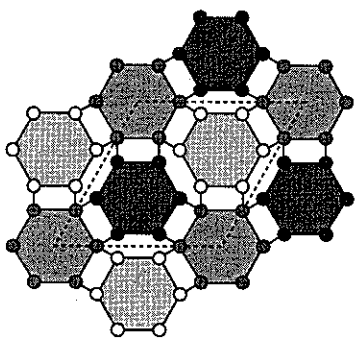

Fig. 7.64. Sodalite projected on (111) with a hexagonal cell outlined. Open circles at 1/6, shaded circles at 1/2 and filled circles at 5/6 of the repeat unit 1/2<111>. Edges joining vertices at 5/6 to those at 7/6 (i.e. 1/6) are not shown.

In § 7.3.5 (p. 306) we commented on **cancrinite** which we described as a stacking of plane hexagons centered at 1/3,2/3,1/4 and 2/3,1/3,3/4. By analogy with the nomenclature

used for sphere packing (§ 6.1.1), we could describe that stacking sequence *AB*... The inclined edges linking the hexagons formed double zig-zag rods. Similarly in **gmelinite** (§ 7.3.7. p. 310) there are hexagonal prisms centered at 1/3,2/3,1/4 and 2/3,1/3,3/4 and the stacking of hexagons could be described as *AABB*.. and the edges not perpendicular to the stacking direction form a double crankshaft rod.

A sequence of hexagons stacked *AAB*... produces a structure based on saw-tooth rods. This is found in the zeolite offretite.

The primitive cell of **sodalite** (§ 7.3.10) is rhombohedral with $a = \sqrt{6}$, $\alpha = \cos^{-1}(-1/3) = 109.47°$ and contains six vertices with x,y,z equal to the six permutations of 1/4,1/2,3/4. These comprise a planar hexagon normal to [111] and centered at 1/2,1/2,1/2. Packing the rhombohedral cells will result in the hexagons being stacked *ABC* along a 3-fold axis as shown in Fig. 7.65.[1]

Nets derived by stacking hexagons in positions *A*, *B* or *C* are known as ABC-6 nets and about a dozen have been recognized in natural and synthetic zeolites.[2] Some of these are summarized in Table 7.3. The entries under "vertex types" are the numbers of topologically-distinct kinds of vertex.

Chabazite is $Ca_3Al_6Si_{12}O_{36}{\cdot}20H_2O$; The net contains a rhombohedral stacking of hexagonal prisms (contrast **sodalite** which has a rhombohedral stacking of single hexagons). The remaining space consists of large (36-vertex) polyhedra as illustrated in Fig. 7.65. Data for the net are:

chabazite $R\bar{3}m$, $a = 4.404$, $c = 4.757$, $r = 0.451$
4·4·4·8·6·8 in 36 *i*: $R \pm (x,y,z$; etc.), $x = 0.106$, $y = 0.439$, $z = 0.062$

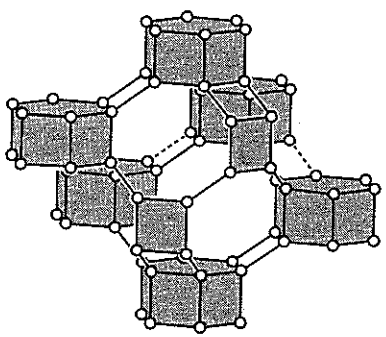

Fig. 7.65. The large polyhedron in **chabazite** formed by a linked stacking of hexagonal prisms. For two hexagonal prisms only one square face is shown (shaded).

[1]The skeptical reader may wish to transform **sodalite** to a hexagonal cell as outlined in § 4.4.2. The cell has $a = 4$ and $c = \sqrt{6}$ and contains 18 vertices. Compare with the 12-vertex cell of **cancrinite** given in § 7.3.5 (p. 306) which has the same a, and c two-thirds as large.

[2]For a systematic discussion of possible ABC-6 structures and their symmetries, see J. V. Smith & J. M. Bennett, *Amer. Mineral.* **66**, 777 (1981).

Table 7.3. Some ABC-6 nets

sequence	*net*	*vertex types*
AB	**cancrinite**	1
ABC	**sodalite**	1
ABAC	**losod**	2
ABABAC	**liottite**	3
ABABACAC	**afghanite**	3
AABB	**gmelinite**	1
AABBCC	**chabazite**	1
AABBCCBBAACC	**AlPO$_4$-52**	3
AAB	**offretite**	2
ABBACC	**TMA-E**	2
AABAAC	**erionite**	2
AABCCABBC	**levyne**	2

**7.8.6 Pentasils (silicalites), clathrasils and related structures*

We have already met the frameworks of **melanophlogite** (SiO_2) and **dodecasil-3C** in § 7.6 where they were identified as the frameworks of clathrate hydrates called **Type I** and **Type II** respectively. (A zeolite named ZSM-39 also has the latter structure). Another simple structure based on a space filling of polyhedra is **octadecasil** (the same framework has been found in AlPO$_4$-16). In this structure cubes pack with truncated rhombic dodecahedra in the ratio 1:1 to fill space as shown in Fig. 7.66. The large polyhedron with 18 faces (an octadecahedron = $[4^6.6^{12}]$) may be derived by truncating the acute vertices (where four edges meet) of a rhombic dodecahedron. The centers of each set of polyhedra fall on points of an *fcc* lattice; accordingly, taken together the centers have a **NaCl** arrangement. Data for this net are given on the next page.

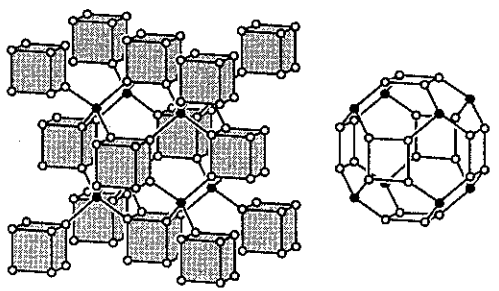

Fig. 7.66. The **octadecasil** net. Left: as cubes connected by isolated tetrahedral vertices (filled circles). Right: the octadecahedron.

octadecasil $Fm\bar{3}m$, $a = 4.309$, $r = 0.500$
6·6·6·6·6·6 in 8 *c*: $F \pm (1/4,1/4,1/4)$
4·6·4·6·4·6 in 32 *f*: $F \pm (\pm x,x,x)$, $x = 0.116$

A particularly beautiful clathrasil known as sigma-2 has recently been described. This is based on a packing of 36-vertex icosahedra $[5^{12}.6^8]$ and enneahedra $(4^3.5^6]$. The large polyhedron, which has symmetry $\bar{4}2m$, is called the "tennis ball" because the pentagons form an endless strip rather like the seam of a tennis ball (see Fig. 7.67).[1] Like that of most clathrasils, the structure is difficult to illustrate satisfactorily, but it is easy to make a model. In **sigma-2** the "tennis balls" share opposite hexagonal faces to form rods along <100> as indicated in Fig. 7.67, and the smaller polyhedra (also shown in the figure) fill the interstices of the packing. The rods of face-sharing tennis balls are packed as in the 4-layer cylinder packing of § 6.7.2 (b) (p. 264).

The crystallographic description is fairly simple:

sigma-2 $I4_1/amd$, $a = 3.28$, $c = 11.17$, $r = 0.53$
5·6·5·6·5·6 in 16 *h*: $I \pm (0,y,z$; etc.), $y = 0.098$, $z = 0.7133$
4·6·5·5·5·5 in 16 *h*: $I \pm (0,y,z$; etc.), $y = 0.038$, $z = 0.3669$
4·6·5·5·5·5 in 16 *h*: $I \pm (0,y,z$; etc.), $y = 0.098$, $z = 0.5529$
4·6·5·5·5·5 in 16 *f*: $I \pm (x,0,0$; etc.), $x = 0.274$

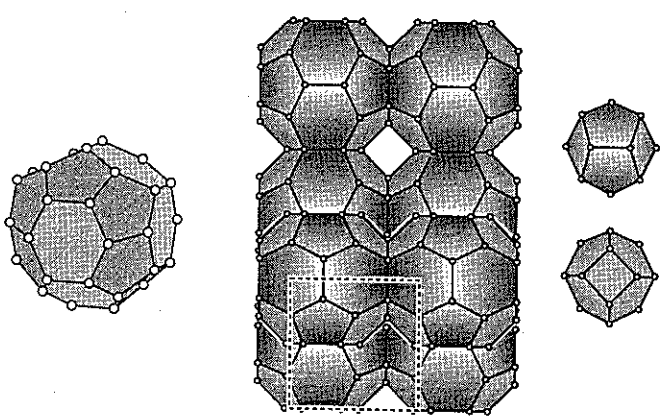

Fig. 7.67. Left: The "tennis ball" icosahedron as it appears in **sigma-2**. The $\bar{4}$ axis is vertical on the page. Middle: part of the icosahedron packing of **sigma-2** viewed down [001]. Right: the enneahedra that fill the interstices are shown in two different orientations.

A zeolite named **$AlPO_4$-22** is included here because it is another simple example of a 4-

[1]For more on this and related polyhedra see Appendix 4.

connected net derived from packing polyhedra. (As the net contains 8-rings, most authors would not classify this material as a clathrasil.) The net is shown in projection in Fig. 7.68. Model builders will discover that it is made up of equal numbers of two kinds of polyhedra; one with 10 faces $[4^6.6^4]$ and the other with 18 faces $[4^8.6^8.8^2]$ (Fig. 7.68). Each kind of polyhedron forms rods along **c** by sharing opposite faces. Crystallographic data for the ideal net are:

$AlPO_4$-22 $P4/nmm$, $a = 4.324$, $c = 2.547$, $r = 0.504$
4·4·4·6·6·6 in 8 *g*: $\pm (x,\bar{x},0$ etc.), $x = 0.134$
4·4·6·6·6·8 in 16 *k*: $\pm (x,y,z$, etc.), $x = 0.029$, $y = 0.866$, $z = 0.345$

The 4·4·4·6·6·6 vertices form squares at $z = 0$ and the 4·4·6·6·6·8 vertices form octagons at $z = \pm 0.35$. How the polygons are connected should be evident from Fig. 7.68.

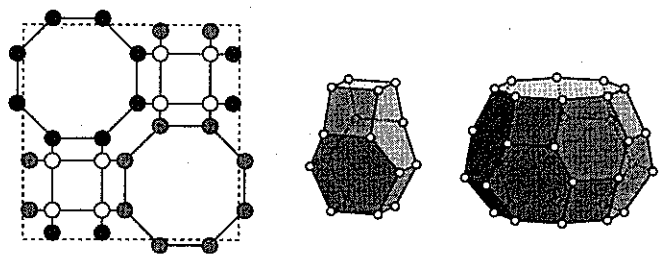

Fig. 7.68. Left: the **$ALPO_4$-22** net projected on (001). Open, shaded and filled circles are at $z = 0$, 0.35 and 0.65 respectively. Right: the two kinds of polyhedra in the structure (**c** is vertical). The top and bottom faces of the polyhedra are separated by *c*.

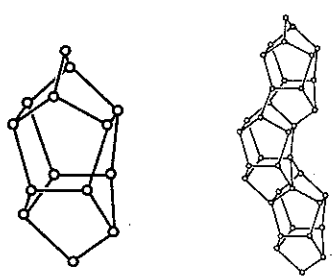

Fig. 7.69. Left: a pentasil unit. Right: three condensed pentasil units

The structures known as *silicalites* are rather more complicated. The net of silicalite 1 (ZSM-5) has twelve different kinds of vertex and that of silicalite 2 (ZSM-11) has eight different kinds. 5- and 6-rings dominate but there are also 4- and 10-rings in the structures. A basic building block in these structures is the "pentasil unit" (shown in Fig. 7.69) which

is a polyhedron with eight pentagonal faces (a "pentagonal octahedron") and two divalent vertices. These can be condensed into corrugated slabs as hinted in the figure. The silicalite structures are then derived by joining the slabs either across mirror planes to form silicalite 2 or through inversion centers to form silicalite 1.[1]

*7.8.7 Fibrous zeolites

The materials under this heading are a group of natural and synthetic zeolites with some fascinating crystal chemistry. The basic building unit is the rod of vertices shown on the left in Fig. 7.70. These rods can be linked in two directions perpendicular to the rod axis as shown on the right in the figure which illustrates the linkage in edingtonite.

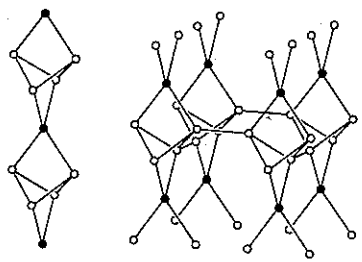

Fig. 7.70. Left the building unit of the fibrous zeolites. Right: the linkage of rods in **edingtonite**.

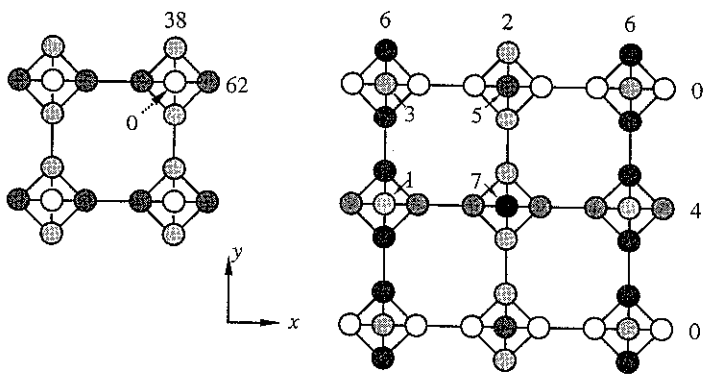

Fig. 7.71. Left: **edingtonite** projected on (001); numbers are elevations in multiples of *c*/100. Right: **natrolite** projected on (001); numbers are approximate elevations in multiples of *c*/8.

[1]Good illustrated accounts of these structures are given by C. A. Fyfe *et al.*, *J. Amer. Chem. Soc.* **111**, 2470 (1989) and D. H. Olsen *et al.*, *J. Phys. Chem.* **85**, 2238 (1981). Silicalites are important commercial catalysts.

The two simplest topologies are:

edingtonite $P\bar{4}m2$, $a = 2.204$, $c = 2.122$, $r = 0.485$
$4_2{\cdot}4_2{\cdot}8_4{\cdot}8_4{\cdot}8_4{\cdot}8_4$ in 1 *a*: 0,0,0
$4{\cdot}8_3{\cdot}4{\cdot}8_3{\cdot}4_2{\cdot}8_4$ in 4 *j*: $(\pm x,0,z\ ;\ 0,\pm x,\bar{z})$, $x = 0.273$, $z = 0.376$

natrolite $I4_1/amd$, $a = 4.406$, $c = 2.124$, $r = 0.485$
$4_2{\cdot}4_2{\cdot}8_4{\cdot}8_4{\cdot}8_4{\cdot}8_4$ in 4*b*: $I \pm (0,1/4,3/8)$
$4{\cdot}8_2{\cdot}4{\cdot}8_2{\cdot}4_2{\cdot}8_4$ in 16*h*: $I \pm (0,y,z\ ;\ 1/2,y,1/2-z\ ;\ 1/4+y,1/4,3/4+z\ ;$
$1/4+y,3/4,1/4-z)$, $y = 0.387$, $z = -0.001$

Fig 7.71 shows, on the left, **edingtonite** in projection. The rods project as centered squares and together with the links between rods form a 4.8^2 pattern. It is important to recognize that we have described the net in its most-symmetrical minimum-density form. In real material (edingtonite has the ideal formula $BaAl_2Si_3O_{10}{\cdot}H_2O$) the framework collapses as discussed for scapolite in § 7.3.8 (see Fig. 7.25, p. 312) and the unit cell is doubled. In the real material the symmetry is further lowered by Si,Al ordering and is in fact $P2_12_12$.

Fig. 7.71 also shows **natrolite** in projection. The links between rods are now at four different elevations and form rods arranged as in the four-layer cylinder packing of § 6.7.2 (b). Natrolite itself has the ideal composition $Na_2Al_2Si_3O_{10}{\cdot}2H_2O$. The same framework is found in other minerals such as scolecite, $CaAl_2Si_3O_{10}{\cdot}3H_2O$ (note the substitution of 2Na by $Ca+H_2O$) and also in anhydrous synthetic materials such as $Rb_2Ga_2Ge_3O_{10}$. Again the framework is partly collapsed and its symmetry is lowered from $I4_1/amd$ to $I\bar{4}2d$. Si,Al ordering in natrolite further lowers the symmetry to $Fdd2$ (with a doubled cell) and in scolecite Ca, H_2O ordering reduces the symmetry further to Cc. It is common to use the same size of cell for these structures: this entails using a face centered cell for all four symmetries. The tetragonal space groups become $F4_1/ddm$ and $F\bar{4}d2$ (see § 3.3.4, p.73) and Cc becomes Fd. The descent in symmetry is in terms of full symbols:

parent structure	F	$4_1/d$	$2/d$	$2/m$
collapsed	F	$\bar{4}$	d	2
Si/Al order	F	d	d	2
Ca/H_2O order	F	1	d	1

The conventional Cc cell is obtained from Fd by $(0\ 0\ \bar{1}\ /\ 0\ 1\ 0\ /\ 1/2\ 0\ 1/2)$.

Thompsonite, which has approximate composition $NaCa_2Al_5Si_5O_{20}{\cdot}6H_2O$, has a closely related structure with a different linkage of rods.[1]

*7.8.8 Zeolite net nomenclature and index

The bewildering variety of names for natural and synthetic zeolites has lead the Structure Commission of the International Zeolite Association to establish three-letter symbols for

[1]For a systematic account of linkages and symmetries possible for fibrous silicates, see J. V. Smith, *Zeits. Kristallogr.* **165**, 191 (1983).

structure topologies.[1] These are given in Table 7.4 for the zeolite nets discussed in this chapter (three of these are in the Exercises § 7.12) together with the names that we have used, so this section can serve as an index to those structures. It is a pity that no generally agreed symbols are available for other common nets (such as **diamond** and **keatite**) which occur in many different contexts.

Table 7.4. Symbols, names and sections for some zeolite nets

ABW	$SrAl_2$	§ 7.3.5	GIS	**gismondine**	§ 7.3.6
AEL	$AlPO_4$-11	§ 7.8.4	GME	**gmelinite**	§ 7.3.7
AET	$AlPO_4$-8	§ 7.8.4	JBW	**NaJ**	§ 7.8.1
AFG	**afghanite**	§ 7.8.5	KFI	**ZK-5**	§ 7.4.3
AFI	$AlPO_4$-5	§ 7.3.8	LEV	**levyne**	§ 7.8.5
AFO	$AlPO_4$-41	§ 7.8.4	LIO	**liottite**	§ 7.8.5
AFS	**MAPSO-46**	§ 7.12.12	LOS	**losod**	§ 7.8.5
AFT	$AlPO_4$-52	§ 7.8.5	LTA	**Linde A**	§ 7.4.1
AFY	**CoAPO-50**	§ 7.4.5	LTL	**Linde L**	§ 7.8.3
ANA	**analcime**	§ 7.12.6	MAZ	**mazzite**	§ 7.8.3
APC	$AlPO_4$-C	§ 7.8.2	MEL	**silicalite 2 (ZSM-11)**	§ 7.8.6
AST	**octadecasil**	§ 7.8.6	MEP	**melanophlogite**	§ 7.6
ATN	**MAPO-39**	§ 7.3.5	MER	**merlinoite**	§ 7.3.6
ATO	$AlPO_4$-31	§ 7.3.4	MFI	**silicalite 1 (ZSM-5)**	§ 7.8.6
ATS	**MAPO-36**	§ 7.8.1	MFS	**ZSM-57**	§ 7.8.3
ATT	$AlPO_4$-12	§ 7.8.2	MON	**montesommaite**	§ 7.12.7
ATV	$AlPO_4$-25	§ 7.8.4	MOR	**mordenite**	§ 7.8.3
AWW	$AlPO_4$-22	§ 7.8.6	MTN	**type II (ZSM-39)**	§ 7.6
BIK	**bikitaite**	§ 7.8.1	MTT	**ZSM-23**	§ 7.8.1
CAN	**cancrinite**	§ 7.3.5	MTW	**ZSM-12**	§ 7.8.1
CAS	$CsAlSi_5O_{12}$	§ 7.8.1	NAT	**natrolite**	§ 7.8.7
CHA	**chabazite**	§ 7.8.5	OFF	**offretite**	§ 7.8.5
DAK	**dachiardite**	§ 7.8.3	PHI	**phillipsite**	§ 7.8.2
EAB	**TMA-E**	§ 7.8.5	RHO	**rho**	§ 7.4.2
EDI	**edingtonite**	§ 7.8.7	SGT	**sigma-2**	§ 7.8.6
EMT	**hex. faujasite**	§ 7.4.4	SOD	**sodalite**	§ 7.3.10
ERI	**erionite**	§ 7.8.5	TON	**theta-1**	§ 7.8.1
FAU	**faujasite**	§ 7.4.4	VFI	**VPI-5**	§ 7.8.4
FER	**ferrierite**	§ 7.8.3			

7.9 5-connected nets

Five-connected nets have received comparatively little attention. Describing them by Schläfli symbols gets a little cumbersome as there are now ten angles and they cannot be all equivalent.[2] Some examples are to be found in the structures of borides which often have extended B-B bonding with connectivity ranging from 2 (forming rods) through 3 (forming layers) to 4, 5 or 6 (forming three-dimensional frameworks).

[1]The index of the *Atlas of Zeolite Structure Types* has 332 entries.

[2]This follows from the fact that the complete graph with five points is not planar and therefore cannot represent the vertices and edges of a three-dimensional polyhedron.

Our first three examples also represent space filling by regular and Archimedean polyhedra. The first of these is a space-filling by octahedra and truncated cubes (3.8^2) and is found in nature as the B structure of CaB_6 and similar borides such as KB_6 and LaB_6. It is illustrated in Fig.7.72. This is a simple cubic structure; data for unit edge length are:

CaB_6 $Pm\bar{3}m$, $a = 1 + \sqrt{2} = 2.4142$, $r = 0.426$
vertices in 6 *e*: $\pm(x,0,0)\kappa$, $x = 1/(2 + \sqrt{2}) = 0.2929$

In CaB_6 a = 4.151 Å, Ca is at 1/2,1/2,1/2 in the center of the truncated cube (24-coordinated by B), and the x parameter (0.302) for B is close to the ideal value given above.

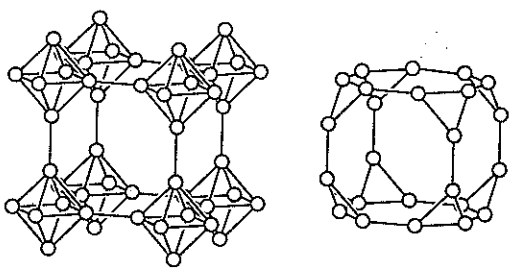

Fig. 7.72. Left: the net of B atoms in CaB_6. Right: a truncated cube formed by 24 vertices of the net.

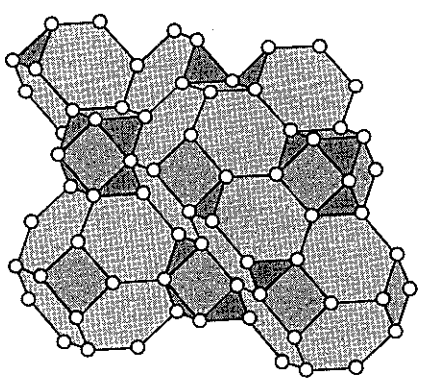

Fig. 7.73. The boron arrangement in UB_{12}.

The second five-connected structure is a space-filling by truncated octahedra, cuboctahedra and truncated tetrahedra that is the B structure of UB_{12} and isostructural borides (e.g. NiB_{12}, LuB_{12}). The crystallographic description is again very simple:

UB_{12} $Fm\bar{3}m$, $a = \sqrt{18} = 4.2426$, $r = 0.629$ [$a = 7.473$ Å for UB_{12}]
vertices in 48 *i*: $F \pm (1/2,x,\pm x)\kappa$, $x = 1/3$

A sketch of part of the structure is shown in Fig. 7.73. In UB_{12}, U atoms in 4 *a*: F + (0,0,0) center the B_{24} truncated octahedra. The centers of the cuboctahedra are at 4 *b*: F + (1/2,1/2,1/2) and the centers of the truncated tetrahedra are at 8 *c*: $F \pm (1/4,1/4,1/4)$.

If the truncated octahedra and half the truncated tetrahedra are omited, the remaining truncated tetrahedra and cuboctahedra form an infinite polyhedron $3.4.6^2.4$. The symmetry of the figure is now $F\bar{4}3m$, but the positions of the vertices are the same (see Fig. 7.74).

The third polyhedron packing is a space-filling by cubes, octagonal prisms, rhombicuboctahedra (3.4^3) and truncated cubes (3.8^2). In Fig. 7.74 the network of cubes and rhombicuboctahedra is shown as an infinite polyhedron 3.4^4. The complementary polyhedron (also 3.4^4) consists of truncated cubes (3.8^2) joined with octagonal prisms.

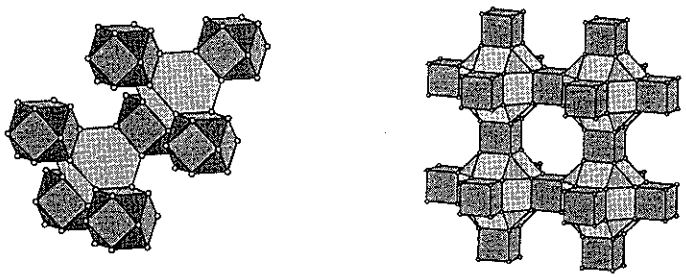

Fig. 7.74. Left: a fragment of an infinite polyhedron $3.4.6^2.4$. Right: Rhombicuboctahedra and cubes forming an infinite polyhedron 3.4^4.

Crystallographic data for this structure are:

3.4^4 $Pm\bar{3}m$, $a = 2 + \sqrt{2} = 3.4142$, $r = 0.603$
vertices in 24 *m*: $(\pm x,\pm x,\pm z)\kappa$, $x = 1/(4 + \sqrt{8}) = 0.1465$, $z = 1/2{-}x$

Per unit cell there is one rhombicuboctahedron (center at cell corner), one truncated cube (center at cell center), three octagonal prisms (centers in cell faces) and three cubes (centers in middle of cell edges). As an example of the occurrence of this structure we cite the structure of $Pd_{17}Se_{15}$ (for crystallographic data see Appendix 5) which is truly a polyhedrist's delight. In the unit cell of this structure, 24 Pd atoms make up the 5-coordinated packing and additionally: $\{Pd\}Se_6$ octahedra center the rhombicuboctahedra, Pd_6Se_{12} clusters consisting of Pd_6 octahedra edge-capped by Se forming a Se_{12} cuboctahedron (cf. § 5.2.4, Fig. 5.32, p. 159) center the truncated cube and $\{Pd\}Se_4$ squares center the octagonal prisms. The unit cell content is accordingly $PdSe_6{\cdot}Pd_6Se_{12}{\cdot}(PdSe_4)_3{\cdot}Pd_{24} = Pd_{34}Se_{30}$. $Rh_{17}S_{15}$ is isostructural.

Two more five-connected infinite polyhedra follow. The first (Fig. 7.75) is $3^3.6^2$ and is made up of truncated tetrahedra sharing triangular faces with octahedra (so that two

opposite faces of an octahedron are shared with truncated tetrahedra). Crystallographic data are :

$3^3.6^2$ $Fd\bar{3}m$, $a = 6.6024$, $r = 0.333$
vertices in 96 *g*: $F \pm (x,x,z$ etc.), $x = 0.0714$, $z = -0.0357$

In this structure, the connectivity of the truncated tetrahedra (by octahedra acting as links) has the **diamond** topology (the centers of the truncated tetrahedra form a **diamond** net). The structure can also be considered as octahedra joined to six neighboring octahedra by a fifth edge, as in $\mathbf{CaB_6}$, but now the topology is different—the centers of the octahedra are at the points of the *T* lattice complex.

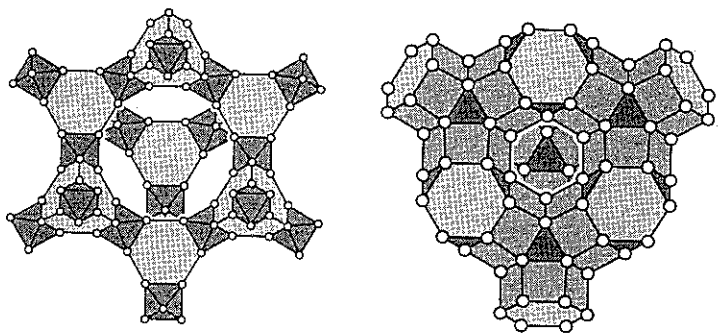

Fig. 7.75. Left: part of an infinite polyhedron $3^3.6^2$. Right: part of an infinite polyhedron 3.4^4.

Another infinite polyhedron with vertices 3.4^4 consists of truncated tetrahedra sharing hexagonal faces with hexagonal prisms (Fig. 7.75). This arrangement is a conspicuous part of the so-called *E* structure which occurs for compositions such as $Mg_3Al_{18}Cr_2$, $ZrZn_{22}$ and $Al_{10}V$. Crystallographic data for the five-coordinated packing are:

3.4^4 $Fd\bar{3}m$, $a = 5.138$, $r = 0.709$
vertices in 96 *g*: $F \pm (x,x,z$ etc.), $x = 0.0562$, $z = 0.3314$

7.10 Nets with mixed connectivity

Nets with mixed connectivity inevitably involve more than one kind of vertex. Here we give some examples of such nets with just two kinds of vertex.

**7.10.1 (3,4)-connected nets*

A very simple cubic structure (Fig. 7.76) has been proposed for Pt_3O_4 in which the atoms lie on invariant lattice complexes:

Pt_3O_4 $Pm\bar{3}n$, $a = 5.58$ Å
Pt in 6 *c*: $\pm(1/4,0,1/2)\kappa$
O in 8 *e*: $\pm(1/4,1/4,1/4\ ;\ 1/4,3/4,3/4)\kappa$

In this structure there are $\{Pt\}O_4$ squares and $\{O\}Pt_3$ equilateral triangles with the Pt-O distance equal to $a/\sqrt{8}$. The O atoms are on the points of a primitive cubic lattice. The Pt atom positions correspond to lattice complex *W* and form non-intersecting rods of Pt atoms a distance $a/2$ apart. The rods, parallel to the cube axes, are packed as in the **β-W** cylinder packing (§ 6.7.3).

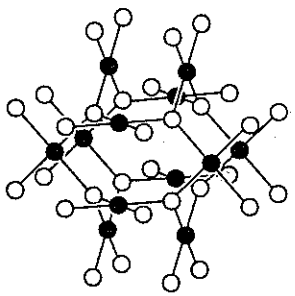

Fig. 7.76. The structure of Pt_3O_4 as a (3,4) connected net.

Boron in borates is commonly found as $\{B\}O_3$ triangles and $\{B\}O_4$ tetrahedra forming frameworks by sharing vertices. Exercise 2 gives an example of a 4-connected net derived from vertex sharing tetrahedra in CaB_2O_4 and the structure of B_2O_3 was cited (§ 7.2) as providing an example of a 3-connected net derived from vertex-sharing triangles. The structure of boracite, $Mg_3B_7O_{13}Cl$, which contains $\{B\}O_3$ triangles and $\{B\}O_4$ tetrahedra provides an elegant example of a (3,4) connected net of B atoms. Per formula unit there are $4BO_{3/2} + 3BO_{4/2} = B_7O_{12}$ in the B-O-B framework.

Here we describe just the idealized (3,4)-connected net. The basic unit consists of an octahedron of 4-connected vertices (*B*) with 3-connected vertices (*A*) centering four of the octahedron faces to form an A_4B_6 cluster (shown in Fig. 5.31, p. 159). Joining these octahedra by vertex sharing as shown in Fig. 7.77 [in the same way as in the *J* lattice complex (Fig. 6.27)] produces stoichiometry $A_4B_{6/2} = A_4B_3$. For unit edge the crystallographic description is:

boracite net $P\bar{4}3m$, $a = \sqrt{6}$
3-connected in 4 *e*: $(x,x,x\ ;\ \bar{x},\bar{x},x)\kappa$, $x = 1/6$
4-connected in 3 *d*: $(1/2,0,0)\kappa$

In the real structure of boracite at high temperature, the unit cell edge is doubled to allow suitable B-O-B configurations, and the symmetry is $F\bar{4}3c$. Below 300 °C, the symmetry is lowered to $Pca2_1$ but the topology of the framework is unaltered.

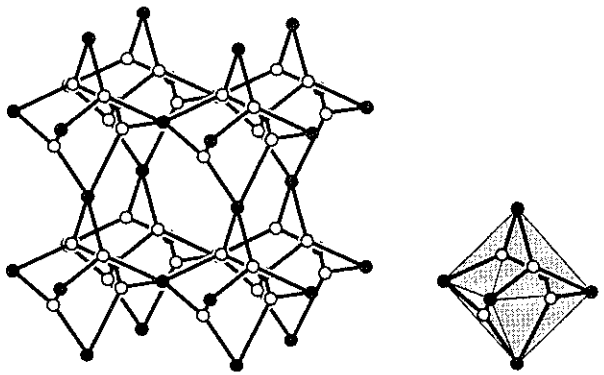

Fig. 7.77. The (3,4)-connected net of B atoms in boracite. On the right one A_4B_6 cluster is shown.

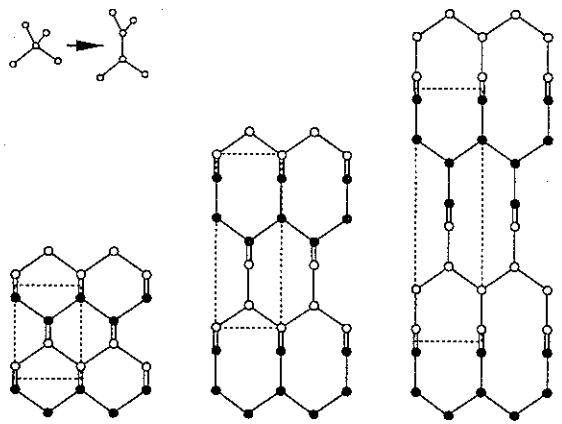

Fig. 7.78. Generation of 3- and (3,4)-connected nets from **diamond** (left). The (3,4)-connected net discussed in the text is shown in the middle and the **$ThSi_2$** net is shown on the right. In each case a body-centered tetragonal cell is shown and in the projection on (100), **c** is vertical, and points shown as filled and empty circles have elevations differing by $\delta x = 1/2$.

3-connected nets can simply be derived from 4-connected nets by replacing each 4-connected vertex by a pair of 3-connected vertices as shown in Fig. 7.78. The figure shows how to generate the **$ThSi_2$** net from **diamond** in this way. On the left **diamond** projected on (110) (cf. Fig. 7.11, p. 302) and on the right the **$ThSi_2$** net is projected on (100) of its tetragonal ($I4_1/amd$) cell (cf. Fig. 7.8, p. 298). Notice how each **diamond** vertex becomes a pair of 3-connected vertices with their edges in planes mutually at right

angles. If only half the **diamond** vertices are so altered, a simple (3,4)-connected net is obtained. The ring size (all 8-rings) is intermediate between that in **diamond** (all 6-rings) and in **ThSi$_2$** (all 10-rings). The net has only three vertices in the repeat unit and is probably the simplest (3,4)-connected net. The cell is again body-centered tetragonal:

(3,4)-connected net — $I\bar{4}m2$, $a = 1.800$, $c = 3.744$
4-connected in 2 *a*: $I + (0,0,0)$
3-connected in 4 *f*: $I + (0,1/2,z\ ;\ 1/2,0,\bar{z})$, $z = 0.3836$

7.10.2 (4,6)-connected nets

Simple examples of (4,6)-connected nets with two kinds of vertex occur as the structures of corundum ($^{vi}Al_2{}^{iv}O_3$) and $^{vi}Ni_2{}^{iv}S_3$.

In structures based on a framework of tetrahedra sharing corners with octahedra (and *vice versa*), the central tetrahedral and octahedral atoms form vertices of a (4,6)-connected net. Examples of such structures are those of the polymorphs of $Fe_2(SO_4)_3$ and $Al_2(WO_4)_3$; in these structures -O- links serve as the edges of the net. Just as for structures based on tetrahedral frameworks, "stuffed" variants are also found. In the following examples the atoms in bold face are on the net (different in every case and with -O- links again serving as edges) and the remaining metal atoms are in cavities in the framework: garnet, $Ca_3\mathbf{Al}_2(\mathbf{Si}O_4)_3$; langbeinite, $K_2\mathbf{Mg}_2(SO_4)_3$; nasicon[1] = $Na_4\mathbf{Zr}_2(\mathbf{Si}O_4)_3$ and $\mathbf{Al}_2(\mathbf{W}O_4)_3$.

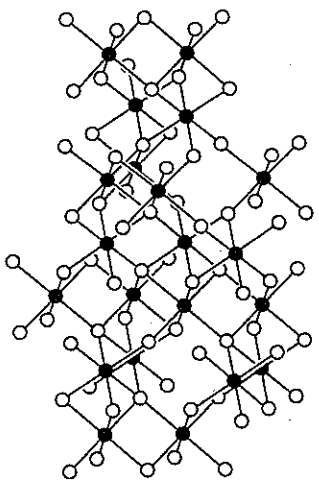

Fig. 7.79. Corundum as a (4,6)-connected net.

[1]Nasicon is a good Na-ion conducting silicate (**Na** silicate **con**ductor).

As for 4-connected nets, the same topology is often found in different contexts; for example, the same (4,6)-connected net is found in corundum, rhombohedral $Fe_2(SO_4)_3$ and in nasicon. We call it the **corundum** net. The corundum structure is possibly best appreciated as a packing of $\{Al\}O_6$ octahedra (see § 6.1.6), however it is shown as a bond (Al-O) network in Fig. 7.79.[1] Fig 7.80 shows the connection of octahedra and tetrahedra in rhombohedral $Fe_2(SO_4)_3$.

The occurrence of the **corundum** net in crystal structures illustrates the hierarchical way structures can develop. In $\mathbf{Al_2O_3}$, the edges of the net are Al-O bonds, in $\mathbf{Fe_2S_3O_{12}}$ the edges are Fe-O-S bonds. In $K_2\mathbf{Fe_2Zn_3}(CN)_{12}.xH_2O$, the edges are Fe-C-N-Zn bond groups (atoms in bold correspond to the vertices of the net). The molar volume of the last compound is over eight times that of the first one.

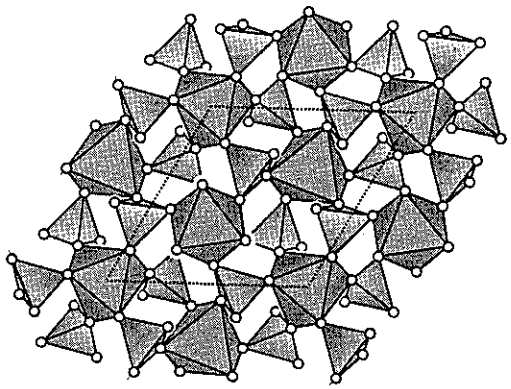

Fig. 7.80. The rhombohedral $Fe_2(SO_4)_3$ structure as a network of vertex-sharing $\{Fe\}O_6$ octahedra and $\{S\}O_4$ tetrahedra. The structure is projected down **c**. Although two kinds of octahedra are apparent in the drawing, they are topologically equivalent.

The different (4,6)-connected nets we have mentioned are readily distinguished by comparing their coordination sequences. The example below shows (a) that the (4,6)-nets of garnet and $Al_2(WO_4)_3$ are topologically distinct (despite a statement to the contrary sometimes encountered), and (b) that there are two topologically-distinct W atoms in $Al_2(WO_4)_3$.

net	*atom*	n_1	n_2	n_3	n_4	n_5	n_6
garnet	Al	6	12	42	50	114	110
	Si	4	16	28	74	76	162
$Al_2(WO_4)_3$	Al	6	14	42	50	114	110
	W(1)	4	17	28	70	76	163
	W(2)	4	16	28	72	76	162

[1]For many people, Fig. 7.79 will merely illustrate the difficulty of interpreting "ball and stick" diagrams of structures!

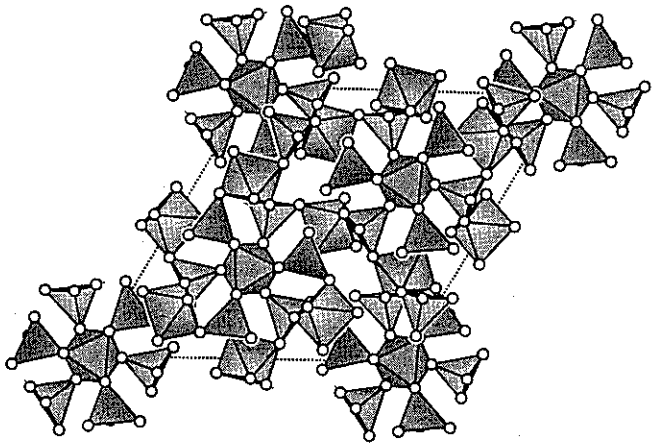

Fig. 7.81. A part of the garnet structure shown as linked $\{Si\}O_4$ tetrahedra and $\{Al\}O_6$ octahedra projected down [111]. For clarity only about a half of the polyhedra in the repeat unit [$\simeq$ (**a** + **b** + **c**)/2] out of the page are drawn.

The common, and important, structure of garnet is remarkably difficult to illustrate or describe. Here we illustrate (Fig. 7.81) just the connectivity of octahedra and tetrahedra which correspond to a (4,6)-connected net with -O- links as edges. Note that the vertices of the net (Al and Si positions) are at the sites of invariant lattice complexes (see § 3.4 for a list of coordinates); in § 6.6.4 we showed how the cation positions are related to **Cr_3Si**.

For some low-density (4,6)-connected nets see Exercise 15.

7.11 Notes

7.11.1 More 3-connected nets

Wells (reference in § 7.11.10) made a special study of uniform 3-connected nets (those in which the shortest rings at each angle are the same size). In contrast to uniform 4-connected nets, which are all 6^6, Wells found nets 7^3, 8^3, 9^3, 10^3 (see § 7.2) and 12^3. Here we list coordinates for a few of the simpler 3-connected nets with one kind of vertex. The reader may enjoy drawing them. They serve to illustrate the topologies that can occur.

A simple net $12_4{\cdot}12_7{\cdot}12_7$, which cannot be constructed with all angles equal to 120°, is for maximum volume:

12^3 — $P6_222$, $a = 2.475$, $c = 2.026$
vertices in 6 *g*: $\pm(x,0,0\ ;\ x,x,1/3\ ;\ \bar{x},\bar{x},1/3\ ;\ 0,\pm x,2/3)$, $x = 0.298$

There are many 8^3 nets. Known nets with one kind of vertex are all $8{\cdot}8{\cdot}8_2$. The first cannot have all angles equal to 120°, so we give coordinates for maximum volume; for the other two (Fig. 7.82), the coordinates are for bond angles of 120°:

I. $Im\bar{3}m$, $a = 6.352$
vertices in 96 *l*: $I + (\pm x,\pm y,\pm z\ ;\ \pm y,\pm x,\pm z)$, $x = 0.349$, $y = 0.190$, $z = 0.079$

II. $P6_222$, $a = 5/\sqrt{3}$, $c = \sqrt{6}$
vertices in 6 *i*: $(x,2x,0\ ;\ \bar{x},2\bar{x},0\ ;\ x,\bar{x},1/3\ ;\ \bar{x},x,1/3\ ;\ 2x,x,2/3\ ;\ \bar{x},2\bar{x},2/3)$, $x = 2/5$

III. $R\bar{3}m$, $a = 5$, $c = \sqrt{6}$
vertices in 18 *f*: $R \pm (x,0,0\ ;\ 0,x,0\ ;\ x,x,0)$, $x = 2/5$

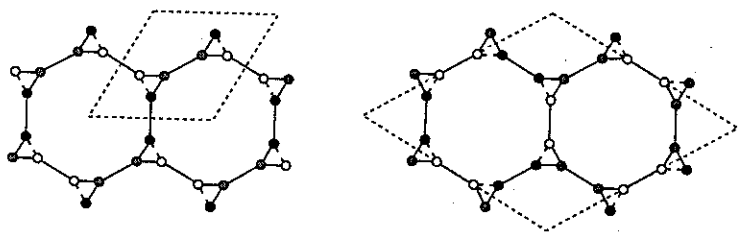

Fig. 7.82. The nets II (left) and III (right) projected down **c**. Open, shaded and filled circles are at elevations 0, 1/3 and 2/3, respectively.

Net II occurs as the (Cu,S) net in $BiCu_3S_3$ (Cu and S are 3-coordinated to each other).

As the 10^3 Y^* (§ 7.2) net is the only 3-dimensional 3-connected net with equivalent edges it is the only one that can be decorated with triangles to produce a uninodal 3-connected net (cf. § 7.5.2).[1] The 3-dimensional net is $3{\cdot}20_5{\cdot}20_5$ and is probably the least dense three-dimensional uninodal net ($c_{10} = 207$), we call it Y^*3. Data for this net are:

Y^*3 — $I4_132$, $a = 4/(\sqrt{24} - \sqrt{18}) = 6.0944$, $r = 0.106$, $\rho = 0.0555$
vertices in 24 *g*: $I + (1/8,x,1/4{-}x\ ;\ 3/8,\bar{x},3/4{-}x\ ;\ 5/8,1/2{-}x,3/4{+}x\ ;$
$7/8,1/2{+}x,1/4{+}x)$K, $x = (\sqrt{12} - 3)/8 = 0.0580$

The quasiregular 4-connected NbO (J^*) net could not be decorated with tetrahedra as the edges are coplanar; however if each vertex is replaced by a square, a 3-connected uninodal net is obtained[2] with symbol $4{\cdot}12_2{\cdot}12_2$:

4.12^2 — $Im\bar{3}m$, $a = 2 + \sqrt{8}$
vertices in 24 *g*: $I \pm (x,0,1/2\ ;\ 0,x,1/2)$K, $x = 1/(4 + \sqrt{8}) = 0.1464$

"Five-electron" compounds AB, where A is an alkali metal and B is from group 4A

[1]The analogous process in two dimensions produces 3.12^2 from 6^3.
[2]The analogy in two dimensions is the generation of 4.8^2 from 4^4.

(column 14) of the periodic table, have some fascinating structures, usually with *B* in three-coordination. The most common structures are **KGe** and **NaPb** in which *B* atoms form tetrahedral groups. In LiGe, however, a 3-dimensional net is formed in which the vertices are $8{\cdot}8{\cdot}10_3$ (LiSi and MgGa have the same structure). The angles are less than 120° as might be expected[1] and we give the actual coordinates for the structure.

LiGe — $I4_1/a$, $a = 9.75$ Å, $c = 5.78$ Å
Li in 16 *f*: $I \pm (x,y,z\ ;\ 1/2{-}x,\bar{y},1/2{+}z\ ;\ 3/4{-}y,\ 1/4{+}x,1/4{+}z\ ;$
$3/4{+}y,\ 3/4{-}x,\ 3/4{+}z)$, with $x = 0.100$, $y = 0.100$, $z = -0.055$
Ge ($8{\cdot}8{\cdot}10_3$) in 16 *f*, with $x = 0.106$, $y = 0.051$, $z = 0.394$

With these parameters, the Ge-Ge distances are 2.55 (2×) and 2.60 Å. The next shortest Ge-Ge distances are 4.10 Å (2×). A sketch of the Ge structure is shown in Fig. 7.83.

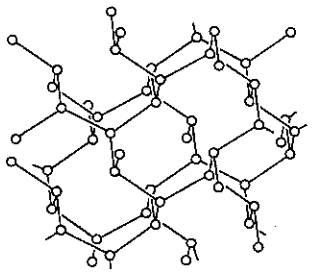

Fig. 7.83. The Ge net in LiGe.

Finally, a cubic net 6·9·9 which cannot be made with angles of 120°, so is given in its maximum volume form:

6.9^2 — $Fd\bar{3}m$, $a = 6.521$
vertices in 96 *g*: $F \pm (x,x,z\ ;\ x.1/4{-}x,1/4{-}z\ ;\ 1/4{-}x,x,1/4{-}z\ ;\ 1/4{-}x,1/4{-}x,z)\kappa$,
$x = 0.0708$, $z = 0.8875$

7.11.2 Model building

Most three-dimensional nets are best appreciated by building models. Fortunately, "spaghetti" models of 3- and 4-connected nets are easily and cheaply built from readily available triangular and tetrahedral connectors and plastic tubing.[2] Connectors with 3 mm (1/8 inch) diameter spokes are suitable. As considerable bond strain occurs in small (3- or 4-) circuits, it is best to use tightly-fitting flexible plastic tubing and to make the edges just over twice the length of the spokes from the vertices.

[1] LiGe may be written as Li^+Ge^-; Ge^- with five valence electrons is expected to have three 2-electron bonds pyramidally disposed and a non-bonding electron pair in an orbital at the apex of the pyramid. Compare $CaSi_2$ (§ 7.2)

[2] Available from many chemical supply houses. These are often sold as carbon, nitrogen, *etc.* atoms for building models of organic molecules, although the tetrahedral stars (also known as "caltrops" or "calthrops") probably more often end up as vertices in zeolite frameworks.

7.11.3 Identifying nets

It is sometimes quite difficult to identify nets in crystal structures, particularly when the structure is of low symmetry. A good way is to count numbers of (topological) neighbors using a computer (it is a good idea to count out to $n_k = 10$). *Usually* edges in nets correspond to shortest distances between vertices and it is very simple to count neighbors in this case. We have given the signature of a number of common nets in this chapter. It is also fairly simple also to get a computer to determine the Schläfli symbols of the vertices. Counting rings and numbers of neighbors by hand from a model can sometimes prove remarkably difficult (nets are known with more than 1000 shortest rings at an angle). If the net matches in both regards with a known net it is a *fairly* safe bet that they are the same.

The Exercises give some examples that are suitable for computer study; they are all done readily using EUTAX.

7.11.4 Diamond and SiC *polytypes*

In § 7.3.1 we discussed polytypes of diamond. Polytypes of SiC are derived from these by replacing half the vertices by Si so that each Si is surrounded by four C and *vice versa*. In a formal sense the structure can be considered as **cp** Si with C in one half the tetrahedral sites (either all "up" or all "down"). The polytypes of SiC (a large number have been characterized) are usually named for the nature of the close packing, e.g. as *hcc* or 6*H* or, in Zhdanov notation 33 (see § 6.1.4).

There is an important distinction to be made between the description of SiC polytypes and the description of close packing. In the *hcc* sphere packing all the *c* spheres are related by symmetry (see Exercise 6.8.2), but in *hcc* SiC the *c* layers of Si are not so related (there are two distinct kinds) and to know which is which, it is necessary to know which of the two sets of tetrahedral sites is occupied by C. Usually the sequence of layers along the **c** axis is written on a line; here we use the convention that the direction from left to right is along the direction of a Si to C vector of a SiC bond parallel to **c**. Thus with Greek letters for carbon positions 6*H* SiC is coded (see § 6.1.4):

$$A{\cdot\cdot}\alpha B{\cdot\cdot}\beta A{\cdot\cdot}\alpha C{\cdot\cdot}\gamma B{\cdot\cdot}\beta C\ldots$$

In this sequence $A{\cdot\cdot}\alpha$, $B{\cdot\cdot}\beta$, $C{\cdot\cdot}\gamma$ correspond to Si-C bonds along **c**. The layer *B* is *h* and the layers *A* and *C* are *c*.

The possible symmetries for polytypes of diamond are the centro-symmetric groups: $Fd\bar{3}m$ (only for cubic diamond itself), $P6_3/mmc$, $R\bar{3}m$, and $P\bar{3}m1$. In each case the center of symmetry is in the midpoint of a C-C bond. In the polytypes of SiC the center of symmetry is destroyed and we have the possible symmetries: $F\bar{4}3m$ (only for the

sphalerite form, polytype symbol 3*C*), $P6_3mc$ (polytype symbol *NH*), *R*3*m* (polytype symbol *NR*), and *P*3*m*1 (polytype symbol *NT*). In giving coordinates for atoms in SiC polytypes it is convenient to take an origin midway along a Si-C bond so that for every Si at *x*,*y*,*z* there is a C at $\bar{x},\bar{y},\bar{z}$. Thus we need only give explicitly coordinates for Si. It might be noted that in all polytypes except 3*C*, the symmetry at atom sites is 3*m*.

Table 7.5. Coordinates for idealized polytypes of SiC (see text)

type	vertex	pos	z_{Si}	type	vertex	pos	z_{Si}
3*C*	**c**						
2*H*	**h**	*b*	1/16	$10H_2$	**cchhh**	*b*	33/80
4*H*	**ch**	*a*	13/32	<311>	**chhhc**	*b*	1/80
<2>	**hc**	*b*	5/32		**hhhcc**	*a*	9/80
6*H*	**cch**	*b*	17/48		**hhcch**	*b*	17/80
<3>	**chc**	*b*	1/48		**hcchh**	*a*	5/16
	hcc	*a*	3/16	$10H_3$	**chchh**	*b*	49/80
9*R*	**chh**	*a*	69/72	<221>	**hchhc**	*a*	17/80
<21>	**hch**	*a*	13/72		**chhch**	*b*	13/16
	hhc	*a*	53/72		**hhchc**	*b*	33/80
$8H_1$	**ccch**	*b*	21/64		**hchch**	*b*	1/80
<4>	**cchc**	*a*	29/64	$15R_1$	**cchch**	*a*	73/120
	chcc	*b*	5/64	<32>	**chchc**	*a*	41/120
	hccc	*b*	45/64		**hchcc**	*a*	3/40
$8H_2$	**chhh**	*a*	29/64		**chcch**	*a*	19/40
<211>	**hhhc**	*b*	5/64		**hcchc**	*a*	7/8
	hhch	*a*	13/64	$15R_2$	**chhhh**	*a*	39/40
	hchh	*b*	21/64	<2111>	**hhhhc**	*a*	17/24
12*R*	**cchh**	*a*	73/96		**hhhch**	*a*	13/120
<31>	**chhc**	*a*	17/96		**hhchh**	*a*	101/120
	hhcc	*a*	19/32		**hchhh**	*a*	29/120
	hcch	*a*	11/32	21*R*	**ccchcch**	*a*	15/56
5*T*	**ccchh**	*c*	9/40	<43>	**cchcchc**	*a*	55/56
<41>	**cchhc**	*a*	17/40		**chcchcc**	*a*	39/56
	chhcc	*b*	5/8		**hcchccc**	*a*	23/56
	hhccc	*c*	33/40		**cchccch**	*a*	19/24
	hccch	*b*	1/40		**chccchc**	*a*	29/168
$10H_1$	**cccch**	*a*	5/16		**hccchcc**	*a*	31/56
<5>	**ccchc**	*b*	33/80				
	cchcc	*b*	1/80				
	chccc	*a*	9/80				
	hcccc	*b*	57/80				

In Table 7.5 we give a name (6*H* etc.) for all polytypes with five or fewer distinct kinds of Si (and hence C) atom and also for a 21*R* polytype. Underneath the name, the shortened Zhdanov symbol.[1] Next is given in bold the symbol (**h** or **c**) for the Si layer followed by

[1]If the number of symbols between angle brackets is odd the Zhdanov symbol is twice as long. Thus <221> refers to 221221.

the symbol for the following layers along the **c** axis in the direction specified by the sense of the Si to C bond. Next we give the Wyckoff symbol of the positions and finally the *z* coordinate for Si in the ideal structure with regular tetrahedra. For this ideal structure $a = \sqrt{(8/3)}d$ where *d* is the Si-C bond length. The coordinates of special positions (*z* is given in the table) and the axial ratios are:

NH — $P6_3mc$, $c/a = N\sqrt{(2/3)}$
2 *a*: (0,0,*z* ; 0,0,1/2+*z*) ; 2 *b*: (1/3,2/3,*z* ; 2/3,1/3,1/2+*z*)

NR — *R*3*m*, $c/a = N\sqrt{(2/3)}$
3 *a* : *R* + (0,0,*z*)

NT — *P*3*m*1, $c/a = N\sqrt{(2/3)}$
1 *a*: (0,0,*z*) ; 1 *b*: (1/3,2/3,*z*) ; 1 *c*: (2/3,1/3,*z*)

Dozens of polytypes of SiC have been characterized. Most are intergrowths of *hc* (4*H*) and *hcc* (6*H*). Some polytypes have been assigned special names:

$$\beta = 3C,\ \text{I} = 15R_1,\ \text{II} = 6H,\ \text{III} = 4H,\ \text{IV} = 21R.$$

7.11.5 Two more nets derived from 6^3: "C" and "D phases"

Many compounds $MTT'X_4$ have structures with nets derived from 6^3 nets (cf. § 7.3.3). These are often described as derived from tridymite but this is only correct if the net of the *T* atoms is **lonsdaleite** (§ 7.3.1). Here we mention two binodal nets derived from 6^3 (Fig. 7.84). The first is found as the (Be,P) net in the structure of **beryllonite**, $NaBePO_4$, and in related compounds, and is often called the "C phase" structure. The second occurs in compounds such as $KAlGeO_4$ [(Al,Ge) net] and is known as the "D phase structure."

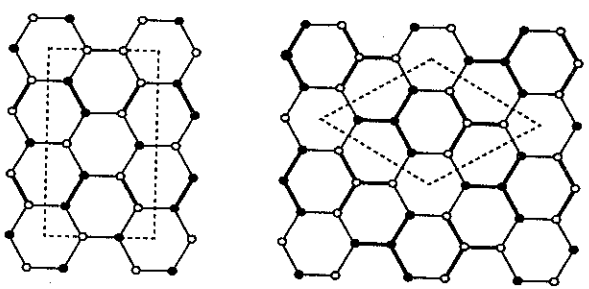

Fig. 7.84. Derivation of two 4-connected nets from 6^3. Fourth bonds go up and down from open and filled circles respectively. Heavy lines are quadrangles seen in projection. Left: **beryllonite** (*C* phase), Right: *D* phase.

In cubanite, $CuFe_2S_3$, all the atoms are 4-connected, and the net of all the atoms is **beryllonite** (for crystallographic data for cubanite see Appendix 5).

7.11.6 Nets in CdP_2 *and* $CdAs_2$

The nets in CdP_2 and $CdAs_2$ provide a treat. Cd is in tetrahedral coordination and each P (or As) atom is bonded to two other P (As) atoms so the net of all the atoms is 4-connected [compare the (Cu,P) net in $BaCu_2P_4$—see § 7.6]. In $CdAs_2$ (Fig 7.85, left), 4_3 helices of As are cross-linked by Cd atoms. The net is remarkable for the large number of 11-rings (see the vertex symbols below). The net of the Cd atoms alone (with -As- acting as edges) is **diamond**, so the structure, considered as a framework of corner-connected {Cd}As_4 tetrahedra, is topologically the same as that of **cristobalite** SiO_2.

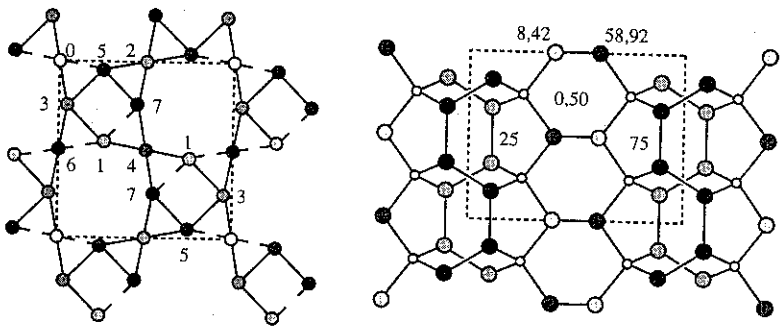

Fig. 7.85. Left: **$CdAs_2$** projected on (001). Numbers are elevations in multiples of $c/8$ with even numbers for **Cd**. Right: **CdP_2** projected on (110). **c** is horizontal on the page and numbers are elevations in units of |**(a+b)**|/100. Smaller circles (at 0 and 50) are the 5·5·5·5·6·6 vertices.

CdP_2 occurs in two forms (α and β) that are topologically the same. The net of all the atoms has two kinds of vertex, but one kind is P and the second kind is alternating Cd and P, so there are three kinds of atom in the structure. The *net* is illustrated in Fig. 7.85 (right).

Crystallographic data for the nets (with unit edge) are:

$CdAs_2$ $I4_122$, $a = 3.1706$, $c = 1.5804$, $r = 0.756$
$5{\cdot}5{\cdot}6{\cdot}6{\cdot}11_{26}{\cdot}11_{26}$ in 4 *a*: $I + (0,0,0\ ;\ 0,1/2,1/4)$
$5{\cdot}5{\cdot}5_2{\cdot}11_{20}{\cdot}6{\cdot}6$ in 8 *f*: $I + (x,1/4,1/8\ ;$ etc.), $x = 0.4549$

CdP_2 $P4_2/ncm$, $a = 2.1912$, $c = 3.9493$, $r = 0.633$
$5{\cdot}5{\cdot}5{\cdot}5{\cdot}6{\cdot}6$ in 4 *b*: $\pm(1/4,3/4,3/4\ ;\ 1/4,3/4,1/4)$
$5{\cdot}6{\cdot}5{\cdot}6{\cdot}5{\cdot}7_2$ in 8 *i*: $\pm(x,x,z\ ;$ etc.), $x = 0.0886$, $z = 0.3942$

ZnP_2 and $ZnAs_2$ are isostructural. The (Zn,P) or (Zn,As) nets have four kinds of vertex with 5-, 6- and 7-rings and are not discussed further. Notice that $BaCu_2P_4$ (p. 334) may be written as $Ba^{2+}[CuP_2^-]_2$ and that CuP_2^- and ZnP_2 are isoelectronic.

7.11.7 More on the **moganite**, **quartz** *and related nets*

On p. 322 we mentioned the net of the Si atoms in the **moganite** form of SiO_2. Here we describe a simple relationship between that net and the **quartz** net. In Fig 7.86 we show projections of the $P6_222$ (^+Q) and $P6_422$ (^-Q) enantiomorphs on $(11\bar{2}0)$ of the conventional hexagonal cell (cf. § 7.3.11, p. 316). The two structures are related by reflection in a mirror plane at elevation 1/4. The bottom left shows the **moganite** net projected on (010) of *Ibam* as it appears in Fig. 7.37 (p. 322). Notice that the net consists of alternating bands of left- and right-hand **quartz** net. Interestingly real **moganite** SiO_2 can similarly decomposed into bands of left- and right-handed **quartz** SiO_2. In the amethyst form of quartz, Brazilian twins (intergrowths of left- and right-) are common and microscopic bands of moganite-structure material separate the two enantiomers [for details see B. G. Hyde & A. C. McLaren, *Aust. J. Chem.* (1996)].

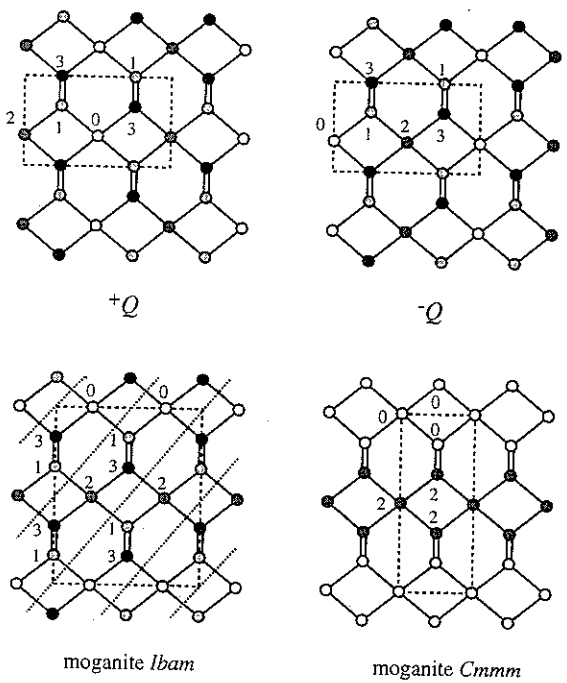

Fig. 7.86. Top: the two enantiomers of the **quartz** net projected on $(11\bar{2}0)$ with the orthohexagonal cell outlined. Numbers are elevations in multiples of |**a+b**|/4. Bottom left: the **moganite** net projected on (010); numbers are now elevation in units of $b/4$. Note the alternating bands of ^+Q and ^-Q (shaded). Bottom right: an alternative conformation of **moganite** with 3 vertices in the repeat unit [projection on (010)].

It should be emphasized that the *Ibam* conformation of the moganite net is a close approximation to the Si structure reported for the mineral and for that reason was used to illustrate the structure.[1] However the figure shows that a simpler, more symmetrical (*Cmmm*) conformation of the net (with of course, the same *topology*) can be realized with only three vertices in the repeat unit. The nets of § 7.3.11 (**quartz**, **NbO** and **W2**) are the only others known with this property. Crystallographic data for this conformation are:

moganite net *Cmmm*, $a = 3.517$, $b = 1.786$, $c = 1.513$
$4{\cdot}4{\cdot}6_2{\cdot}6_2{\cdot}8_2{\cdot}8_2$ in 2 *a*: $C + (0,0,0)$
$4{\cdot}8_6{\cdot}6{\cdot}6{\cdot}6{\cdot}6$ in 4 *h*: $C \pm (x,0,1/2)$, $x = 0.186$

Fig. 7.86 should readily suggest ways of generating other nets in the **quartz-moganite** family. Two simple examples are shown in Fig. 7.87. That on the left (with 6- and 8-rings) is related to **quartz**—but notice that the vertices in 2 *a* (see below) are co-planar with their four neighbors (as in **NbO**). The net (which also has 4-rings) on the right of the figure is closely related to **moganite**. Parameters derived in what should be an obvious way from those for the orthohexagonal cell of **quartz** (with a shift of origin) are:

Fig. 7.87 (left) *Pmna*, $a = \sqrt{8}$, $b = \sqrt{3}$, $c = \sqrt{(8/3)}$
$6_2{\cdot}6_2{\cdot}6_2{\cdot}6_2{\cdot}8_4{\cdot}8_4$ in 2 *a*: (0,0,0 ; 1/2,0,1/2)
$6{\cdot}6{\cdot}6{\cdot}6{\cdot}6_2{\cdot}6_2$ in 4 *g*: $\pm(\pm 1/4, y, 1/4)$, $y = 1/3$

Fig. 7.87 (right) *Pccm*, $a = \sqrt{3}$, $b = \sqrt{(8/3)}$, $c = \sqrt{8}$
$4{\cdot}4{\cdot}6{\cdot}6{\cdot}8_2{\cdot}8_2$ in 2 *e*: $\pm(0,0,1/4)$
$4{\cdot}8_{10}{\cdot}6{\cdot}8_5{\cdot}6{\cdot}8_5$ in 4 *q*: $\pm(x,y,0 ; \bar{x},y,1/2)$, $x = 1/3$, $y = 1/4$

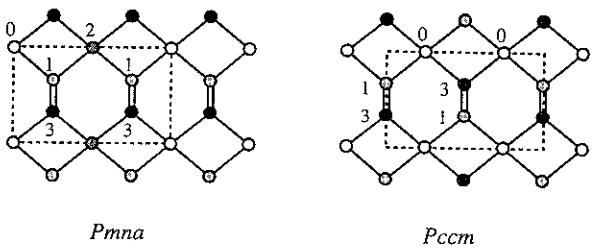

Pmna *Pccm*

Fig. 7.87. Two nets related to **quartz**. Left: projected (001), elevations in multiples of *c*/4. Right: projected on (010), elevations in multiples of *b*/4.

7.11.8 Stereo picture of nets: Y, clathrate hydrates I and II*

Many people find stereo pictures of nets helpful.[2] Here (Figs. 7.88-7.90) are such

[1] BeH_2 has the moganite structure, and the structure has symmetry *Ibam*. See Exercise 17.

[2] Stereo viewers (available in many bookstores) are helpful. Some people find the stereo perception easier when the picture is turned upside down.

pictures of three important nets that are difficult to illustrate.

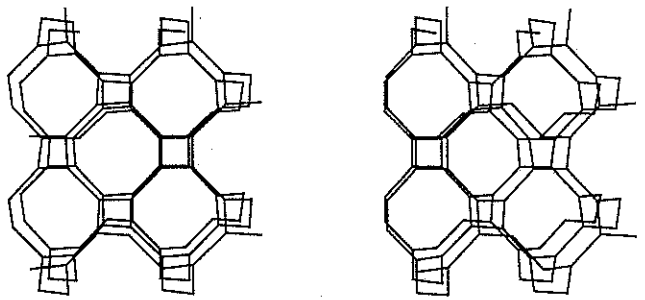

Fig. 7.88. A stereo view of the Y^* net (compare Fig. 7.6).

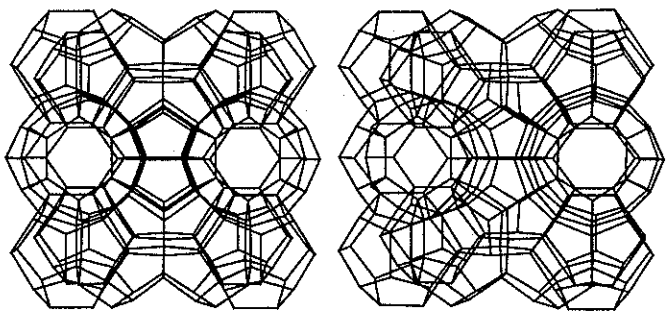

Fig. 7.89. A stereo view of the Type I hydrate net (compare Fig. 7.51).

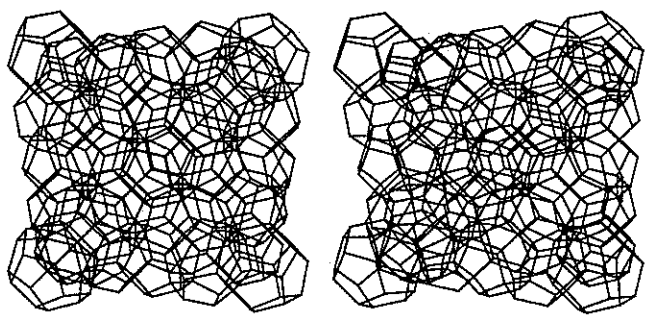

Fig. 7.90. A stereo view of the Type II hydrate net.

7.11.9 Anion positions and the possibility of open zeolite frameworks

We have seen (§ 7.5.2, p. 330) that to make open (rare) nets with low density and large rings, configurations which also have a large concentration of small (3- or 4-) rings are generally needed. We have also seen (§ 5.2.1, p. 150) that small rings (<6-rings) put a constraint on the maximum *T*-*X*-*T* angle possible for catenated regular $\{T\}X_4$ tetrahedra. Thus for a ring of three tetrahedra (Fig. 5.19) the maximum *T*-*X*-*T* angle is 130.5°, and for clusters of 3-rings forming a tetrahedron (to give a supertetrahedron of four regular $\{T\}X_4$ tetrahedra), it should be obvious from Fig. 5.18 that the *T*-*X*-*T* angle is 109.47° [the tetrahedral angle, $\cos^{-1}(-1/3)$]. Similarly for a ring of four tetrahedra (Fig. 5.19) the maximum *T*-*X*-*T* angle is 160.5° and for clusters of 4-rings forming a cube (to give a T_8X_{20} cluster of regular $\{T\}X_4$ tetrahedra, Fig. 5.20) the maximum *T*-*X*-*T* angle is 148.4°. To make a cluster of twelve tetrahedra with *T* atoms at the vertices of a pair of cubes sharing a face, the *T*-*X*-*T* angles are reduced to 109.47° (Fig. 7.91). The "cubes" are no longer cubes, but tetragonal prisms; the faces parallel to those shared are square, but the others have edges in the ratio 1:1.21.

A way of making nets of low density is to replace vertices in a net by tetrahedra of vertices as described in § 7.5.2 (this process can be repeated *ad nauseam* to produce nets of arbitrarily low density). Another way is to replace cubes in nets such as those of **Linde A** (Fig. 7.38) or *W**8 (Fig.7.42) by stacks of *N* cubes sharing faces; nets of arbitrarily low density can be made by increasing *N*. In both these cases however, some *T*-*X*-*T* angles must be as small as 109.47°. In silicas with framework structures the Si-O-Si angle is usually greater than about 140° (with similar values in related oxides), so these open structures cannot be formed.[1] In fact it appears that for alumino-silicates the **faujasite** structure is about the least dense that can be made. We give here coordinates for some tetrahedral framework structures based on simple low-density nets with cubic symmetry. The coordinates are for regular tetrahedra of unit *T*-*X* distance and are such as to maximize the minimum *T*-*X*-*T* angle. It may be seen that the tetrahedral structure based on *W**8 is not very likely to be formed for an alumino-silicate framework.

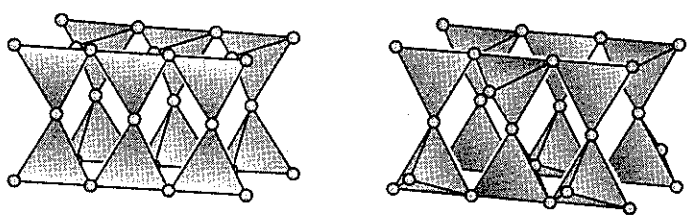

Fig. 7.91. Left: a cluster of twelve regular tetrahedra with centers at the vertices of two "cubes" (actually tetragonal prisms) sharing a common face. Right: a cluster of twelve tetrahedra corresponding to a fragment of a net containing "up-down" tetrahedra and based on rectangles sharing a common edge (see text).

[1]Minimum *T*-*X*-*T* angles are much smaller in sulfides than in oxides, so the former offer much greater promise for making open framework structures. See for example Exercise 16.

In the case of **sodalite** we give coordinates for the maximum *T*-*X*-*T* angle; decreasing the angle (as in the real mineral) will increase the density as described on p. 275. The transition from β-quartz to α-quartz (§ 3.6) corresponds likewise to a decrease in density accomplished (for rigid tetrahedra) by decreasing the *T*-*X*-*T* angle.[1] Thus for a *given* topology, the density of tetrahedral framework structures can often be increased by decreasing the *T*-*X*-*T* angle; but to achieve frameworks of lower minimum density the minimum *T*-*X*-*T* angle has to be decreased (see e.g. the crystallographic data below).

sodalite — $Im\bar{3}m$, a = 5.575, density = 0.0692 *T* vertices per unit volume
T in 12 *d*: (1/4,0,1/2 ; etc.) ; *X* in 24 *h*: (0,*y*,*y* ; etc.), y = 0.3536, *T*-*X*-*T* = 160.6°

rho — $Im\bar{3}m$, a = 9.2733, density = 0.0602 *T* vertices per unit volume
T in 48 *i*: (1/4,*y*,1/2–*y* ; etc.), y = 0.1036
X(1) in 48 *j*: (0,*y*,*z* ; etc.), y = 0.2242, z = 0.3809, *T*-*X*(1)-*T* = 147.6°
X(1) in 48 *k*: (*x*,*x*,*z* ; etc.), x = 0.1658, z = 0.3707, *T*-*X*(1)-*T* = 147.6°

Linde A — $Pm\bar{3}m$, a = 7.4339, density = 0.0584 *T* vertices per unit volume
T in 24 *k*: (0,*y*,*z* ; etc.), y = 0.1831, z = 0.3706
X(1) in 24 *m*: (*x*,*x*,*z* ; etc.), x = 0.1098, z = 0.3447, *T*-*X*(1)-*T* = 148.4°
X(2) in 12 *h*: (*x*,0,1/2 ; etc.), x = 0.2197, *T*-*X*(2)-*T* = 148.4°
X(3) in 12 *i*: (0,*y*,*y* ; etc.), y = 0.2929, *T*-*X*(3)-*T* = 160.5°

faujasite — $Fd\bar{3}m$, a = 15.1618, density = 0.0551 *T* vertices per unit volume
T in 192 *i*: (*x*,*y*,*z* ; etc.), x = 0.0361 y = 0.1240, z = 0.3045
X(1) in 96 *h*: (0,*y*,$\bar{y}$; etc.), y = 0.1059, *T*-*X*(1)-*T* = 140.8°
X(2) in 96 *g*: (*x*,*x*,*z* ; etc.), x = 0.0697, z = 0.3211, *T*-*X*(2)-*T* = 140.8°
X(3) in 96 *g*, x = 0.3284, z = 0.0374, *T*-*X*(3)-*T* = 149.2°
X(4) in 96 *g*, x = 0.2537, z = 0.1395, *T*-*X*(4)-*T* = 152.7°

W*8 — $Im\bar{3}m$, a = 12.5567, density = 0.0485 *T* vertices per unit volume
T in 96 *l*: (*x*,*y*,*z* ; etc.), x = 0.0793 y = 0.3231, z = 0.4267
X(1) in 48 *j*: (0,*y*,*z* ; etc.), y = 0.1655, z = 0.3917, *T*-*X*(1)-*T* = 133.8°
X(2) in 48 *i*: (1/4,*y*,1/2–*y* ; etc.), y = 0.0983, *T*-*X*(2)-*T* = 133.8°
X(3) in 48 *k*: (*x*,*x*,*z* ; etc.), x = 0.1228, z = 0.3897, *T*-*X*(3)-*T* = 133.8°
X(4) in 48 *j*, y = 0.3309, z = 0.4281, *T*-*X*(4)-*T* = 168.7°

An interesting way to obtain tetrahedral frameworks of low density has been described.[2] The nets are based on the "up-down" principle of coupling 3-connected two-dimensional nets. In § 7.3.8 (p. 311) examples are given in which "up-down" rods of vertices are derived from squares of the planar net. In **VPI-5** (§ 7.8.4) the net is derived from a two-dimensional net with pairs of squares sharing an edge (fusion of two up-down rods), and it should be obvious that **VPI-5** (Fig. 7.62) is simply derived from **$AlPO_4$-5** (Fig. 7.23) by replacing a square by two "squares" (actually now rectangles) sharing an edge. In Fig.

[1]Another tetrahedral framework than can have variable density is **cristobalite** (§ 6.3.9, p. 240). Note that in cristobalite (which has all 6-rings) the *T*-*X*-*T* angle can be as much as 180°. In the quartz structure, which has 6- and 8-rings, with regular tetrahedra the maximum angle is 155.6° (in the β- structure).

[2]J. V. Smith & W. J. Dytrych, *Nature* **309**, 607 (1984).

7.91, we show a fragment of the configuration of tetrahedra that results. In Fig. 7.92 we show a net derived analogously from **$TlZn_2Sb_2$** (Fig. 7.23). Clearly the strip of two rectangles could be replaced by strips of arbitrary length, so nets with large rings of any even size could be made, and with density approaching zero for very large strips. In nets of this type, the vertices on the octagon have Schläfli symbol $4{\cdot}6_2{\cdot}6{\cdot}6_3{\cdot}6{\cdot}6_3$; all the rest (on edges between two rectangles) have symbol $4{\cdot}6_3{\cdot}4{\cdot}6_3{\cdot}6{\cdot}6_4$. It may be seen that there at most two 4-rings meeting at a vertex, so that low (in the limit zero) density is achieved in this case with a relatively small number of small rings. For frameworks of regular tetrahedra, some of the *T*-*X*-*T* angles cannot exceed $\cos^{-1}(-5/9) = 123.75°$.

In the real $AlPO_4$ framework of VPI-5 [L. B. McCusker *et al.*, *Zeolites*, **11**, 308 (1991)] the tetrahedra are not very regular; in particular one $\{Al\}O_4$ "tetrahedron" is better thought of as part of an octahedron (with two water molecules completing the coordination sphere). The Al-O-P angles range from 137° to 162° (Al...P = 3.09 to 3.27 Å); compare berlinite $AlPO_4$ in which the values are Al-O-P = 142.5° and Al...P = 3.08 Å.

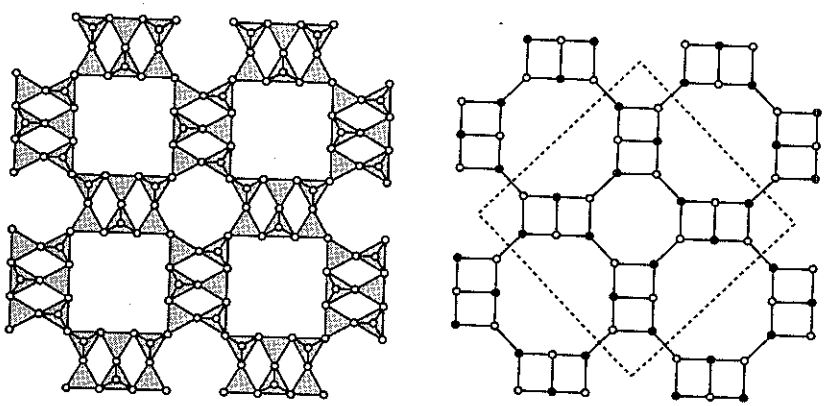

Fig. 7.92. An "up-down" net derived by replacing the squares of **$TlZn_2Sb_2$** (Fig. 7.23) by pairs of rectangles sharing an edge. Left: showing the $\{T\}X_4$ tetrahedra in projection down the 4-fold axis. Right: the *T* network in the same projection. Open (filled) circles are vertices with links to layers above (below).

In TX_2 frameworks of zeolite structures, the *T* atoms can be considered to lie on a surface with *X* atoms on either side. In a polyhedral cavity of *n T* atoms, there are $3n/2$ *X* atoms (one associated with each *T*...*T* "edge") generally slightly closer to the center of the cavity. Thus, for the framework of **Linde A** with the coordinates given above, the following atoms are at the given distances from the center of the cavity:

cavity	*T* atoms	*X* atoms
4.6.8	4.50 (48×)	4.26 (48×), 4.31 (24×)
4.6^2	3.07 (24×)	2.81 (24×), 3.08 (12×)
4^3 (cube)	1.67 (8×)	1.63 (8×), 1.63 (4×)

Similarly the *TXTX*... rings on the surface of cages are usually puckered and, especially for larger rings, with *X* inside the ring. Fig. 7.93 shows the 8-ring in **Linde A**.

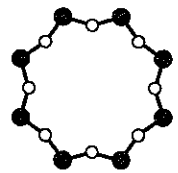

Fig. 7.93. The 8-ring in **Linde A** TX_2 with coordinates given on p. 373. Filled circles are *T*.

7.11.10 References

The pioneering work on nets and infinite polyhedra by A. F. Wells is collected in his *Three-dimensional Nets and Polyhedra* [Wiley, New York (1977)]. A catalog of 4-connected nets (over 500) has been compiled by Smith and Bennett [see J. V. Smith, *Chem. Rev.* **88**, 149 (1988)]. References to zeolite nets are given in § 7.8 (p. 337) and some references to the topology of nets are given in Appendix 3 (§ A3.9). For a review of structures of clathrate hydrates and inclusion compounds see Chapter 7 of *Crystallography in Modern Chemistry* by T. C. W. Mak & G.-D. Zhou [Wiley, New York (1992)].

Those who are skeptical about the relevance of geometry to chemistry should know that some of the beautiful zeolite and other structures based on polyhedron packings that appear in this chapter were first described (and illustrated as models) by A. Andrieni in a classical paper *Sulle reti di poliedri regolari e semiregolari e sulle corrispondenti reti correlative* [*Mem. Soc. Ital. delle Scienze* Ser 3, **14**, 75 (1907)]. The Type I and Type II hydrate structures were predicted (and elegantly illustrated) by W. F. Clausen [*J. Chem. Phys.* **19**, 259 and 662 (1951)]. Many structures now known were predicted in advance, especially by A. F. Wells and by J. V. Smith and collaborators (*loc. cit. supra*). Indeed some zeolite structures could only be solved with the knowledge of possible structures, their symmetries and approximate coordinates. Some nets that were described as "unknown" in earlier drafts of this chapter, were subsequently found in recently determined crystal structures.

7.12 Exercises[1]

1. A body-centered array of cubes connected corner to corner by additional edges will produce a simple 4-connected net somewhat analogous to the connection of octahedra in the 5-connected CaB_6 net.[2]

[1]Most of the Exercises in this chapter will be tedious to do by hand, but are readily done using a computer program such as EUTAX (see the Note to the Reader).

[2]This structure ("*supercubane*") has been proposed as a possible form of carbon. See R. L. Johnston & R. Hoffmann, *J. Amer. Chem. Soc.* **111**, 810 (1989). Compare with the **octadecasil** net (§ 7.8.6).

$Im\bar{3}m$, $a = 2 + 2/\sqrt{3} = 3.1457$
$4{\cdot}8_2{\cdot}4{\cdot}8_2{\cdot}4{\cdot}8_2$ in 16 *f*: $I \pm (\pm x,x,x)$κ, $x = \sqrt{3}/(4 + \sqrt{48}) = 0.1585$

2. The 4-connected net of the B atoms in CaB_2O_4 may described as follows for unit edge (the same net appears in the structures of SrB_2O_4, $BaAl_2S_4$ and $BaGa_2S_4$):

$Pa\bar{3}$, $a = 3.5334$, $r = 0.544$.
$3{\cdot}6{\cdot}7{\cdot}7{\cdot}7_2{\cdot}7_2$ in 24 *d*: $\pm(x,y,z$; $x,1/2{-}y,1/2{-}z$; $1/2{+}x,\ y,1/2{-}z$;
$1/2{-}x,1/2{+}y,z)$κ, $x = 0.1046$, $y = 0.1709$, $z = 0.3295$.

3. γ-$LiAlO_2$ is tetragonal:

γ-$LiAlO_2$ $P4_12_12$, $a = 5.169$, $c = 6.268$ Å
Li and Al in 4 *a* : $(x,x,0$; $\bar{x},\bar{x},1/2$; $\pm(1/2{-}x,1/2{+}x,1/4))$
For Li, $x = 0.688$; for Al, $x = 0.324$
O in 8 *b*: $(x,y,z$; $\bar{x},\bar{y},1/2{+}z$; $1/2{-}y,1/2{+}x,1/4{+}z$; $1/2{+}y,1/2{-}x,3/4{+}z$; $y,x,\bar{z}$;
$\bar{y},\bar{x},1/2{-}z$; $1/2{-}x,1/2{+}y,1/4{-}z$; $1/2{+}x,1/2{-}y,\ 3/4{-}z)$,
$x = 0.210$, $y = 0.164$, $z = 0.228$.

Li and Al are each on **diamond** nets and the atoms taken all together are on a **CrB_4** net (this structure is derived from that of β-BeO by the substitution $2Be \rightarrow Li + Al$).

4. β-$LiGaO_2$ is orthorhombic:

β-$LiGaO_2$ $Pna2_1$, $a = 5.402$, $b = 6.372$, $c = 5.007$ Å
all atoms in 4 *a*: $(x,y,z$; $\bar{x},\bar{y},1/2{+}z$; $1/2{+}x,1/2{-}y,z$; $1/2{-}x,1/2{+}y,1/2{+}z)$
Li: $x = 0.421$, $y = 0.127$, $z = 0.494$; Ga: $x = 0.082$, $y = 0.126$, $z = 0.0$
O(1): $x = 0.070$, $y = 0.112$, $z = 0.371$; O(2): $x = 0.407$, $y = 0.139$, $z = 0.893$

Li and Ga are each on **diamond** nets and the atoms taken all together are on a **lonsdaleite** net (this structure is derived from that of ZnO by the substitution $2Zn \rightarrow Li + Ga$). The O atoms are **hcp**, as are the metal atoms (combined).

5. A 4-connected net considered by Heesch & Laves is derived from a space filling by truncated tetrahedra, truncated cubes and truncated cuboctahedra. We call this net **$HL4_2$**.

$HL4_2$ $Fm\bar{3}m$, $a = 2 + \sqrt{18} = 6.2426$, $r = 0.395$
$3{\cdot}4{\cdot}6{\cdot}8{\cdot}6{\cdot}8$ in 96 *k*: $F + (\pm x,\pm x,\pm z)$κ, $z = 1/(4 + \sqrt{72}) = 0.0801$, $x = (1 + \sqrt{2})z = 0.1934$

A "spaghetti" model is easily made if it is realized that each triangular face of the truncated cubes is shared with a similar face of a truncated tetrahedron and *vice versa*. The truncated cuboctahedra and truncated cubes likewise share octagonal faces.

6. Another uninodal 4-connected net occurs as the (Si,Al) framework of the natural zeolite analcime, $NaAlSi_2O_6{\cdot}H_2O$. A formal description of the net with unit edge length is:

analcime $Ia\bar{3}d$, $a = \sqrt{(96/5)} = 4.3818$, $r = 0.571$; $4{\cdot}4{\cdot}6{\cdot}6{\cdot}8_4{\cdot}8_4$ in 48 *g*: $(1/8,x,1/4{-}x$; etc.), $x = 1/3$

Try to make or find a good picture of this net (difficult!).
In the bixbyite structure of Sc_2O_3, the O atom positions are in positions 48 *e* of $Ia\bar{3}$: x,y,z etc., with $x = 0.390$, $y = 0.155$, $z = 0.380$. Each O atom has four O nearest neighbors. Show that the net of the O atoms has the same topology as that of analcime.

7. The net of the recently described mineral montesommaite [approximate composition $(K,Na)_9Al_9Si_{23}O_{64}{\cdot}10H_2O$] is very simple [hint: project on (100)]:

montesommaite $I4_1/amd$, $a = 2.258$, $c = 5.795$, $r = 0.542$
$4{\cdot}5_2{\cdot}5{\cdot}8_2{\cdot}5{\cdot}8_2$ in 16 *h*: $I \pm (0,y,z$; etc.), $y = 0.028$, $z = 0.0856$

8. The diamond net is ubiquitous (see Exercises 3 and 4). Here are two more examples of its occurrence as the metal arrays in oxides. (Note that we are concerned with the *topology* of the structure, in this instance the topology of the net defined by edges joining the first four nearest neighbors.)

corundum (Al_2O_3) $R\bar{3}c$, $a = 4.759$, $c = 12.991$ Å
Al in 12 *c*: $R \pm (0,0,z$; $0,0,1/2{+}z)$, $z = 0.3523$; O in 18 *e*: 0.3064,0,1/4

anatase (TiO_2) $I4_1/amd$, $a = 3.785$, $c = 9.514$ Å
Ti in 4 *a*: $I \pm (0,3/4,1/8)$; O in 8 *e*: 0,1/4,0.0816

9. Another net that occurs in many different contexts is **$SrAl_2$** (the Al net in $SrAl_2$). Two examples of compounds iso-structural with $SrAl_2$ were given in Exercise 3.8.11. Here are three other examples of its occurrence as the net of (a) Mg and Si in SrMgSi, (b) Both atoms in α-Np and (c) Al and Si in synthetic zeolite Li-A ($LiAlSiO_4{\cdot}2H_2O$):

SrMgSi *Pnma*, $a = 7.78$, $b = 4.56$, $c = 8.49$ Å
Sr in 4 *c*: $\pm(x,1/4,z$; $1/2{+}x,1/4,1/2{-}z)$, $x = 0.515$, $z = 0.683$
Mg in 4 *c*, $x = 0.640$, $z = 0.057$; Si in 4 *c*, $x = 0.276$, $z = 0.110$

α-Np *Pnma*, $a = 6.661$, $b = 4.271$, $c = 4.888$ Å
Np(1) in 4 *c*: $\pm(x,1/4,z$; $1/2{+}x,1/4,1/2{-}z)$, $x = 0.036$, $z = 0.208$
Np(2) in 4 *c*, $x = 0.319$, $z = 0.842$

Li-A $Pna2_1$, $a = 10.31$, $b = 8.18$, $c = 5.00$ Å
Al in 4 *a*: $(x,y,z$; $\bar{x},\bar{y},1/2{+}z$; $1/2{+}x,1/2{-}y,z$; $1/2{-}x,1/2{+}y,1/2{+}z)$,
$x = 0.136$, $y = 0.072$, $z = 0.25$; Si in 4 *a*, $x = 0.358$, $y = 0.378$, $z = 0.252$

10. The compound $NaGaSn_5$ can be considered in a formal sense as $Na^+(Ga^-Sn_5)$ with the (Ga^-Sn_5) part having four valence electrons per atom, so it is not surprising to find these atoms forming a 4-connected net. The (Ga,Sn) structure was reported as:

$NaGaSn_5$ $P3_112$, $a = 6.328$, $c = 6.170$ Å
M1 in 3 *a*: $(x,\bar{x},1/3$; $x,2x,2/3$; $2\bar{x},\bar{x},0)$, $x = 0.431$
M2 in 3 *b*: $(x,\bar{x},5/6$; $x,2x,1/6$; $2\bar{x},\bar{x},1/2)$, $x = 0.903$

with M1 and M2 being a disordered combination of Ga and Sn. Show that the net of the atoms is a uninodal net 5·5·5·5·5·8_4 which, in its most symmetrical form has symmetry $P6_122$. The net is illustrated in Fig. 7.94 below (note that a and c are approximately equal).

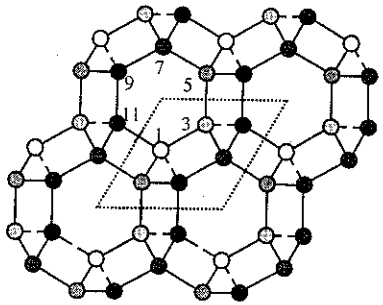

Fig 7.94. A net 5·5·5·5·5·8_4 projected down the c axis of $P6_122$. Elevations are in multiples of $c/12$.

11. The P atom positions in one form of P_2O_5 have been given as:

Fdd2, a = 16.3, b = 8.12, c = 5.25 Å
P in 16 *b*: $F + (x,y,z\ ;\ \bar{x},\bar{y},z\ ;\ 1/4{-}x,1/4{+}y,1/4{+}z\ ;\ 1/4{+}x,1/4{-}y;1/4{+}z)$,
x = 0.075, y = 0.083, z = 0.153

Verify that the five shortest P-P distances are 2.79, 2.92 (2×) and 4.34 (2×) Å and that the three shortest P-P distances define a net with the topology of the Si net in $ThSi_2$.

12. A zeolite we haven't discussed, but which is nice to draw or to explore using computer graphics, is known as **MAPSO-46** (symbol AFS). Here are data for the maximum volume form of the net with unit edge:

MAPSO-46 *P*6_3*/mcm*, a = 4.363, c = 8.034, r = 0.366
4·8·4·8·4·8 in 8 *h*: ±(1/3,2/3,±*z* ; 1/3,2/3,1/2±*z*), z = 0.438
4·4·4·8_2·6_2·8 in 24 *l*: ±(*x*,*y*,*z* ; etc.), x = 0.364, y = 0.496, z = 0.366
4·4·4·6·6·12 in 24 *l*, x = 0.570, y = 0.703, z = 0.312

The net is closely related to that of **CoAPO-50** (Fig. 7.43, p. 328), the main difference being that the cubes in that net are replaced by polyhedra with nine faces.

13. $BaCu_2S_2$ is polymorphic. One form has the $ThCr_2Si_2$ structure (§ 6.4.2) with Ba between tetragonal layers of {Cu}S_4 tetrahedra. A second form forms a three-dimensional 4-connected Cu,S net derived from 4.8^2 by double zig-zag connections in the manner similar to that shown in Fig. 7.17 (p. 306). The vertices are all 4·6·4·6·6·8_2 but there are two topologically-different kinds. Crystallographic data for the compound are:

$BaCu_2S_2$ *Pnma*, a = 9.308, b = 4.061, c = 10.408 Å. Atoms in 4 *c*: ±(x,1/4,z ; 1/2+x,1/4,1/2−z)
Ba: x = 0.240, z = 0.822 ; Cu(1): x = 0.056, z = 0.111 ; Cu(2): x = 0.083, z = 0.545
S(1): x = 0.483, z = 0.169 ; S(2): x = 0.339, z = 0.559

Plot the Cu and S positions in projection down **b** to identify the net.
The net symmetry is *Cmcm*, but Cu,S ordering lowers the symmetry to *Pmcn* (*Pnma*).

14. A 4-connected net with "up-down" rods (§ 7.3.8) occurs as the Ga net in Mg_2Ga_5.

Mg_2Ga_5 *I4/mmm*, a = 8.627, c = 7.111 Å
Mg in 8 *h*: *I* ± (x,±x,0), x = 0.300; Ga(1) in 4 *e*: *I* ± (0,0,z), z = 0.288
Ga(2) in 16 *n*: *I* ± (0,y,±z ; y,0,±z), y = 0.298, z = 0.181

Ga(2) atoms form "up-down" rods (shaded in Fig. 7.95) and Ga(1) atoms link the rods.

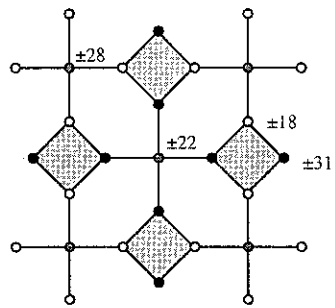

Fig. 7.95. The Ga arrangement in Mg_2Ga_5 projected on (001). Numbers are elevations in units of $c/100$.

The silicate, narsarsukite, was mentioned in § 7.3.8. In that compound Ti atoms link up-down rods of {Si}O_4 tetrahedra to produce the same 4-connected net with stoichiometry $(TiSi_4)O_{10}$. An additional O atom links the Ti atoms in the **c** direction producing distorted {Ti}O_6 octahedra and the composition is often written $Na_2TiOSi_4O_{10}$. Drawing the structure of narsasukite and identifying the net is a nice exercise [for data see D. R. Peacor & M. J. Buerger, *American Mineralogist*, **47**, 539 (1962)]. If you do this, you may notice that the metal atom arrangements are nearly identical (except for a change of scale) in $Mg_2Ga(1)Ga(2)_4$ and $Na_2TiSi_4O_{11}$.

15. Open (zeolite-like) (4,6)-connected networks are often produced by linking clusters of tetrahedra by octahedra and *vice versa* and indeed some authors include such structures under the heading of zeolites. The narsasukite framework (Exercise 14) is a (4,6)-connected net if *all* -O- links are counted. Here are some other examples for exploration:

(a) Part of the pharmacosiderite structure was illustrated as clusters of octahedra linked by tetrahedra in § 5.2.2 (see Fig. 5.23, p. 154). The coordinates of the metal atoms are: space group $P\bar{4}3m$: Fe (octahedral) in 4 *e*: x,x,x ; $(x,\bar{x},\bar{x})\kappa$; As (tetrahedral) in 3 *d*:

(1/2,0,0)κ. Fe has 3 Fe and 3 As neighbors, and As has 4 Fe neighbors. If all edges are equal, $x = 5/\sqrt{2}(\sqrt{6} - 1) = 0.145$ (quite close to the actual value). For the full structure see M. J. Buerger *et al., Zeits. Kristallogr.* **125**, 93 (1967).

(b) An open structure consisting of rings of three tetrahedra (corner sharing) joined by further corner sharing with octahedra occurs in catapleite, $Na_2ZrSi_3O_9.2H_2O$ in which rings of three corner-sharing $\{Si\}O_4$ tetrahedra are joined by $\{Zr\}O_6$ tetrahedra. Data for the non-water atoms are:

catapleite — *P*6$_3$/*mmc*, $a = 7.40$, $c = 10.07$ Å, $V = 477$ Å^3.
Zr in 2 *a*: (0,0,0 ; 0,0,1/2) ; Na in 4 *f*: ± (1/3,2/3,*z* ; 1/3,2/3,1/2+*z*), $z = 0.08$
Si in 6 *h*: ± (x,2x,1/4 ; x,$\bar{x}$,1/4 ; 2$\bar{x}$,$\bar{x}$,1/4), $x = 0.20$; O(1) in 6 *h*, $x = 0.47$
O(2) in 12 *k*: ± (x,2x,z ; x,$\bar{x}$,z ; 2$\bar{x}$,$\bar{x}$,z ; x,2x,z+1/2 ; x,$\bar{x}$,z+1/2 ; 2$\bar{x}$,$\bar{x}$,z+1/2),
$x = 0.135$, $z = 0.125$

In the Zr,Si net, Zr has 6 Si neighbors and Si has 2 Si and 2 Zr neighbors. Not unexpectedly, the Zr-Si distances are rather different (larger) than the Si-Si distances.

(c) A related, but different, structure is found in benitoite, $BaTiSi_3O_9$

benitoite — *P*6̄*c*2, $a = 6.61$, $c = 9.72$ Å, $V = 368$ Å^3
Ba in 2 *f*: (2/3,1/3,0 ; 2/3,1/3,1/2) ; Ti in 2 *c*: (1/3,2/3,0 ; 1/3,2/3,1/2)
Si in 6 *k*: (x,y,1/4 ; $\bar{y}$,x–y,1/4 ; y–x,$\bar{x}$,1/4 ; $\bar{y}$,$\bar{x}$,3/4 ; y–x,y,3/4 ; x,x–y,3/4),
$x = 0.0711$, $y = 0.2894$; O(1) in 6 *k*, $x = 0.2535$, $y = 0.1972$
O(2) in 12 *l*: (as 6 *k* but 1/4 replaced by z and 1/2–z and 3/4 replaced by $\bar{z}$, 1/2+z)
$x = 0.0880$, $y = 0.4302$, $z = 0.1127$

Compare the Zr,Si net in catapleite with the Ti,Si net in benitoite. Note that the latter is much denser (compare the volumes of the unit cells which contain 6 Si atoms in each case).

16. A fascinating open structure based on a 4-connected net is that of the zeolite-like compound: $[N(CH_3)_4]_2MnGe_4S_{10}$ with a framework based on vertex sharing $\{Mn\}S_4$ and $\{Ge\}S_4$ tetrahedra. Ge_4S_{10} "supertetrahedron" units (Fig. 5.18, § 5.2.1) and MnS_4 units are linked as in **diamond** (or better, as in **sphalerite**) so the net of the metal atoms is intermediate between **diamond** and ***D4***. Here are data for the framework (explore!):

$I\bar{4}$, $a = 9.513$, $c = 14.281$ Å.
Mn in 2 *d*, *I* + (0,1/2,1/4)
Ge in 8 *g*: *I* + (x,y,z ; $\bar{x}$,$\bar{y}$,z ; y,$\bar{x}$,$\bar{z}$; $\bar{y}$,x,$\bar{z}$), $x = 0.570$, $y = 0.325$, $z = 0.089$

The vertex symbols are Mn: $9_2{\cdot}9_2{\cdot}9_2{\cdot}9_2{\cdot}9_2{\cdot}9_2{\cdot}9_2$ and Ge: $3{\cdot}9_2{\cdot}3{\cdot}9_2{\cdot}3{\cdot}9_2$.

17. Draw the structure of BeH_2 and show that it is topologically the same as that of moganite (SiO_2).

BeH_2 — *Ibam*, $a = 9.082$, $b = 4.160$, $c = 7.707$ Å ; Be(1) in 4 *a*: *I* ± (0,0,1/4)
Be(2) in 8 *j*: *I* ± (x,y,0 ; 1/2–x,1/2+y,0), $x = 0.1699$, $y = 0.1253$
H(1) in 8 *j*, $x = 0.3055$, $y = 0.2823$
H(2) in 16 *k*: *I* ± (x,y,±z ; 1/2–x,1/2+y,±z), $x = 0.0895$, $y = 0.1949$, $z = 0.1515$

APPENDIX 1

MORE INFINITE SYMMETRY GROUPS

In this appendix we describe some infinite symmetry groups other than the space groups discussed in Chapters 1 and 3. Three-dimensional objects with translational symmetry in only two dimensions are *layers*. The symmetry groups of these objects are the 80 layer groups that are given below. Likewise three-dimensional objects with translational symmetry in only one dimension are *rods*. The 75 crystallographic rod groups are also listed.[1] Two-dimensional objects with one-dimensional translational symmetry are called *bands* or *friezes* and we describe the 7 band groups also.

A convenient way to consider these groups is as derived from space groups by removing translations in one or two dimensions. The reason for doing this is that the coordinates of general and special positions (and their site symmetries), and the nature and location of symmetry elements, can be obtained directly from the space group tables in the *International Tables* (abbreviated here to *IT*). As the coordinates of the general and special positions are the same as those of the space groups from which they are derived, the same labels (Wyckoff notation) are used for them here.

For completeness we also mention the *cylindrical* and *spherical* point groups that describe the symmetries of objects with ∞-fold rotation axes.

A1.1 Layer groups

In the coordinate system used here it is assumed that the translations are along the x and y directions. The lattice can be oblique, either primitive (*p*) or centered (*c*) rectangular, hexagonal or square as for the two-dimensional space groups. The position in the plane group symbol has the same significance as for the three-dimensional space groups.

Once the space group from which the layer group is derived has been identified (and, if necessary, the axes relabeled as explained below) the symmetry elements and their locations and the coordinates of special and general positions are obtained directly from the *IT* (but of course there are no translations along z. In fact z is now to be considered as the height above the $z = 0$ plane, and as such, has dimensions (e.g. z may be measured in Å). The symmetry elements of the layer group are those of the space group which are contained in, or which intersect, the plane $z = 0$.

Comments and examples are taken in order of the system of the corresponding three-dimensional groups. For the full table of groups see § A1.6 (p. 389).

Monoclinic. The cases to be considered are classes 2, *m* and 2/*m*. The 2-fold axis of the layer group can be along z in which case the lattice is oblique. The symbol for the layer

[1] With translations in only one direction, there is no restriction on the nature of rotation axes in rod groups. Here we restrict ourselves to those containing only 1-, 2-, 3-, 4- and 6-fold axes.